SKB

TECHNICAL REPORT 95-31

DECOVALEX I – Test Case 1:

Coupled stress-flow model

Lars Rosengren[1], Mark Christianson[2]

1 Itasca Geomekanik AB,
Borlänge, Sweden
2 Itasca Consulting Group Inc.,
Minneapolis, MN, USA

December 1995

SVENSK KÄRNBRÄNSLEHANTERING AB
SWEDISH NUCLEAR FUEL AND WASTE MANAGEMENT CO

P.O.BOX 5864 S-102 40 STOCKHOLM SWEDEN
PHONE +46 8 665 28 00 TELEX 13108 SKB
FAX +46 8 661 57 19

DECOVALEX I - TEST CASE 1:

COUPLED STRESS-FLOW MODEL

Lars Rosengren[1], Mark Christianson[2]

1 Itasca Geomekanik AB, Borlänge, Sweden
2 Itasca Consulting Group Inc., Minneapolis, MN, USA

December 1995

DECOVALEX I

TEST CASE 1:
COUPLED STRESS-FLOW MODEL

Lars Rosengren (1)
Mark Christianson (2)

(1) Itasca Geomekanik AB
Box 17
S-781 21 Borlänge
Sweden

(2) Itasca Consulting Group Inc.
Thresher Square East
708 South Third Street, Suite 310
Minneapolis, MN 55415
USA

December 1995

Keywords: Numerical Modeling, Fluid Flow in Joints, Coupled Mechanical-Flow

FOREWORD

This report is an integral part of SKB's engagement in the first part of the DECOVALEX project (DECOVALEX I). The work, that was made 1992-1994, is compiled in four reports and two articles.

The following SKB technical reports have been printed:

Börgesson, L. and Hernelind, J. (1995) "DECOVALEX I — Test Case 2: Calculation of the Fanay-Augères THM Test — Thermomechanical modelling of a fractured rock volume," SKB Technical Report TR 95-28.

Börgesson, L. and Hernelind, J. (1995) "DECOVALEX I — Test Case 3: Calculation of the Big Ben Experiment — Coupled modelling of the thermal, mechanical and hydraulic behaviour of water-unsaturated buffer material in a simulated deposition hole," SKB Technical Report TR 95-29.

Israelsson, J. (1995) "DECOVALEX I — Bench-Mark Test 3: Thermo-Hydro-Mechanical Modelling," SKB Technical Report TR 95-30.

Rosengren, L. and Christianson, M. (1995) "DECOVALEX I — Test Case 1: Coupled Stress-Flow Model," SKB Technical Report TR 95-31.

The following articles have been published:

Rehbinder, G. (1995) "Analytical Solutions of Stationary Coupled Thermo-Hydro-Mechanical Problems," *Int. J. Rock Mech. Min. Sci. & Geomech. Abstr.* Vol. 32, No. 5, pp. 453-463, 1995.

Claesson, J., Follin, S., Hellström, G. and Wallin, N-O. (1995) "On the use of diffusion equation in test case 6 of DECOVALEX," *Int. J. Rock Mech. Min. Sci. & Geomech. Abstr.*, Vol. 32, No. 5, pp. 525-528, 1995.

ABSTRACT

This report presents the results of the Coupled Stress- Flow Model, TC1 (Test Case 1) of Decovalex. The model simulates the fourth loading cycle of a Coupled Stress-Flow Test (CSFT) and subsequent shearing up to and beyond peak shear resistance.

The first loading sequence, termed "Sequence A", consists of seven normal loading steps: 0, 5, 15, 25, 15, 5 and 0 MPa. The second loading sequence termed "Sequence B", consists of the following eight steps: unstressed state, normal boundary loading of 25 MPa (no shearing), and then shearing of 0.5, 0.8, 2.0, 4.0, 2.0 and 0 mm.

According to the problem definition, Decovalex (1991), the shearing was to be made by changing the boundary stresses while keeping the joint normal stress at a constant value of 25 MPa. It was found, however, that an applied boundary stress of 25 MPa produces an average joint normal stress, at five monitoring points along the joint, that is significantly greater. Further, it is not possible to specify stress boundary conditions to produce a specific amount of shear displacement after the joint reaches peak shear strength. Therefore, displacement boundary conditions were applied so that the average joint normal stress from the 25 MPa normal boundary loading step was kept constant during shearing.

The normal stress along the joint is not constant, but higher at the joint ends due to bending in the model. A higher normal stress results in a smaller aperture at the ends of the joint. The ends of the joint will control the flow rate for the entire joint. If the flow rate is used to determine an average joint aperture, this will lead to errors.

Two different options regarding the rock joint behavior were modeled in accordance with the problem definition. In Option 1 a linear elastic joint model with a Coulomb slip criterion was used. In Option 2 a non-linear empirical (i.e. Barton-Bandis) joint model was used.

The hydraulic condition during both Loading Sequence A and B was a constant head of 5 m at the inlet point and 0 m at the outlet point.

All model runs presented in this report were performed using the two-dimensional distinct element computer code UDEC, version 1.8.

SAMMANFATTNING

Denna rapport redovisar resultatet från den kopplade spännings-flödesmodellen, TC1 (Test Case 1) utförd inom ramen för Decovalex. Modellen simulerar den fjärde belastningscykeln av ett kopplat spännings-flödestest och efterföljande skjuvning upp till och efter maximalt skjuvmotstånd.

Normalbelastningssekvensen, kallad "Sekvens A", utgörs av sju belastningssteg: 0, 5, 15, 25, 15, 5 och 0 MPa, och den efterföljande skjuvsekvensen, kallad "Sekvens B", av följande åtta steg: obelastat tillstånd, 25 MPa normalbelastning på ränderna (ingen skjuvning), och sedan skjuvning på 0.5, 0.8, 2.0, 4.0, 2.0 och 0 mm.

Enligt problemdefinitionen, Decovalex (1991), skulle skjuvningen utföras genom att ändra normalspänningen på ränderna under det att normalspänningen i sprickan skulle hållas på ett konstant värde av 25 MPa. Men, resultaten från modellerna visade att en normalspänning på 25 MPa ränderna resulterar i en medelspänning vinkelrätt mot sprickan som är betydligt större. Vidare, är det inte möjligt att specificera spänningar som randvillkor för att producera ett specifikt belopp på skjuvrörelsen efter det att sprickans skjuvhållfasthet uppnåtts. Därför applicerades förskjutningar på ränderna på ett sådant sätt att medelspänningen vinkelrätt mot sprickan hölls konstant under skjuvningen.

Normalspänningen längs sprickan är inte konstant utan högre vid sprickändarna än i mitten. Detta beror på böjning i modellen. En högre normalspänning resulterar i mindre spricköppning vid sprickans ändar, vilket leder till att dessa kommer att bestämma flödets storlek längs hela sprickan. Om flödet genom sprickan används för att bestämma medelspricköppningen kommer detta att leda till avvikelser från den verkliga medelspricköppningen.

I enlighet med problemdefinitionen modellerades sprickans uppförande på två olika sätt, dels som linjärelastisk med ett Coulomb skjuvningsvillkor, dels med hjälp av en icke linjär empirisk modell (d.v.s. Barton- Bandis sprickmodell).

De hydrauliska villkoren för båda belstningssekvenserna var: konstant tryck på 50 kPa vid insläppspunkten och 0 kPa vid utsläppspunkten.

Alla modellkörningar presenterade i denna rapport utfördes med det datorbaserade två-dimensionella distinkta elementprogrammet UDEC, version 1.8.

TABLE OF CONTENTS

SUMMARY AND CONCLUSIONS

This report presents the results of the Coupled Stress-Flow Model, TC1 (Test Case 1) of Decovalex. The model simulates the fourth loading cycle of a Coupled Stress-Flow Test (CSFT) and subsequent shearing up to and beyond peak shear resistance.

The normal loading sequence, termed "Sequence A", consists of seven loading steps: 0, 5, 15, 25, 15, 5 and 0 MPa. The shear sequence termed "Sequence B", consisted of the following eight steps: unstressed state, normal boundary loading of 25 MPa (no shearing), and then shearing of 0.5, 0.8, 2.0, 4.0, 2.0 and 0 mm.

Each loading sequence were performed with two different options regarding the rock joint behavior. In Option 1 a linear elastic joint model with a Coulomb slip criterion was used. In Option 2 a non-linear empirical (i.e. Barton-Bandis) joint model was used.

The hydraulic conditions for all models presented in this report was a constant head of 5 m at the inlet point and 0 m at the outlet point.

Based on the modeling, the following general conclusions could be drawn for Option 1 and 2:

- A boundary normal stress of 25 MPa produces an average joint normal stress that is significantly greater than 25 MPa.

- It is not possible to specify stress boundary condition to produce a specific amount of shear displacement after the joint reaches peak shear strength.

- The normal stress along the joint is not constant, but higher at the joint ends. This is due to bending in the model.

- The higher normal stress at the joint ends results in smaller joint apertures at the joint ends than along the rest of the joint. The ends of the joint will therefore control the flow rate for the entire joint. If the flow rate is used to determine an average joint aperture, this will lead to errors.

- Normal stress boundaries produce more bending in the model compared to displacement boundaries. This larger bending results in larger difference in stress between the joint ends and the middle of the joint, although the average stress is the same.

- The average normal stress could be held fairly constant during the

The following specific conclusions could be drawn for Option 1:

- The joint closes to it's residual aperture at the joint ends for all loading steps except for the case of 5 Map normal boundary loading.

- When shearing a non-dilatant joint as in this problem, the joint apertures should remain constant during the shearing sequence. However, a slight change (<1 μm) in the average aperture occurs resulting in a slight change in flow rate. If the flow rates are plotted in the same scale as for Option 2, they will appear constant. Consequently, this minor change in aperture and flow can essentially be considered as noise.

The following specific conclusions could be drawn for Option 2:

- Because of dilation, it is difficult to maintain a constant average normal stress in the joint during shear using a displacement boundary condition. A component of normal displacement must be estimated and removed during shear. The sample is not allowed to rotate when a displacement boundary is used so that any change in normal stress distribution caused by rotation may not be evident.

- The use of relatively low joint stiffness limit (200 GPa/m) produces a more constant stress distribution along the joint compared to Option 1 where a joint stiffness of 500 GP/m was used.

- In the Barton-Bandis joint model implementation in UDEC the joint dilation is a function of the shear displacement and the mobilized roughness. It does not take into account displacement from the original start point during shear reversal. This results in the dilation being recovered immediately upon shear reversal since the mobilized roughness goes to zero. The dilation is then accumulated during the reverse shear displacement and is nearly the same as at the end of the original 4.0 mm shear. This error in implementation has been fixed in the current UDEC version.

1 INTRODUCTION

This report presents the results of the Coupled Stress-Flow Model, TC1, of Decovalex. The model simulates the fourth loading cycle of a Coupled Stress-Flow Test (CSFT) and subsequent shearing up to and beyond peak shear resistance.

The normal stress boundary loading sequence is termed "Loading Sequence A" and the subsequent shearing is termed "Loading Sequence B". Loading Sequence A consists of seven loading steps, including the initial unstressed state. The following boundary normal stress loading steps are included in Loading Sequence A: 0, 5, 15, 25, 15, 5, and 0 MPa. Loading Sequence B consists of eight steps, which are as follows: unstressed state, normal boundary loading of 25 MPa (no shearing), and then shearing of 0.5, 0.8, 2.0, 4.0, 2.0 and 0 mm. The first values up to 4 mm, represent forward shearing and the remaining values represent reverse shearing. The shearing sequence was to be made under constant joint normal stress.

In the problem specification the shearing was to be made by changing the boundary stresses. However, it is not possible to specify stress boundary conditions to produce specific amounts of shear displacement after the joint reaches peak shear strength. Therefore, displacement boundary conditions were applied so that joint normal stress from the 25 MPa normal boundary stress step was kept constant during shearing.

Two different options regarding the rock joint behavior are modelled in accordance with the problem definition, Decovalex (1991). In Option 1 a linear elastic joint model with a Coulomb slip criterion was used. In Option 2 a non-linear empirical (i.e. Barton-Bandis) joint model was used.

The hydraulic condition during both Loading Sequence A and B was a constant head of 5 m at the inlet point and 0 m at the outlet point.

All model runs presented in this report are performed using the two-dimensional distinct element computer code UDEC, version 1.8.

2 BRIEF MATHEMATICAL BACKGROUND TO THE CODE

There are numerous references which describe the theoretical background and numerical formulation used in UDEC. One of the most comprehensive descriptions is given by Board (1989). The description of the mechanical and hydromechanical code formulation presented here is adapted from Hart (1991). The description of the thermomechanical code formulation is adapted from Board (1989).

In the distinct element method, a rock mass is represented as an assemblage of discrete blocks. Joints are viewed as interfaces between distinct bodies — i.e., the discontinuity is treated as a boundary condition rather than a special element in the model. The contact forces and displacements at the interfaces of a stressed assembly of blocks are found through a series of calculations which trace the movements of blocks. Movements result from the propagation through the block system of a disturbance applied at the boundary. This is a dynamic process in which the speed of propagation is a function of the physical properties of the discrete system. The dynamic behavior is described numerically by using a timestepping algorithm in which the size of the timestep is selected such that velocities and accelerations can be assumed constant within the timestep. The distinct element method is based on the concept that the timestep is sufficiently small that during a single step disturbances cannot propagate from one discrete element in the model further than its immediate neighbors. This solution scheme is identical to that used by the explicit finite difference method for continuum numerical analysis. The timestep restriction applies to both contacts and blocks. For rigid blocks, the block mass and interface stiffness between blocks define the timestep limitation; for deformable blocks, the zone size is used, and the stiffness of the system includes contributions from both the intact rock modulus and the stiffness at the contacts.

The calculations performed in the distinct element method alternate between application of a force-displacement law at the contacts and Newton's second law of motion at the blocks. The force-displacement law is used to find contact forces from displacements. Newton's second law gives the motion of the blocks resulting from the forces acting on it. If the blocks are deformable, motion is calculated at the gridpoints of the triangular finite-difference (constant-strain) elements within the blocks. Then, the application of the block material constitutive relations gives new stresses within the elements. Figure 2-1 shows schematically the calculation cycle for the distinct element method.

This numerical formulation satisfies momentum and energy conservation laws by satisfying Newton's laws of motion exactly. Although some error may be introduced in the computer programs by the numerical integration process, this error may be made arbitrarily small by the use of suitable timesteps and high precision coordinates.

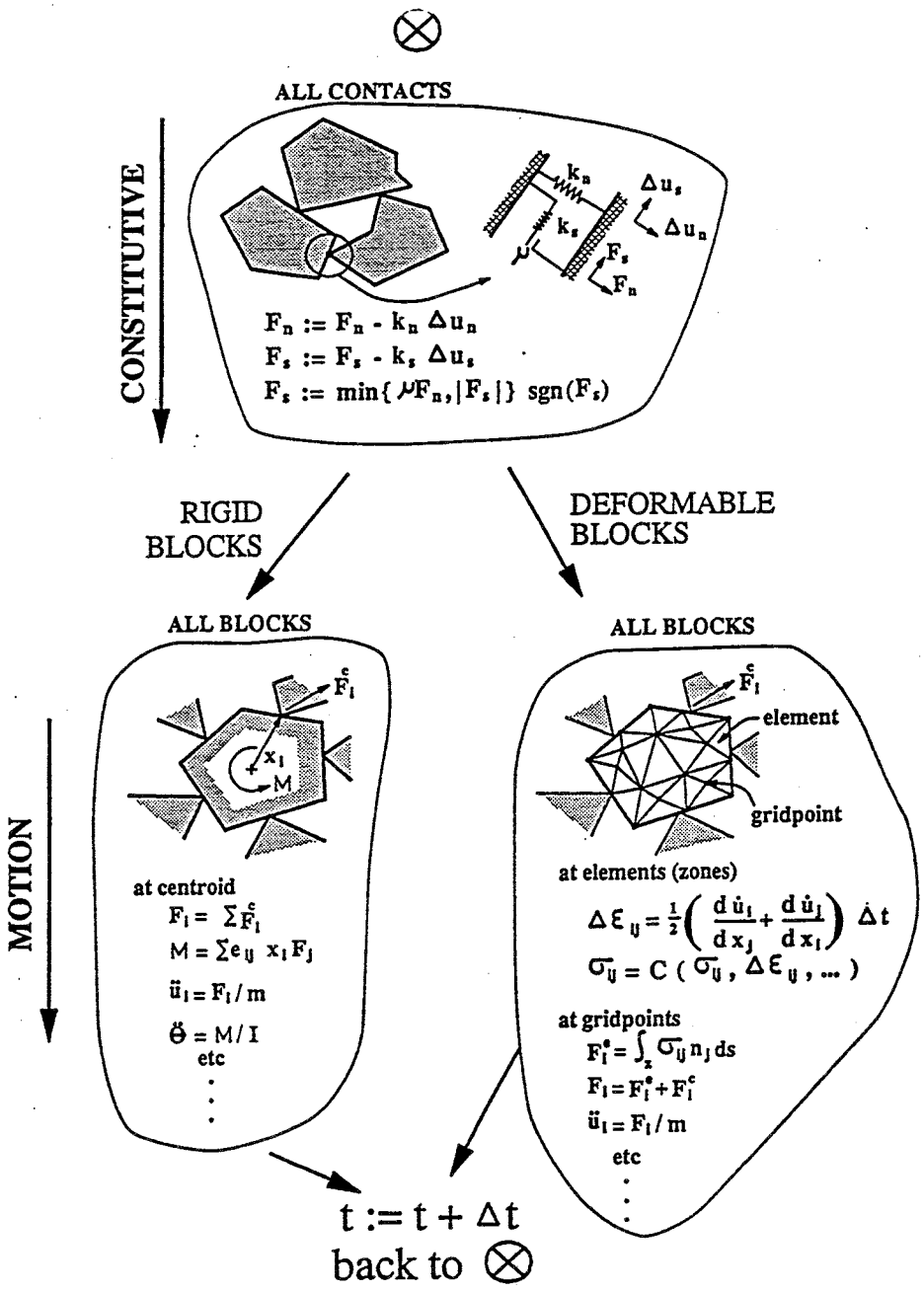

Figure 2-1. *Calculation Cycle for the Distinct Element Method (symbols defined in the appendix I) [Hart, 1991]*

2.1 Rock Joint Representation

A rock joint is represented numerically as a contact surface (composed of individual point contacts) formed between two block edges. In general, for each pair of blocks that touch (or is separated by a small enough gap), data elements are created to represent point contacts. In UDEC, adjacent blocks can touch along a common edge segment or at discrete points where a corner meets an edge or another corner. For rigid blocks, a contact in UDEC is created at each corner interacting with a corner or edge of an opposing block (Fig 2-2). If the blocks are deformable (internally discretized into finite difference elements), point contacts are created at all gridpoints located on the block edge in contact. Thus, the number of contact points can be increased as a function of the internal zoning of the adjacent blocks.

A specific problem with contact schemes is the unrealistic response that can result when block interaction occurs close to or at opposing block corners. Numerically, blocks may become locked or hung-up. This is a result of the modeling assumption that block corners are sharp or have infinite strength. In reality, crushing of the corners would occur as a result of a stress concentration. Explicit modeling of this effect is impractical. However, a realistic representation can be achieved by rounding the corners so that blocks can smoothly slide past one another when two opposing corners interact. Corner rounding is used in UDEC by specifying a circular arc for each block corner. The arc is defined by the distance from the true apex to the point of tangency with the adjoining edges. By specifying this distance rather than a constant radius, the truncation of sharp corners is not severe.

In UDEC, the point of contact between a corner and an edge is located at the intersection between the edge and the normal taken from the center of the radius of the circular arc at the corner to the edge (Fig 2-3(a)). If two corners are in contact, the point of contact is the intersection between the line joining the two opposing centers of radii and the circular arcs (Fig 2-3(b)). The directions of normal and shear force acting at a contact are defined with respect to the direction of the contact normal (Fig 2-3). Contacts along the edge of a deformable block are represented by corners with very large rounding lengths.

Corner rounding only applies to the contact mechanics calculation in UDEC. All other calculations and properties such as block and zone mass are based on the entire block. Corner rounding can introduce inaccuracy in the solution if the rounding is too large. If the rounding length is kept to approximately one percent (1%) of the representative block edge length in the model, good accuracy is achieved.

Contact points in UDEC are updated automatically as block motion occurs. The algorithms to perform this updating must be computationally efficient, particularly for dynamic analysis, in which large displacements may require deleting and adding hundreds of contacts during the dynamic simulation. UDEC takes advantage of a network of "domains" created by the two-

dimensional block assembly. Domains are the regions of space between blocks which are defined by the contact points — e.g., D_1 and D_2 in Fig 2-4. During one timestep, new contacts can be formed only between corners and edges within the same domain, so local updates can be executed efficiently whenever some prescribed measure of motion is reached within the domain. The main disadvantage of this scheme is that it cannot be used for very loose systems because the domain structure becomes ill-defined.

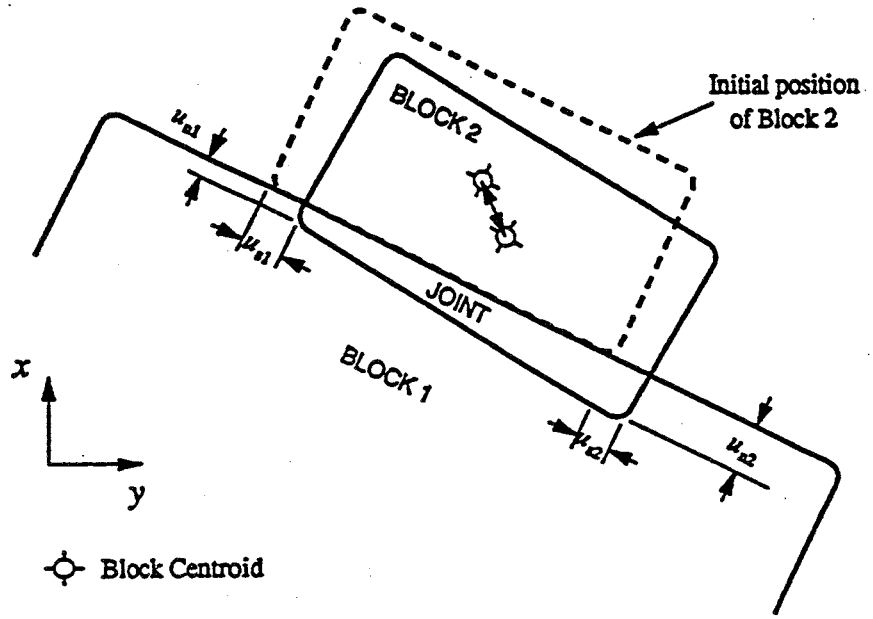

Figure 2-2. *Contacts Between Two Rigid Blocks in UDEC (Block overlap is exaggerated.) [Hart, 1991]*

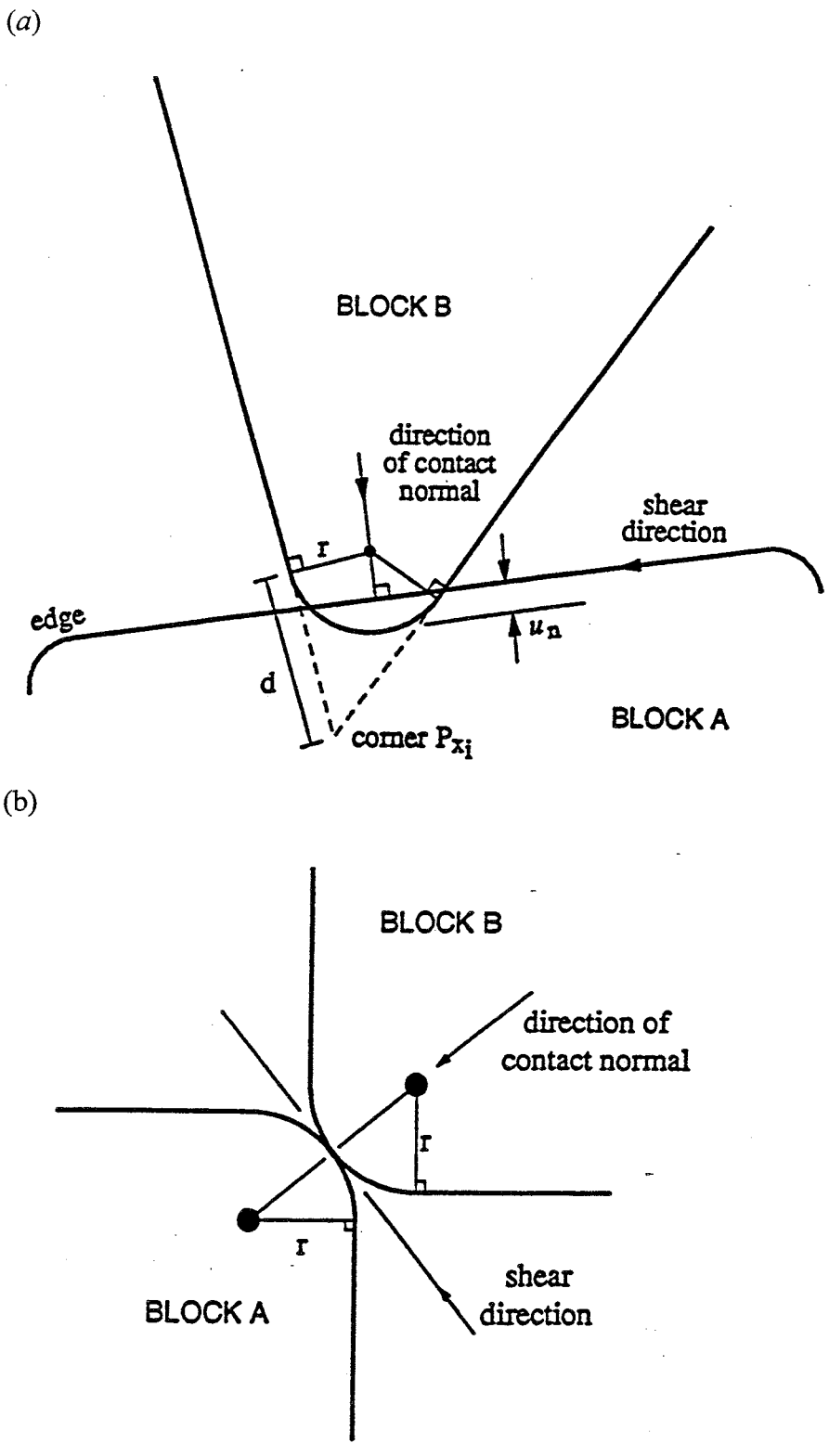

Figure 2-3. *Definition of Contact Normal in UDEC: (a) detail of rounded Corner-to-edge contact (rounding length exaggerated); (b) smooth interaction of corner-to-corner contact [Hart, 1991]*

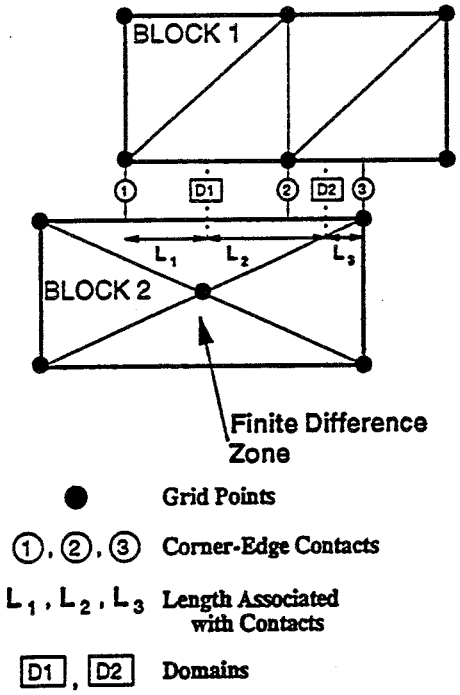

Figure 2-4. *Contacts and Domains Between Two Deformable Blocks [Hart, 1991].*

2.2 Rock Joint Behavior

Numerically, a joint is a special contact type which is classified as an edge-to-edge contact. In UDEC, a joint is recognized when a domain is defined by two point contacts. The joint is assumed to extend between the two contacts and be divided in half with each half-length supporting its own contact stress (Fig 2-4). Incremental normal and shear displacements are calculated for each point contact and associated length (i.e., L_1, L_2 and L_3 in Fig 2-4).

UDEC uses several joint behavior relations to describe the mechanical response at the interface. The basic joint model used in the codes captures several of the features which are representative of the physical response of joints. In the normal direction, the stress-displacement relation is assumed to be linear and governed by the stiffness k_n such that

$$\sigma_n = k_n u_n \qquad 2\text{-}1$$

where σ_n is the effective normal stress, and
u_n is the normal displacement.

There is also a limiting tensile strength, T, for the joint. If the tensile strength is exceeded (i.e., if $\sigma_n < -T$), then $\sigma_n = 0$. Similarly, in shear, the response is controlled by a constant shear stiffness, k_s. The shear stress, τ_s, is limited by a combination of cohesive (C) and frictional (ϕ) strength. Thus, if

$$|\tau_s| \leq C + \sigma_n \tan\phi = \tau_{max} \qquad 2\text{-}2$$

then

$$\tau_s = k_s u_s^e \qquad 2\text{-}3$$

or else, if

$$|\tau_s| \geq \tau_{max} \qquad 2\text{-}4$$

then

$$\tau_s = sign(\Delta u_s)\, \tau_{max} \qquad 2\text{-}5$$

where u_s^e is the elastic component of the shear displacement, and
Δu_s is the incremental shear displacement.

This model is described as the Coulomb slip model. In addition, joint dilation may occur at the onset of slip (non-elastic sliding) of the joint. Dilation is governed in the Coulomb slip model by a specified dilation angle ï. The accumulated dilation is generally limited by either a high normal stress level or by a large accumulated shear displacement which exceeds a limiting value U_{cs}. The limitation on dilation corresponds to the observation that crushing of asperities at high normal stress or large shearing would eventually prevent the joint from dilating.

In the Coulomb model, the dilation is restricted such that if $|\tau_s| \leq \tau_{max}$, then $\gamma = 0$, and if $|\tau_s| = \tau_{max}$ and $u_s \geq U_{cs}$, then $\gamma = 0$.

The Coulomb model can approximate a displacement-weakening response which is often observed in physical joints. This is accomplished by setting both the tensile strength, T, and cohesion, C, to zero whenever either the tensile or shear strength is exceeded.

A more comprehensive displacement-weakening model is also available in UDEC. This model, the continuously-yielding joint model (Cundall and Lemos, 1990) is intended to simulate the intrinsic mechanism of progressive damage of the joint under shear.

UDEC also includes an empirical joint model described by Barton et al. (1985). In this joint model, the effect of surface roughness on joint deformation and strength is described in terms of empirical relations between normal stress and closure, mobilized roughness and normalized shear displacements, and a non-linear strength criterion.

2.3 Block Deformability

In UDEC, each block can be automatically discretized into triangular constant-strain elements. These elements may follow an arbitrary, nonlinear constitutive law (e.g., Mohr-Coulomb failure criterion with non-associated flow rule). Other nonlinear plasticity models recently added to UDEC include a ubiquitous joint model and strain-softening models for both shear and volumetric (collapse) yield. The complexity of deformation of the blocks depends on the number of elements into which the blocks are divided.

2.4 Hydromechanical Coupling

UDEC has the capability to model the flow of a fluid through the fractures of a system of impermeable blocks. A fully-coupled mechanical-hydraulic analysis is performed in which fracture conductivity is dependent on mechanical deformation and, conversely, joint water pressures affect the mechanical behavior. Joint apertures and water pressures are updated at every timestep.

The fluid logic takes advantage of the domain network logic used in UDEC to monitor changes in contacts. The domains are considered to be fluid volumes which fluctuate as a function of contact normal displacement at the two ends of the domain. Each contact is assigned a conducting (hydraulic) aperture, a, which is related to normal displacement by

$$a = a_o + u_n \qquad 2\text{-}6$$

where a_o is the aperture at zero normal stress, and
u_n is the joint normal displacement (positive denoting opening).

A minimum residual value, a_{res}, is assumed at higher confining stresses. This allows for some fluid conductivity always to be maintained, in keeping with experimental observation.

Joint dilation will modify the basic relation, and is assumed to be irrecoverable. A maximum contact aperture is also defined which limits the magnitude of the conductivity when the joint opens.

Flow in planar rock fractures is idealized as a case of laminar viscous flow between parallel plates. In this model, the flow rate per unit width, q, if given by

$$q = Ca^3\left[\frac{\Delta p}{L}\right] \qquad 2\text{-}7$$

$$C = \frac{1}{12\mu} \qquad 2\text{-}8$$

where C is the fluid flow joint property which is assumed to remain constant,

μ is the dynamic viscosity of the fluid,

Δp is the change in pressure across a contact between adjacent domains, and

L is the length assigned to the contact.

The rate of fluid flow thus is assumed to be dependent upon the cubic power of the aperture.

The domain pressures are updated by taking into account the net flow into the domain and changes in domain volume due to incremental motion of the surrounding blocks. The new domain pressure is

$$p = p_0 + K_w Q\left[\frac{\Delta t}{V}\right] - K_w\left[\frac{\Delta V}{V_m}\right] \qquad 2\text{-}9$$

where p_0 is the domain pressure in the preceding timestep,

Q is the sum of flow rates into the domain from all surrounding contacts,

K_w is the bulk modulus of the fluid, and

$$\Delta V = V - V_0, \quad V_m = \frac{V + V_0}{2} \qquad 2\text{-}10$$

where V and V_0 are the domain volumes at the present and previous timesteps.

The domain pressures are resolved into forces exerted by the fluid at the contacts and are added to the mechanical contact forces and external loads to be applied at the block boundaries. Thus, total stresses will result inside the impermeable blocks, while effective normal stresses are obtained for the mechanical contacts.

Lemos and Lorig (1990) describe the following limitations of the current procedure as well as an adaptive procedure for determining steady-state condition. For transient flow analysis, the numerical stability requirements may be rather severe, and may make some analyses very time-consuming or impractical, especially if large contact apertures and very small domain areas are present. A scheme that can be used to enhance computational efficiency consists in assigning to domains at the intersection of the joints part of the volume of the joints meeting at the point, and correspondingly reducing the volume of the joint domains. Furthermore, the fluid filling a joint also increases the apparent joint stiffness by K_w/a, thus possibly requiring a reduction of the timestep used in the mechanical calculation.

In many studies, only the final steady-state condition is of interest. In this case, several simplifications are possible which make the present algorithm very efficient for many practical problems. The steady-state condition does not involve the domain volumes. These can thus be scaled to improve the convergence to the solution. A scheme that was found to produce good results consists in assigning to a given domain a volume V that, inserted in the timestep expression above, leads to the same timestep for all domains. The contribution of the change in domain volume to the pressure variation can also be neglected, thus eliminating the influence of the fluid stiffness in the mechanical timestep. Furthermore, as the steady-state condition is approached, the pressure variation in each fluid step becomes very small, allowing the execution of several fluid steps for each mechanical step without loss of accuracy. An adaptive procedure was implemented in UDEC which "triggers" the update of the mechanical quantities, whenever the maximum increment of pressure in any domain exceeds some prescribed tolerance (for example, 1% of the maximum pressure).

2.5 Thermomechanical Coupling

The heat transfer in UDEC is based on conductive transfer within the medium with the provision for temperature, flux, convective or radiative boundaries. The standard equations for transient heat conduction can be found in many texts, such as Karlekar and Desmond (1982), and are reviewed here. The basic equation of conduction heat transfer is Fourier's law, which can be written in one dimension as

$$Q_x = -k_x \frac{\partial T}{\partial x} \qquad 2\text{-}11$$

where Q_x = flux in the x-direction (W/m^2), and
k_x = thermal conductivity in the x-direction (W/m °C).

A similar equation can be written for Q_y. Also, for any mass, the change in temperature can be written as

$$\frac{\partial T}{\partial t} = \frac{Q_{net}}{C_p M} \qquad 2\text{-}12$$

where Q_{net} = net heat flow into mass (M),
C_p = specific heat (J/kg °C), and
M = mass (kg).

These two equations form the basis of the thermal logic in UDEC. Equation 2-12 can be written as

$$\frac{\partial T}{\partial t} = \frac{1}{C_p \rho}\left[\frac{\partial Q_x}{\partial x} + \frac{\partial Q_y}{\partial y}\right] \qquad 2\text{-}13$$

where ρ is the mass density.

Combining this with Eq. 2-11,

$$\frac{\partial T}{\partial t} = \frac{1}{C_p \rho}\frac{\partial}{\partial x}\left[k_x \frac{\partial T}{\partial x}\right] + \frac{\partial}{\partial y}\left[k_y \frac{\partial T}{\partial y}\right] = \frac{1}{\rho C_p}\left[k_x \frac{\partial^2 T}{\partial x^2} + k_y \frac{\partial^2 T}{\partial y^2}\right] \qquad 2\text{-}14$$

if k_x and k_y are constant. This is the standard two-dimensional diffusion equation.

Temperature changes cause stress changes for fully-deformable blocks according to the equation

$$\Delta\sigma_{ij} = -\delta_{ij} K\beta\Delta T \qquad 2\text{-}15$$

where $\Delta\sigma_{ij}$ = change in ij stress component,

δ_{ij} = Kronecker delta function,

$$\begin{bmatrix} 1 & 0 \\ 0 & 1 \end{bmatrix}$$

K = bulk modulus,
ß = volumetric thermal expansion coefficient ß, and
ΔT = temperature change.

Note that ß = 3α, where α = linear thermal expansion coefficient.

Equation 2-15 assumes a constant temperature in each triangular zone which is interpolated from the surrounding gridpoints. The incremental change in stress is added to the zone stress state prior to application of the constitutive law.

The mechanical changes can also cause temperature changes as en~ergy is dissipated in the system. This coupling is not modeled in UDEC because the heat produced in usually negligible for quasi-static problems.

2.6 Performing Coupled Analysis

In performing coupled analyses, it is important to be clear about the relative time scales associated with heat flow, fluid flow and mechanical loading. Mechanical effects occur almost instantaneously in the real world — in the order of milliseconds. Fluid flow effects in jointed rock usually take somewhat longer, on the order of seconds, hours or even days, depending on joint permeability. However, heat flow is a much longer-term process, taking place over months and years.

As discussed previously, UDEC is an explicit code, which means that it takes "timesteps" to solve a problem. Thus, although mechanical effects take place almost instantaneously, UDEC takes a finite number of steps to reach mechanical equilibrium. However, there is no true time period associated with these steps; they are merely an internal mechanism for the code to attain equilibrium. An alternative way in which to think of these mechanical steps is to imagine that each step represents a microsecond or less of time, so that, even if many steps are taken, almost no time elapses.

The procedure for running a coupled thermomechanical simulation is shown in Fig 2-5. The fundamental requirement in performing the simulation is that temperature increases between successive thermal time cause only "small" out-of-balance forces in blocks. Out-of-balance forces are "small" if they do not adversely affect the solution. For non-linear problems, some experimentation may be necessary to obtain a feeling of what "small" means in the particular problem being solved. This is performed by trying different allowable temperature increases when running the problem. An important point to note is that the same temperature increase is not necessarily acceptable to all times in a problem. While the system is far from yield (i.e., inelastic behavior), large temperature changes may be acceptable but, near yield, only relatively small increases can be tolerated.

In many studies involving coupled thermal, hydrological and mechanical analyses, only the steady-state condition at specified times are of interest. For these problems, the adaptive hydromechanical coupling scheme described at the end of Section 2.4 can be used. If this procedure is used to determine the steady-state fluid flow condition, then, again, no true time period is associated with the fluid flow steps and the procedure for running a coupled simulation is similar to that shown in Fig 2-5.

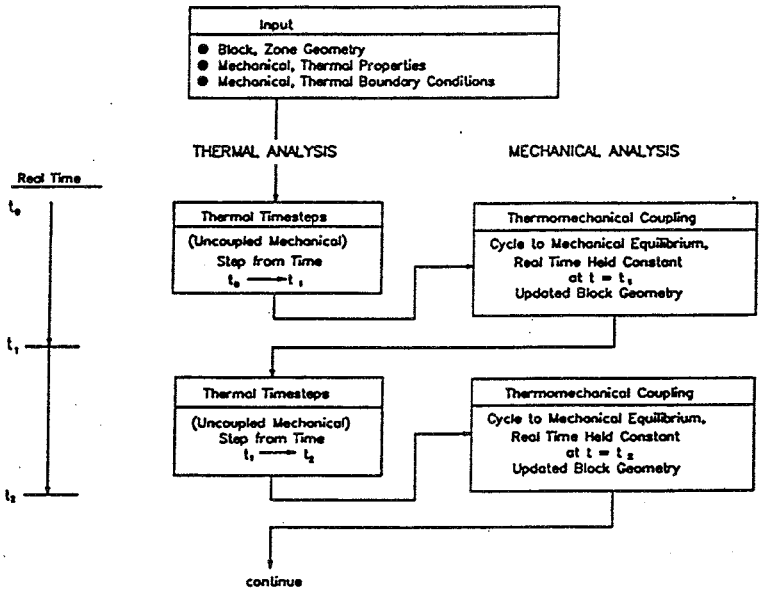

Figure 2-5. *Method of Running A Coupled Thermomechanical Simulation with UDEC [Board, 1989]*

The three main differences would be that:

(1) hydrologic properties and boundary conditions would be specified under "input";

(2) mechanical analysis would be replaced by hydromechanical analysis; and

(3) mechanical equilibrium would be replaced by mechanical and hydrologic equilibrium.

This method of performing coupled analysis results in the following interactions.

- Temperature change is not affected by fluid flow (convective heat transfer).
- Pore pressure in fractures is not affected by temperature change.
- Mechanical stress is affected by temperature change.
- Temperature is not affected by volume change.
- Mechanical stress is affected by pore pressure.
- Pore pressure is not affected by aperture change.
- Thermal conductivity is constant.

3 CODE DESCRIPTION

Formulation and development of the distinct element method has progressed for over 20 years, beginning with the initial presentation by Cundall (1971). The method was created originally as a two-dimensional representation of a jointed rock mass, but has been extended to applications in particle flow research (Walton, 1980), studies on micromechanics of granular media (Cundall and Strack, 1983) and crack development in rocks and concrete (Plesha and Aifantis, 1983; Lorig and Cundall, 1987). The most recent two-dimensional program, UDEC (**U**niversal **D**istinct **E**lement **C**ode) was developed in 1980 (Cundall, 1980; Lemos et al., 1985) to combine into one code the formulation to represent both rigid and deformable blocks separated by discontinuities. In 1983, work was begun on the development of a three-dimensional version of the method. This work is embodied in a computer program entitled 3DEC (**3**-Dimensional **D**istinct **E**lement **C**ode) (Cundall, 1988; Hart et al., 1988). The chronology of development of the distinct element method, and UDEC in particular, is shown in Fig 3-1.

Over the years, the performance of UDEC has been verified for specific problems through through numerous studies (Board, 1989; Brady et al., 1990a,b; Lemos and Lorig, 1990; Itasca, 1991). These verification studies have shown reasonable agreement with analytical solutions and/or results obtained using other codes.

UDEC has also been used to analyze the results of field tests (Brady et al., 1985; Hart et al., 1985) and to predict the results of laboratory tests. UDEC models of jointed rock problems involving response to storage of high-level nuclear waste have been made by many investigators (e.g., Johansson et al., 1991a,b; Board, 1989; Christianson, 1989; Lorig and Dasgupta, 1989).

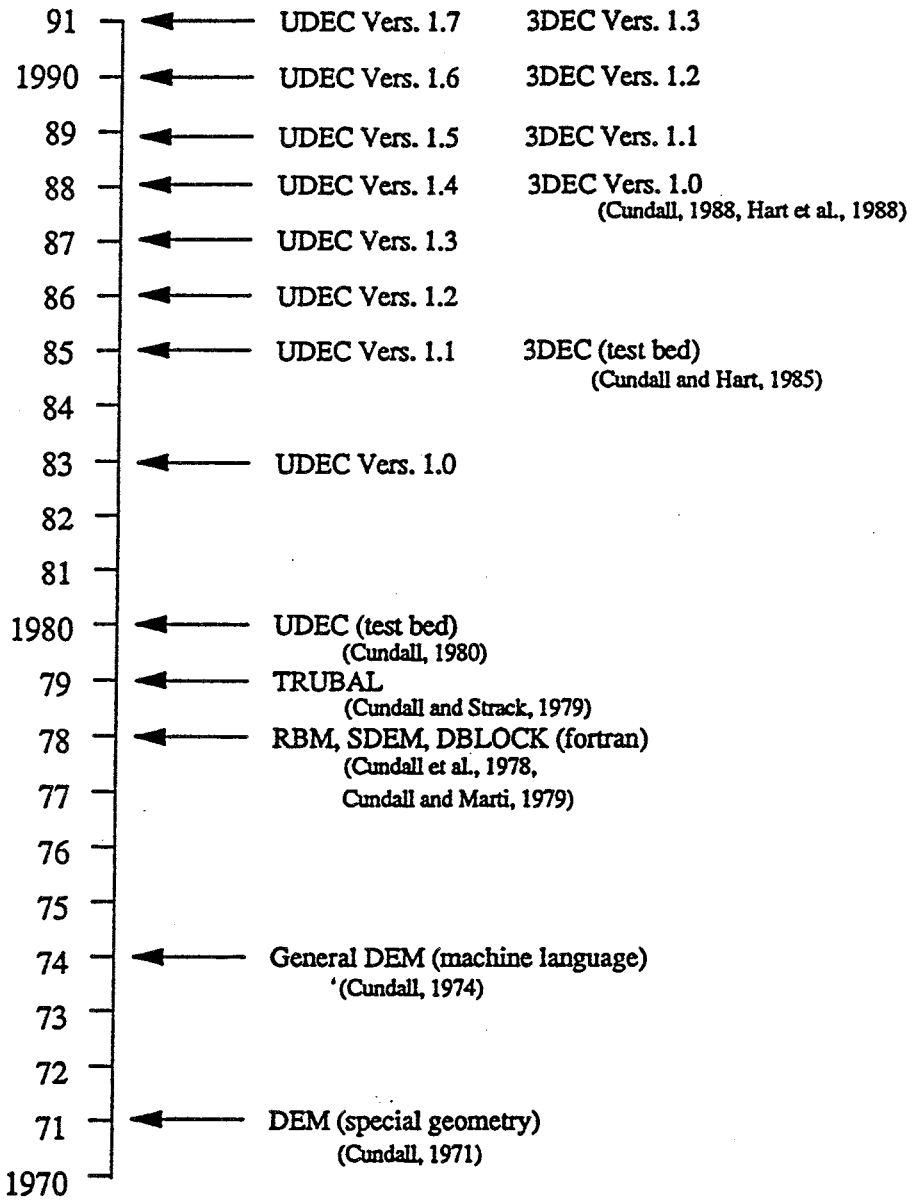

Figure 3-1. *Chronology of the Distinct Element Method*

4 COMMENTS ON THE GIVEN SPECIFICATIONS OF COUPLED STRESS-FLOW MODEL, TC1

4.1 General Comments for Option 1 and Option 2

General comments regarding the specifications for Option 1 and Option 2 are as follows.

1. The specified normal stiffness (1 GPa/m) for the steel-epoxy interface (I4) is too low. The specified maximum normal stress (25 MPa) applied at the boundary produces a normal displacement of 25 mm, which is 2.5 times greater than the steel thickness. In order to overcome this difficulty, the normal stiffness for the steel-epoxy interface was increased from 1 GPa/m to 100 GPa/m.

   A similar problem arises at the epoxy-epoxy interface (I5). The normal stiffness for this interface was not increased as it was assumed that there is actually a gap between halves in the laboratory apparatus.

2. The problem specification implies that (i) normal stress along the length of the rock joint from 25 MPa boundary loading is constant, and (ii) that the average stress is 25 MPa. Neither of these statements are correct. The normal stress varies considerably along the joint due to bending in the epoxy which results in high normal stresses at the joint ends and lower stresses at the middle of the joint. The bending in the epoxy is due to the lower stiffness (compared to the rock joint stiffness) in the epoxy-epoxy interface and to the lower stiffness of the epoxy itself. From knowledge of the test set-up, the boundaries are loaded only over a width which roughly corresponds to the diameter of the specimen. In the specified model, however, the entire width of the boundaries are loaded. This is the main reason that the average joint normal stress in the model is much higher than the specified boundary stresses.

   The induced average joint normal stress from 25 MPa boundary loading was taken as the stress which should be kept constant during the shear sequence. Another way to perform this modelling would be to determine the boundary stresses required to produce an average joint normal stress of 25 MPa and then keep this stress value constant during the shear sequence. This procedure was not used.

3. Displacement boundaries were used for the shear sequence since it is impossible to obtain post peak results with pressure boundaries.

4. The properties for the rock-epoxy interface are not specified in the problem definition. The following properties are used: cohesion, C=1E6 MPa, friction angle, ϕ=45 degrees, normal stiffness, Kn=500 GPa/m, and shear stiffness Ks=16 GPa/m.

4.2 Specific Comments for Option 1

Comments regarding the specifications for this problem are as follows.

1. The residual hydraulic aperture specified for the linear stiffness model is 0.8 μm. At the normal loads at the ends of the joint and the joint normal stiffness specified the joint will close to this value. The hydraulic aperture for the Barton-Bandis joints at this stress level would be 18 μm.

2. There is no dilation angle specified for the linear joints. Since the joint will not change in aperture during shear, Loading Sequence B should not produce a change in flow rate.

3. Plane strain conditions are specified for this problem but not for option 2.

4.3 Specific Comments for Option 2

Comments regarding the specifications for this problem are as follows.

1. On page 16, it is stated that "the displacement needed to mobilize peak shear strength of the rock joint is slightly above 0.8 mm." This statement is true for values of JRC greater than 5. In this problem, JRC is less than 5 and, hence, the displacement needed to mobilize the peak shear strength is 2x0.84 mm = 1.68 mm.

2. Reference for the Barton-Bandis type of joint model (see page 11) is not provided. The joint model used in this exercise is described by Barton (1982) and Barton et al. (1985).

3. On page 11, it states "Each Research Team has therefore to decide whether plane strain or plane stress conditions should be used in a two-dimensional model." However, no information about end conditions is provided. Specification of end conditions would allow proper determination of whether plane strain or plane stress conditions are appropriate. Plane strain was used to be consistant with Option 1.

4. Page 12 provides the relation to be used between hydraulic aperture, e, and mechanical aperture, b. This relation is defined by Barton et al. (1985). However, this reference is not provided. It is believed that, in this relation, b must be specified in microns. A value of JRCo used in the relation is not specified. The value of JRCo = 1.95 was used (see number 6, below). The relation also specifies that the hydraulic aperture be less than or equal to the mechanical aperture. If JRCo = 1.95, then

   $e = 0.19b^2$

   Therefore, the hydraulic aperture will equal the mechanical aperture for mechanical apertures greater than about 5 microns. In this problem, mechanical apertures are greater than 5 microns; therefore, the mechanical and hydraulic apertures are equal.

5. Gravity was neglected in the analysis presented here.

6. Values for JRCo and JCSo were not provided. In the analysis presented here, these values were back-calculated based on joint length. The following values were used in the analysis presented here:

   JRCo = 1.95
   JCSo = 156.21

7. The boundary conditions for the upper block for sequence B are defined as 25 MPa $\pm\Delta\sigma$. It is impossible to specify stress boundary conditions to produce specific amounts of joint shear displacement after the joint reaches peak shear strength. Therefore, displacement boundary conditions were estimated for the analysis presented here. However, difficulties arise when attempting to do this.

   The problem specification states that joint normal stress be kept constant during shearing (see page 15). This means that joint dilation resulting from shear must be accounted for in the boundary conditions. For the results shown here, it was assumed that a dilation angle of 0.5 degrees would result from shearing of the joint under constant normal stress. This value was determined based on use of a joint exerciser (i.e., spread sheet) assuming a joint normal stress of 25 MPa.

8. The problem specification implies that normal stress along the length of the rock joint is constant (see page 20). However, the normal stress varies considerably along the length of the joint. The highest normal stresses are obtained at the ends of the rock joint. The lowest values of normal stress are at the middle of the joint length. This result is exactly what is expected, since the epoxy-epoxy interface at the joint ends has a much lower normal stiffness than the rock joint. In order to reduce the normal stress concentration, and at least try to approach a condition of constant normal stress, the normal stiffness of the rock joint was limited to a normal stiffness of 200 GPa/m. This will also reduce problems with numerical stability caused by joint dilation.

The use of this stiffness limit has relatively minor effects other than reducing the variation in normal stress along the joint. The joint aperture in the Barton-Bandis model in UDEC is calculated from the joint normal stress using a hyperbolic stress displacement function. The use of a stiffness limit in the normal direction, therefore, does not affect apertures. The stiffness limit will result in a slightly greater displacement of the blocks on either side of the joint. The magnitude of this additional displacement is usually several orders of magnitude less than the displacements due to elastic compression of the block.

The output specifications for the model ask for the "average" normal stress across the joint. The concept of an "average" normal stress may be misleading in the problem, since the maximum stresses may be of importance in determining flow characteristics and shear deformations.

9. The initial aperture is calculated from the Barton-Bandis model assuming parameters previously given and assuming a rock compressive strength of 240 MPa. The resultant initial unstressed aperture is 81 microns. Initial closure at the beginning of the fourth normal load cycle is 30 microns. Consequently, the initial unstressed aperture at the beginning of normal loading sequence is 51 microns.

5 HARDWARE - TIMING

The model runs were performed on different computers resulting in different runtimes. Table 5-1 shows the different computers used and approximate runtimes.

Table 5-1. Computers Used and Approximate Runtimes.

RUN	COMPUTER	RUNTIME [h]
Option 1		
Loading Sequence A	Dell 325, 386, 25 Mhz	6
Loading Sequence B	Dell 325, 386, 25 MHz	10
Option 2		
Loading Sequence A	Dell 310, 386, 20 Mhz	8
Loading Sequence B	Gateway 2000, 486, 33 Mhz	4

All runs were conducted using UDEC version 1.8. The data files used are given in Appendices II through V.

6 RESULTS

6.1 Results According to Given Specifications

The results according to the given specifications are divided into four groups, representing the different runs given in Table 5-1 above. Each group of results consist of the following type of figures.

1. Tables showing the value of a specific parameter at a specific point at each loading/shearing step. The given parameters may be either rock matrix parameters or joint parameters depending on where in the model the actual point is specified. Points A through D refer to rock matrix parameters such as the stress components SXX, SYY and SXY, etc. (negative stresses are compressive), and points E through I refer to joint parameters such as joint normal and shear displacement, joint normal stress, pore pressure, etc. For the location of monitoring points, see Fig 6-1. The tables are presented in Appendices VI through XIII.

2. Diagrams showing relations between different parameters for the different loading sequences, e.g. average normal stress versus average normal deformation across the joint.

   The following diagrams are presented for Loading Sequence A:

   (i) Average normal stress across the joint as a function of the average normal deformation between points A-D and B-C. The average normal stress is the average of the normal stress values at points E-I. The normal deformation is defined as the relative displacement of the specified points in a direction orthogonal to the joint. This implies that the orthogonal deformation of the joint includes deformation of the joint and the intact rock material between points A-D and B-C.

   (ii) Average normal stress across the joint versus average mechanical and conducting aperture. The stress and aperture values are average values at points E-I.

   (iii) Average normal stress across the joint versus flow rate at the outlet point (E).

For Loading Sequence B, the following diagrams are presented:

(i) Average shear stress along the joint as a function of the average shear deformation between points A-D and B-C. The average shear stress, is the average of the shear stress values at points E-I. The shear deformation is defined as the relative shear displacement of points A-D and B-C in a direction parallel to the joint. This implies that the parallel deformation includes deformation of the joint and intact rock material between point A-D and B-C.

(ii) Average mechanical and conducting aperture versus average shear displacement along the joint. All values are average values at points E-I.

(iii) Flow rate at the outlet point (E) as a function of average shear displacement along the joint.

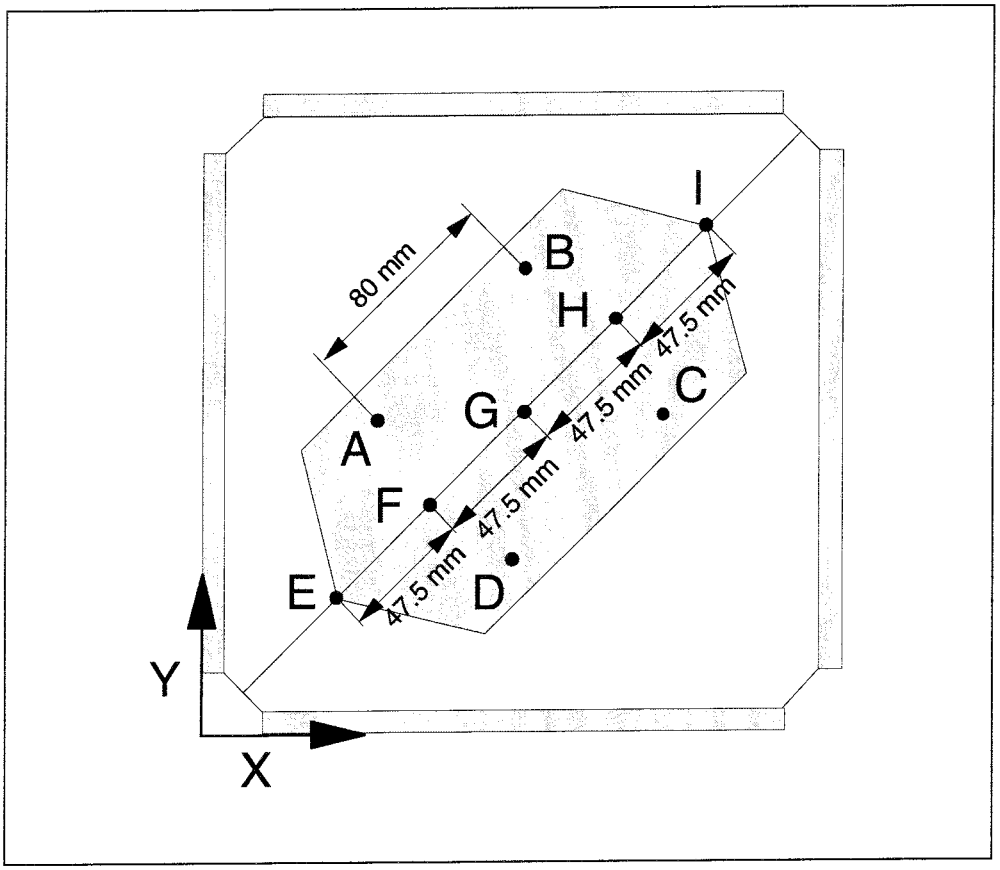

Figure 6-1 *Monitoring point locations.*

3. Plots provided directly from UDEC. The following UDEC plots are presented for each option:

Loading Sequence A; (i) Model geometry prior to loading of the entire model including finite difference zone discretisation

(ii) Vector plot of principal stresses for the case of 25 MPa boundary loading

Loading Sequence B; (i) Model geometry prior to loading of the entire model including finite difference zone discretisation

(ii) Vector plots of principal stresses at 0.0, 0.8 and 4.0 mm forward shearing

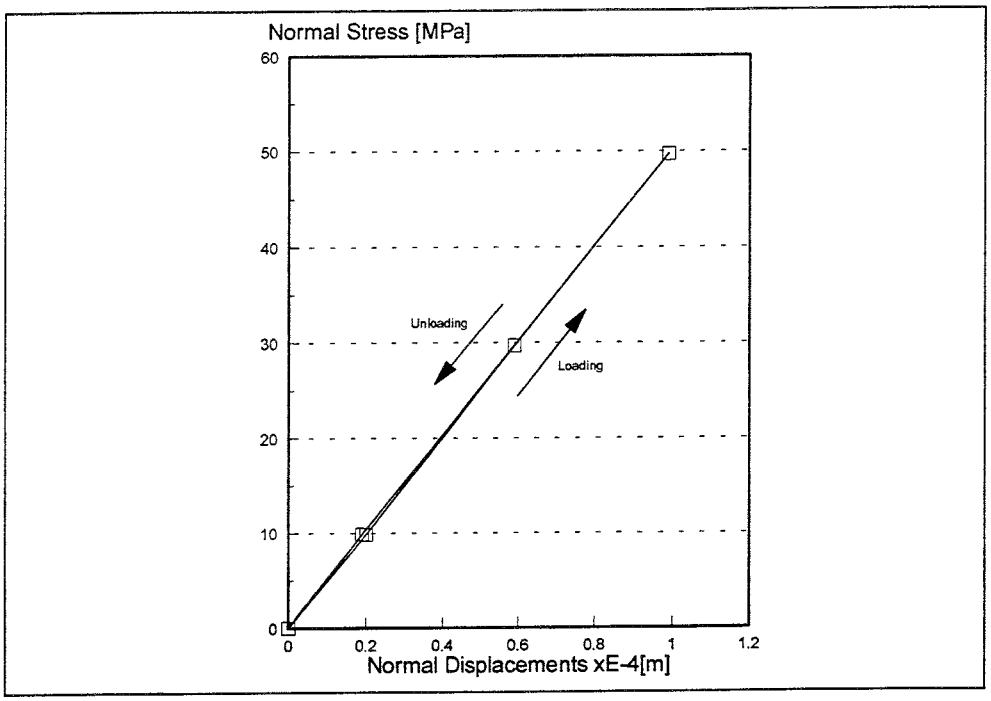

Figure 6-2. *Average normal stress versus the average orthogonal deformation across the joint at points A-D and B-C, Option 1, Loading Sequence A.*

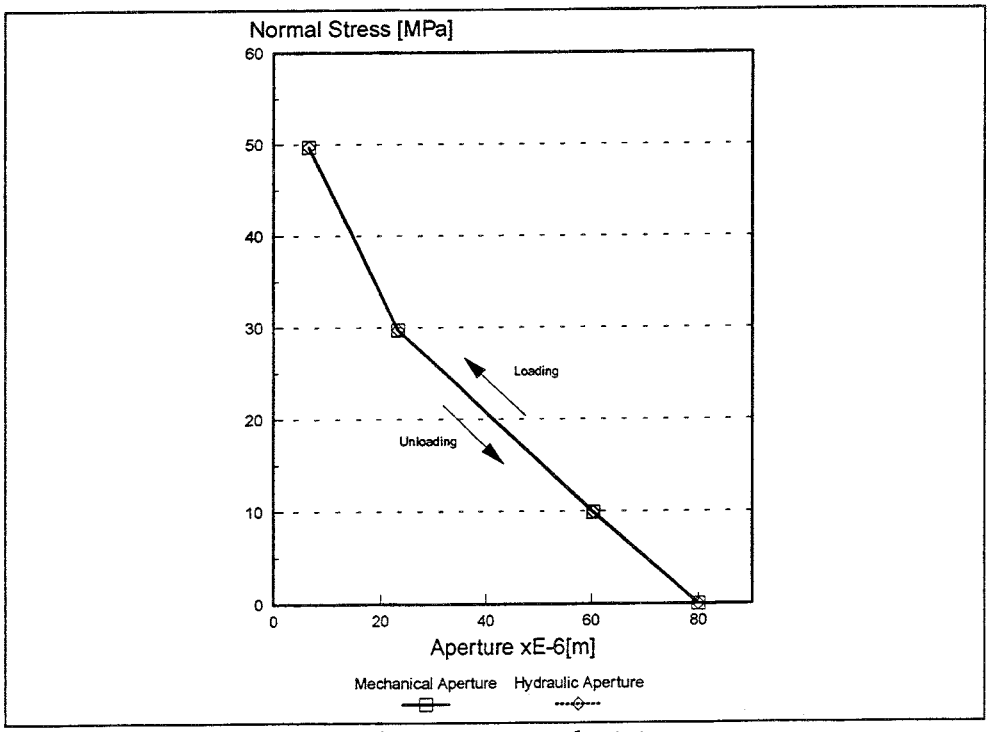

Figure 6-3. *Average normal stress across the joint versus average mechanical and conducting aperture at points E-I, Option 1, Loading Sequence A*

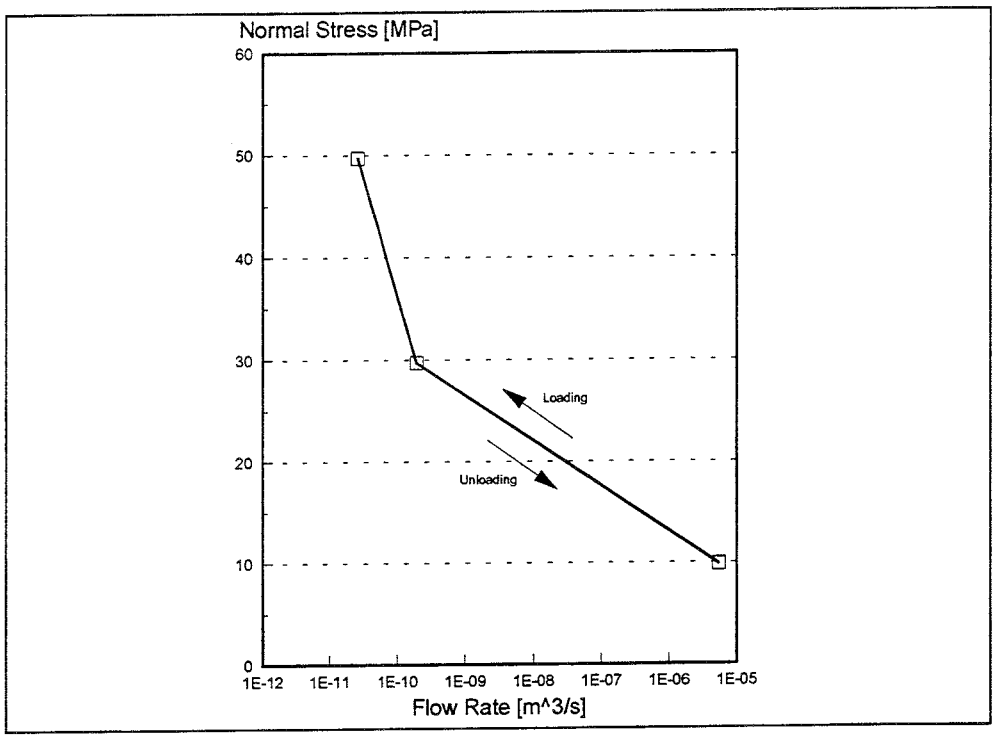

Figure 6-4. *Average normal stress across the joint versus flow rate at the outlet point (E), Option 1, Loading Sequence A.*

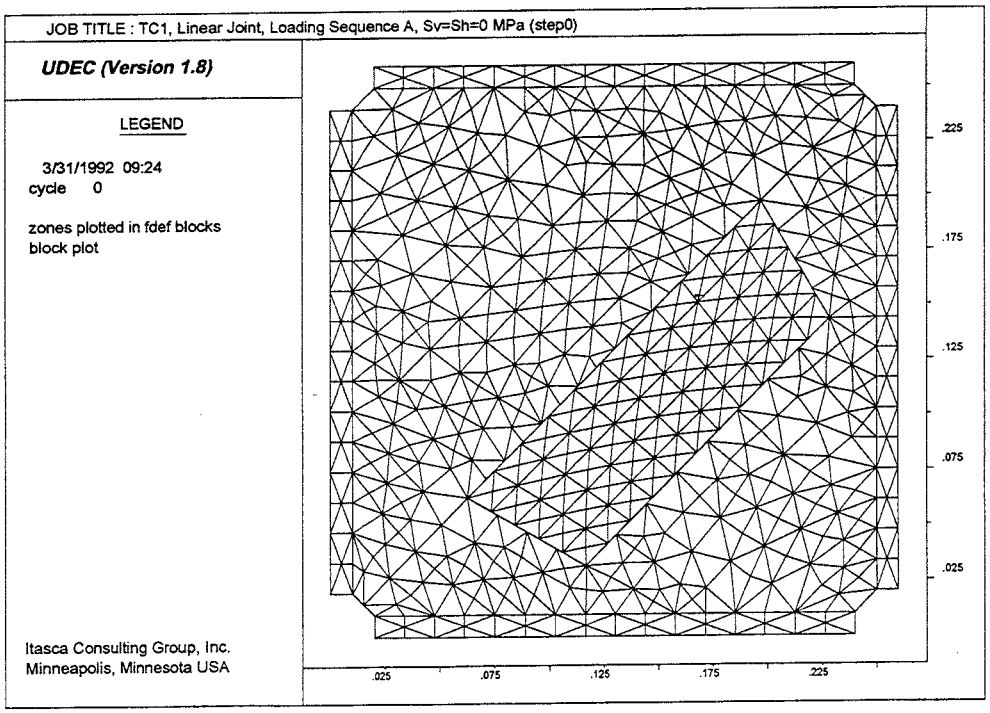

Figure 6-5. *Model goemetry prior to loading of the entire model including finite difference zone discretisation, Option 1, Loading Sequence A.*

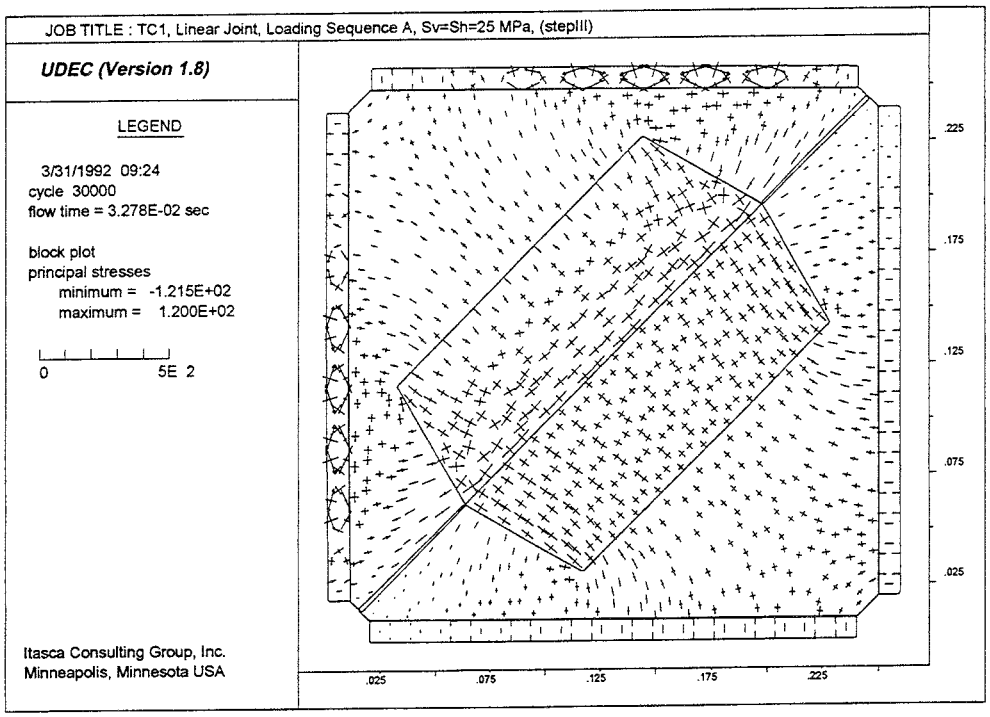

Figure 6-6. *Principal stress vectors for the case of 25 MPa boundary loading, Option 1, Loading Sequence A.*

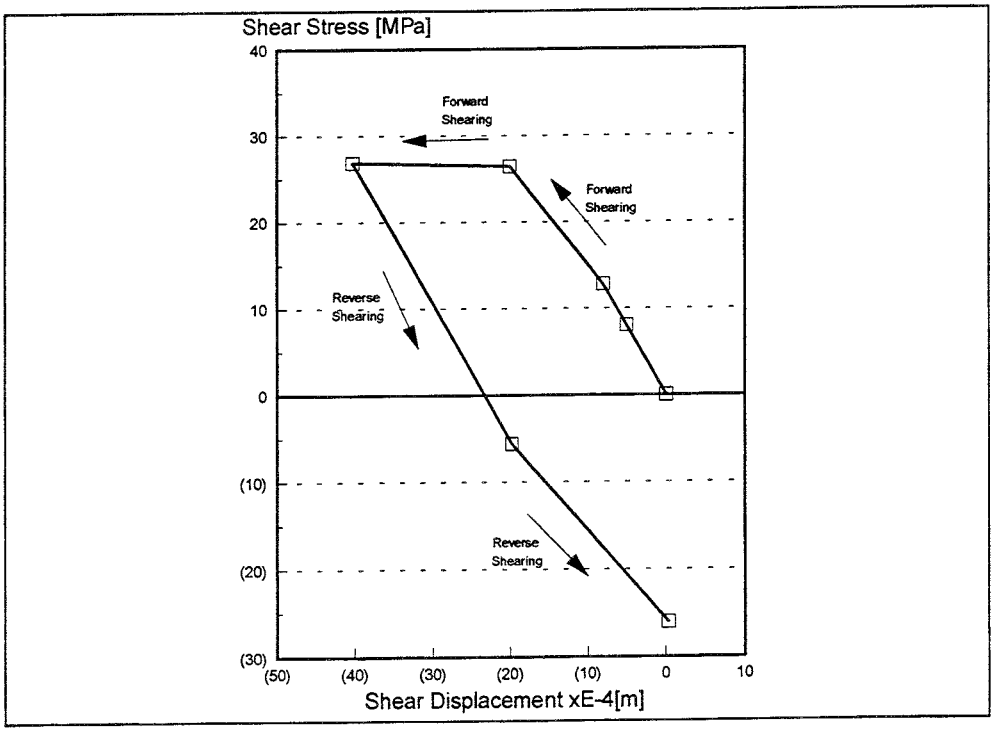

Figure 6-7. *Average shear stress along the joint versus the average shear deformation between points A-D and B-C, Option 1, Loading Sequence B.*

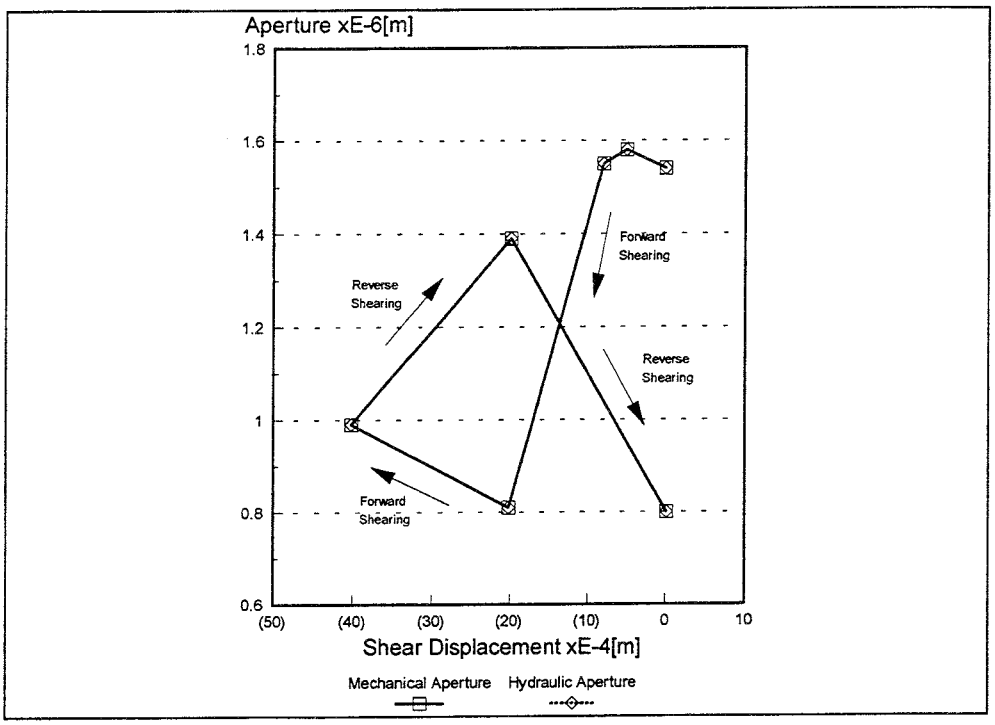

Figure 6-8. *Average mechanical and conducting aperture versus average shear displacement along the joint at points E-I, Option 1, Loading Sequence B.*

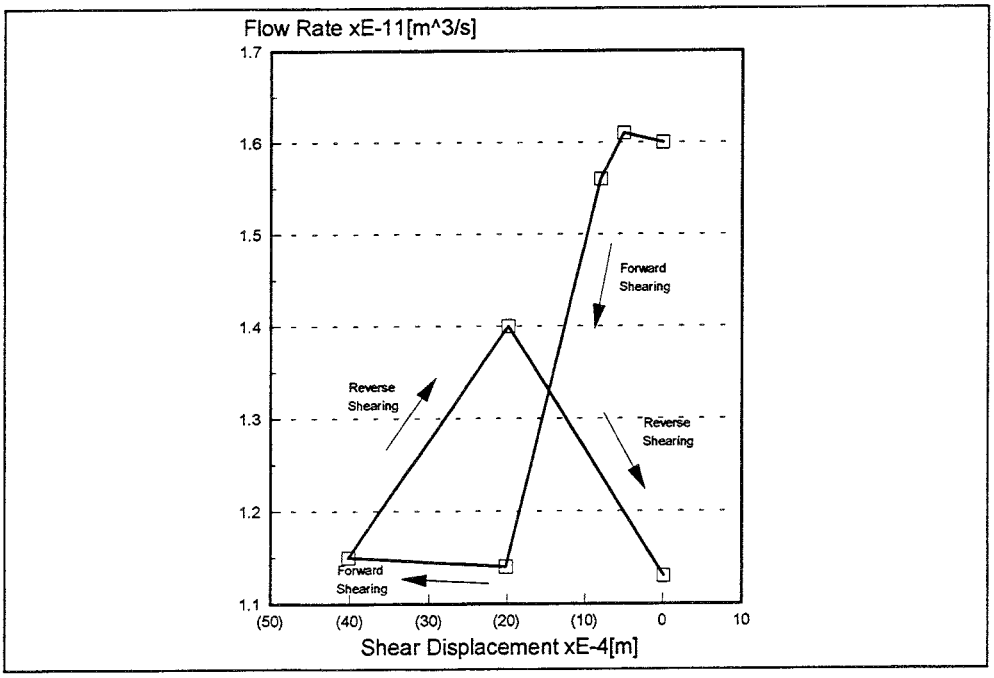

Figure 6-9. *Flow rate at the outlet point (E) versus average shear displacement along the joint, Option 1, Loading Sequence B.*

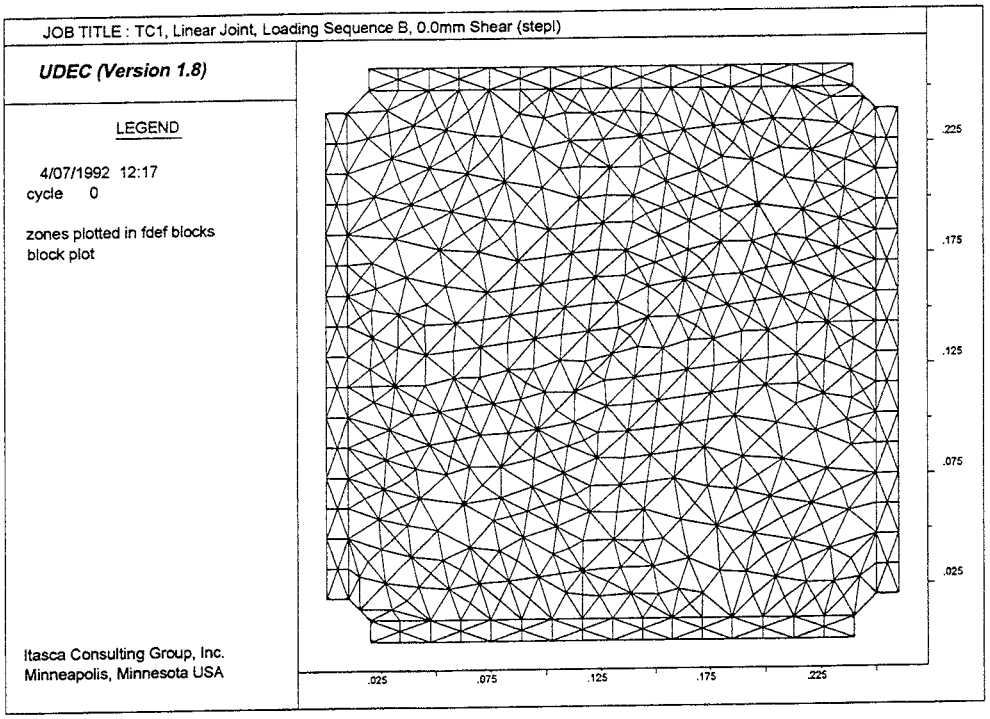

Figure 6-10. *Model geometry prior to loading of the entire model including finite difference zone discretisation, Option 1, Loading Sequence B.*

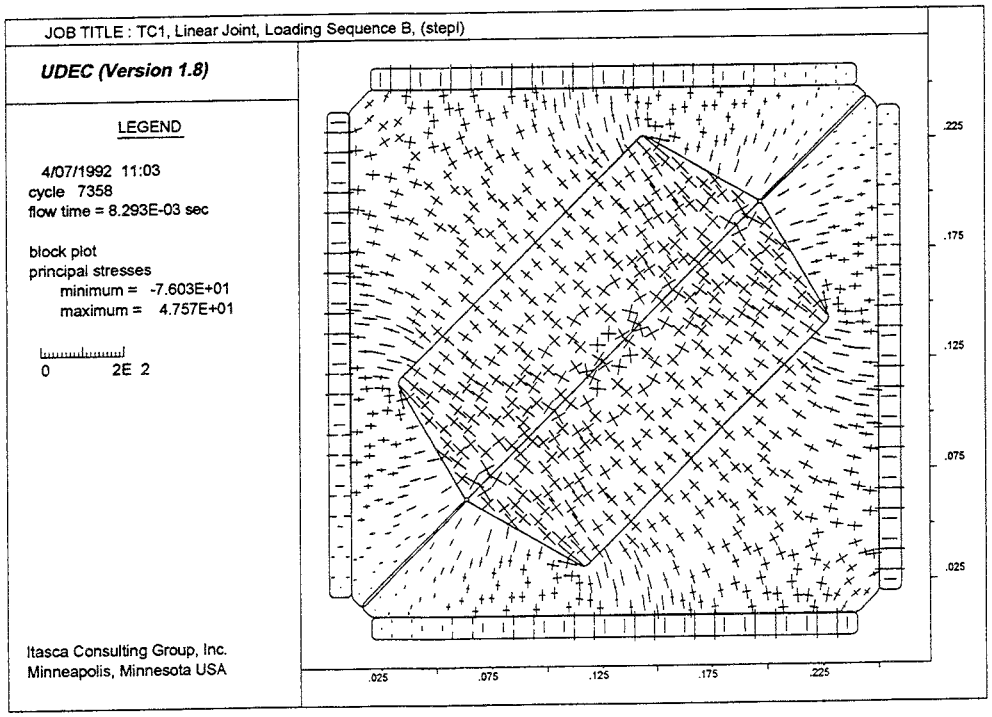

Figure 6-11. *Principal stress vectors at 0.0 mm forward shearing, Option 1, Loading Sequence B.*

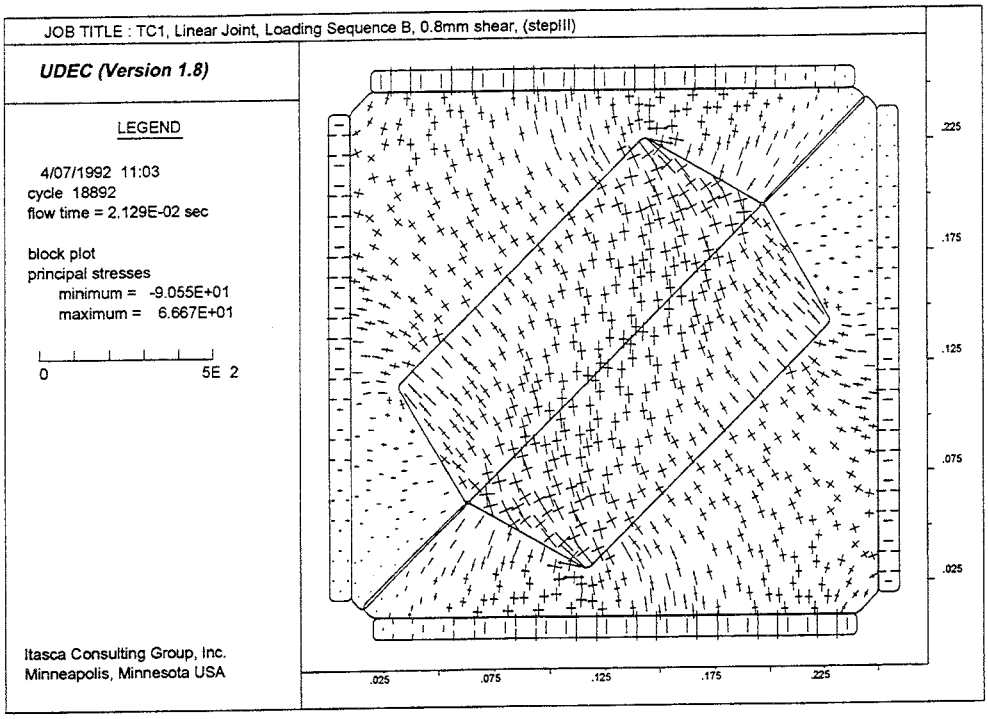

Figure 6-12. *Principal stress vectors at 0.8 mm forward shearing, Option 1, Loading Sequence B.*

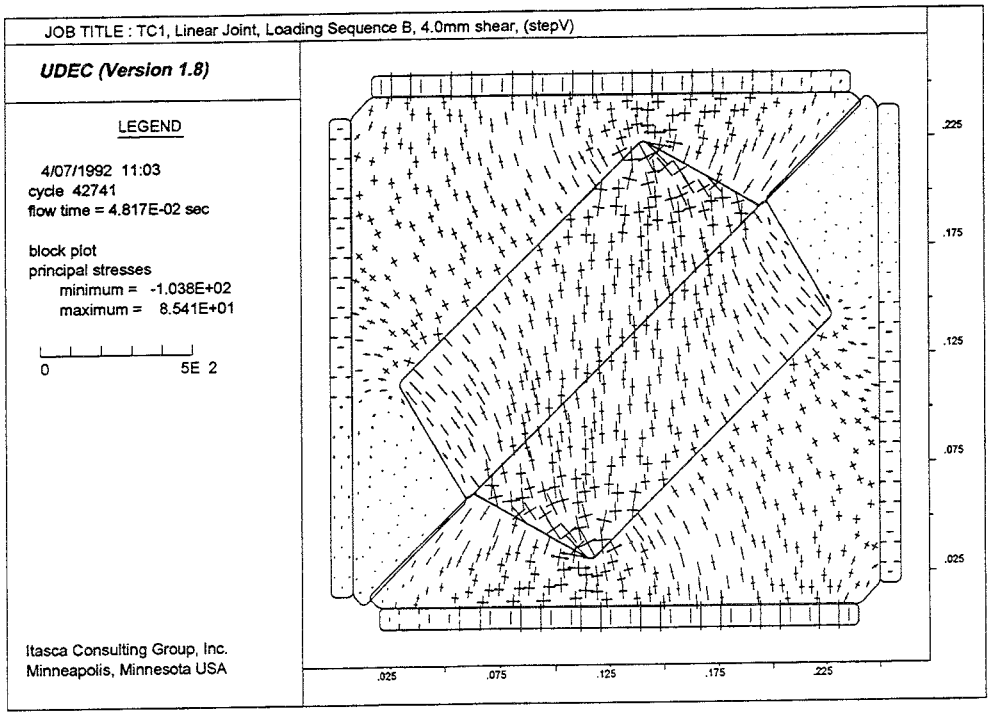

Figure 6-13. *Principal stress vectors at 4.0 mm forward shearing, Option 1, Loading Sequence B.*

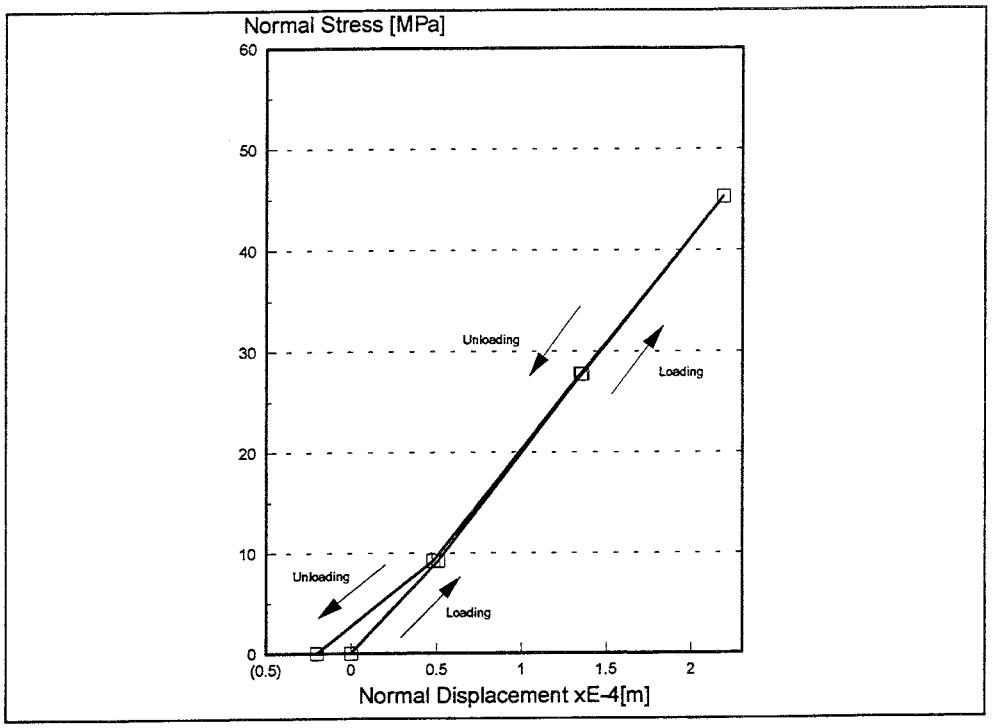

Figure 6-14. *Average normal stress versus the average orthogonal deformation across the joint at points A-D and B-C, Option 2, Loading Sequence A.*

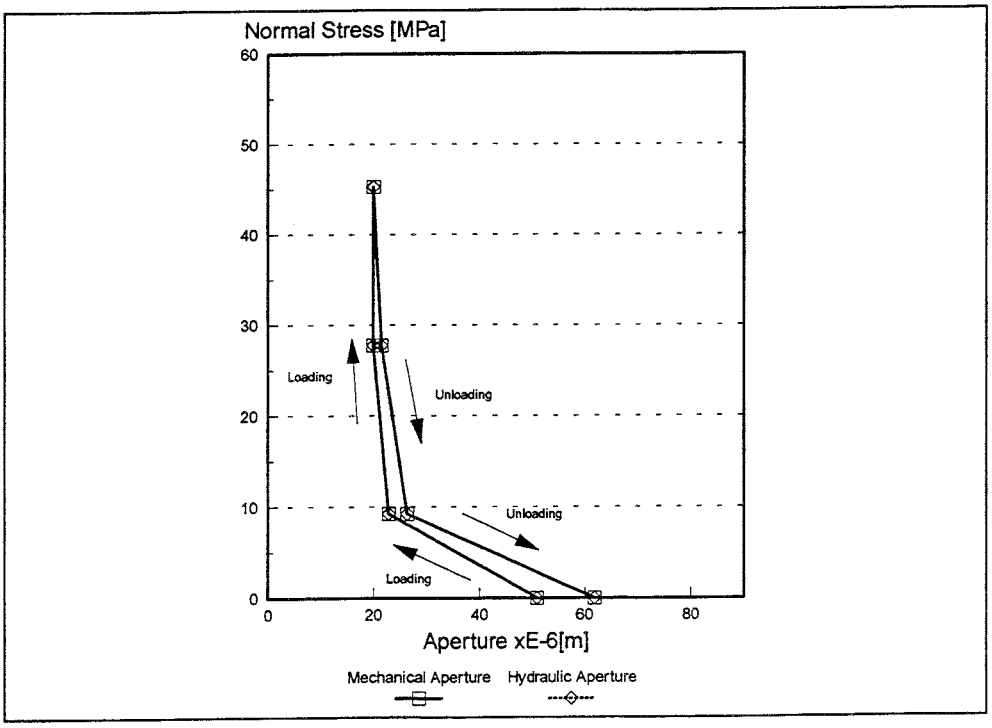

Figure 6-15. *Average normal stress across the joint versus average mechanical and conducting aperture at points E-I, Option 2, Loading Sequence A.*

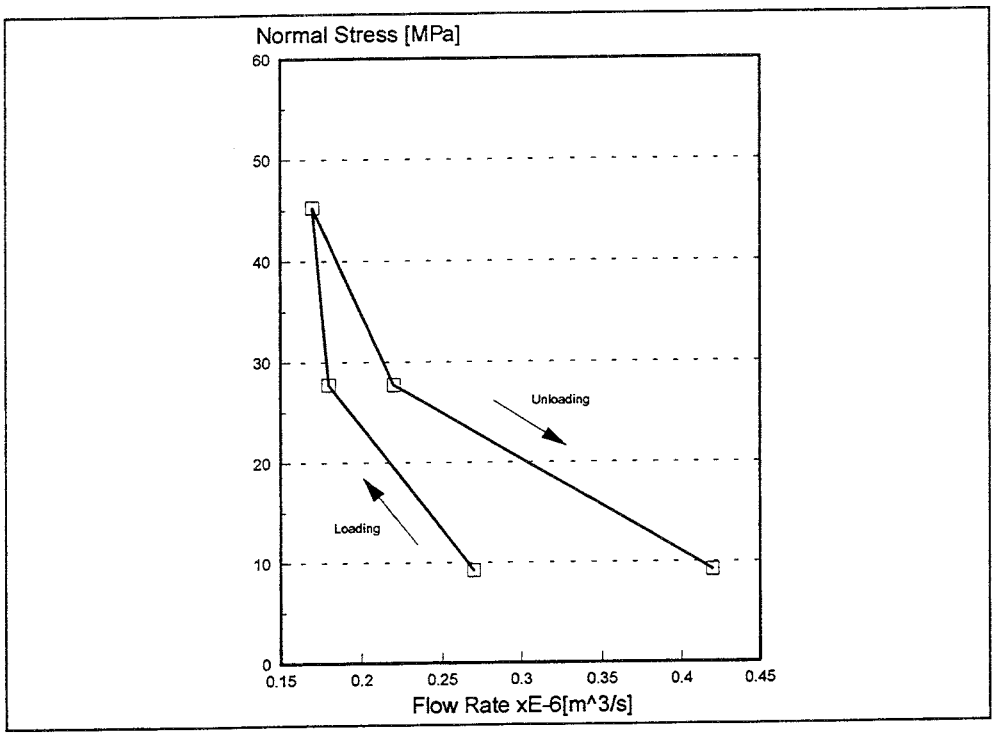

Figure 6-16. *Average normal stress across the joint versus flow rate at the outlet point (E), Option 2, Loading sequence A.*

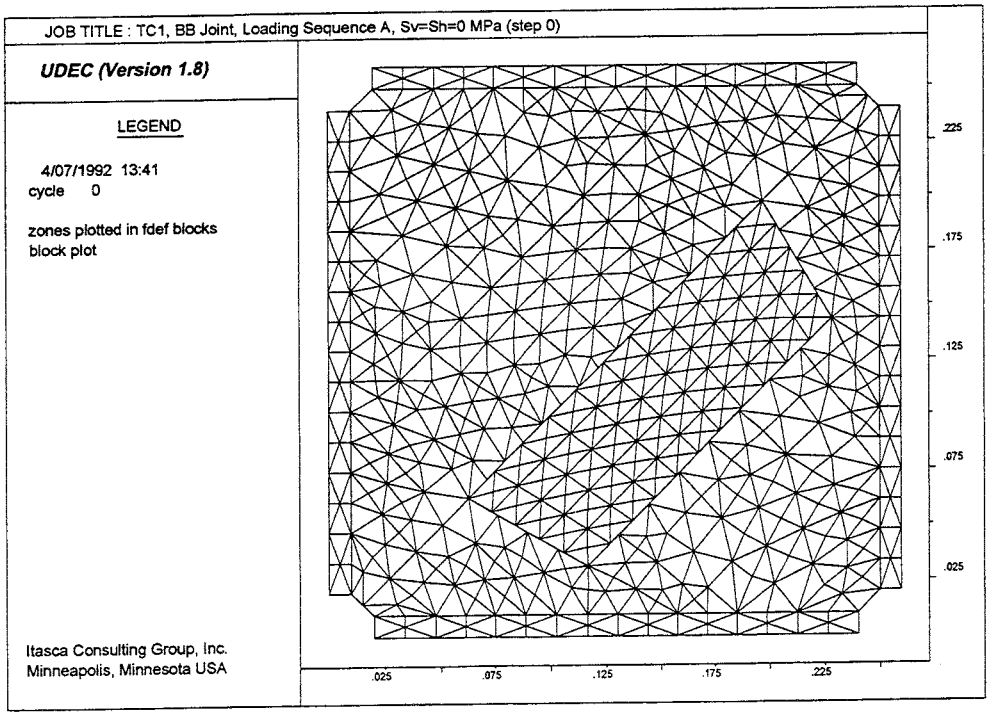

Figure 6-17. *Model goemetry prior to loading of the entire model including finite difference zone discretisation, Option 2, Loading Sequence A.*

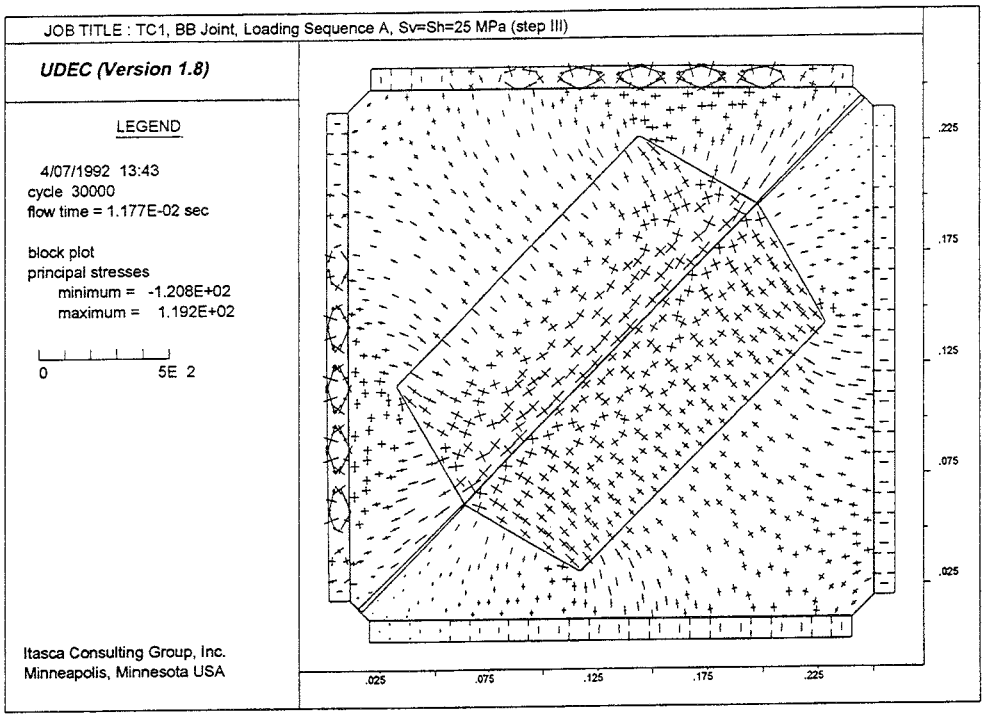

Figure 6-18. *Principal stress vectors for the case of 25 MPa boundary loading, Option 2, Loading Sequence A.*

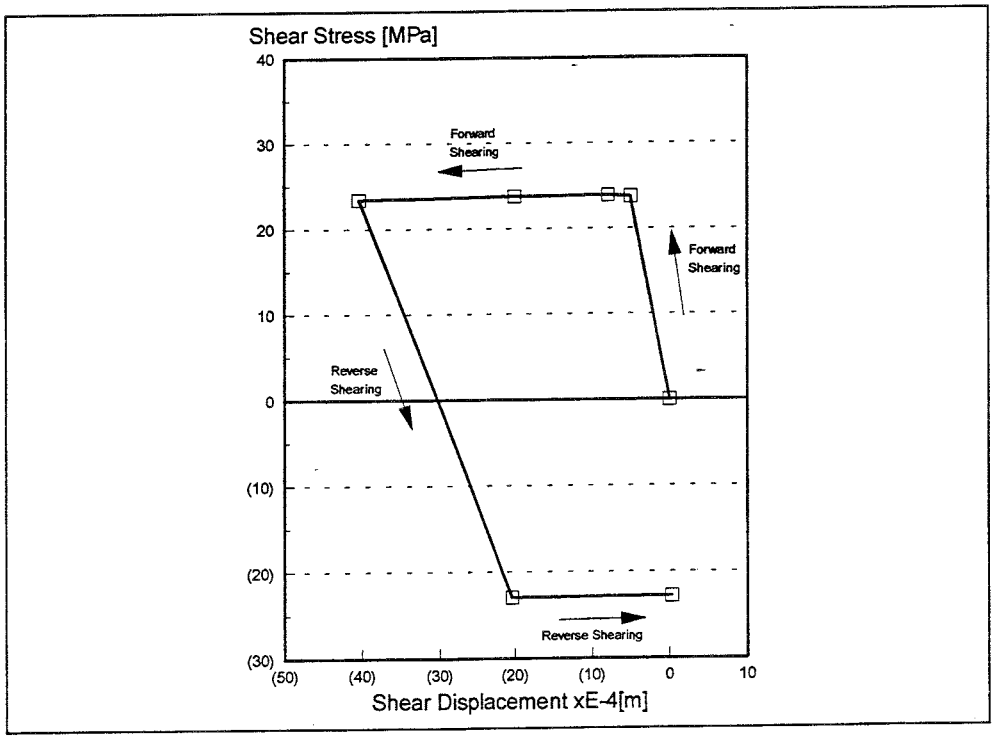

Figure 6-19. *Average shear stress along the joint versus the average shear deformation between points A-D and B-C, Option 2, Loading Sequence B.*

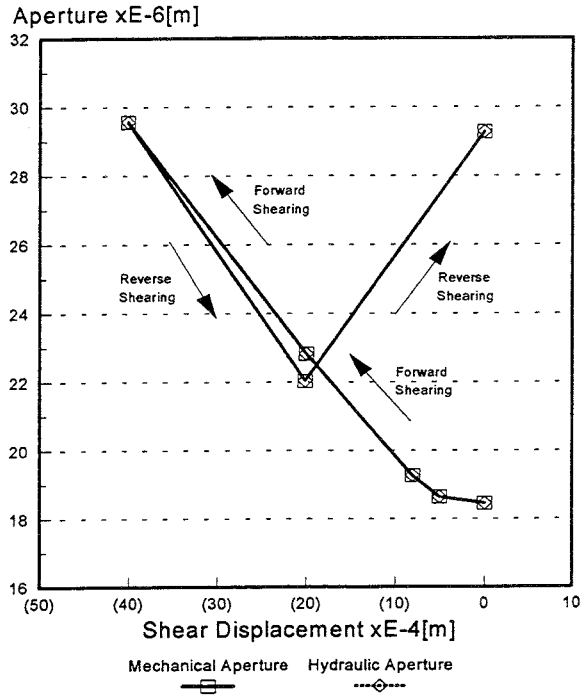

Figure 6-20. *Average mechanical and conducting aperture versus average shear displacement along the joint at points E-I, Option 2, Loading Sequence B.*

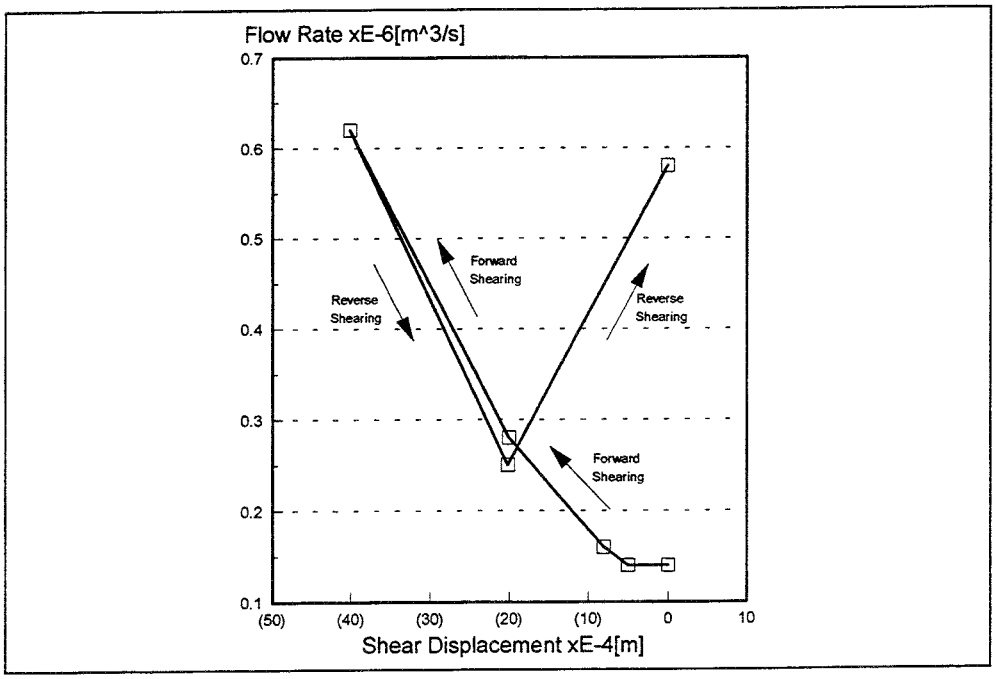

Figure 6-21. *Flow rate at the outlet point (E) versus average shear displacement along the joint, Option 2, Loading Sequence B.*

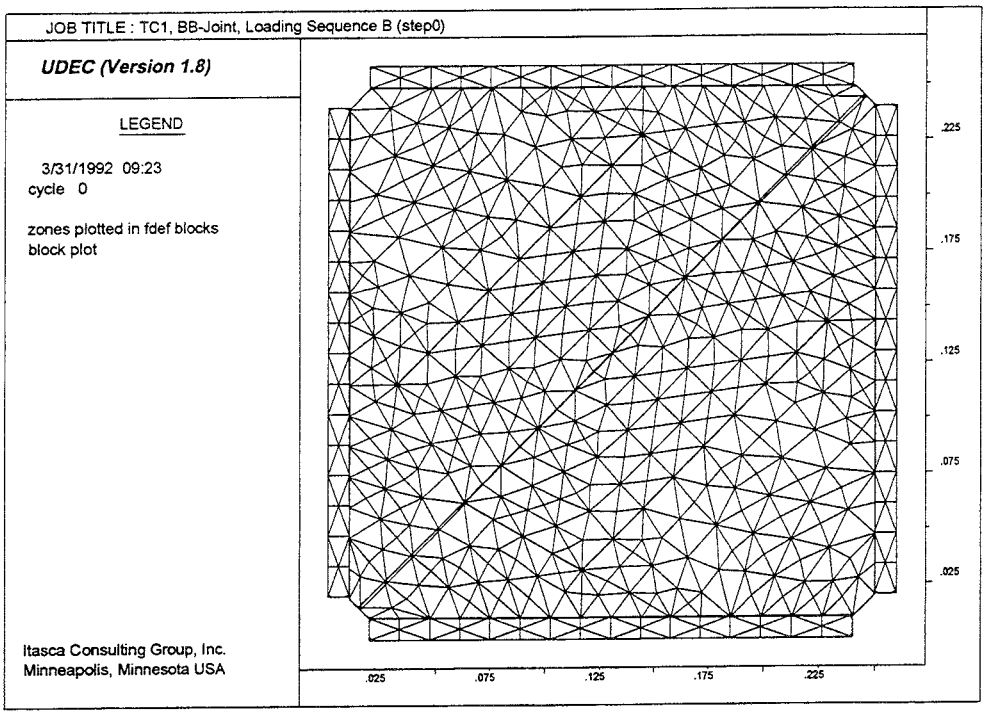

Figure 6-22. *Model geometry prior to loading of the entire model including finite difference zone discretisation, Option 2, Loading Sequence B.*

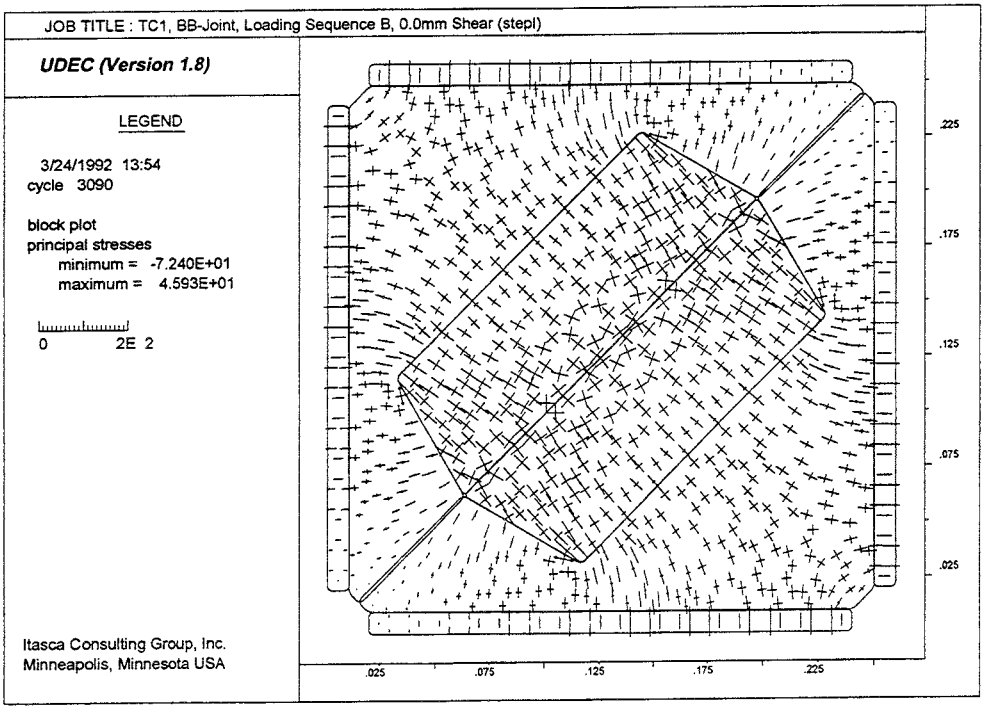

Figure 6-23. *Principal stress vectors at 0.0 mm forward shearing, Option 2, Loading Sequence B.*

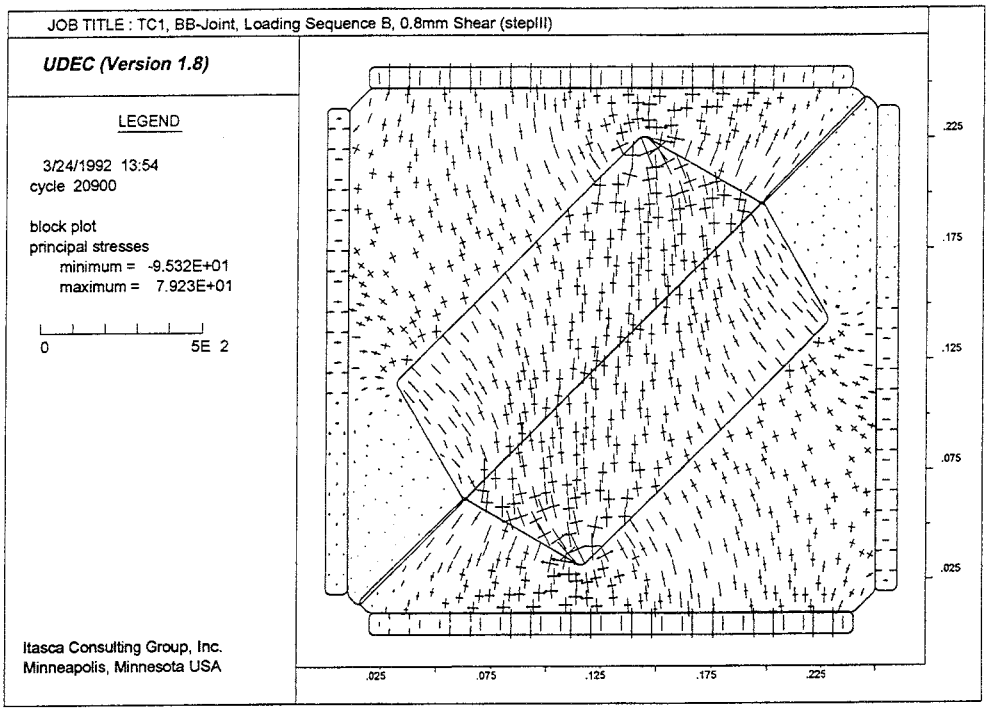

Figure 6-24. *Principal stress vectors at 0.8 mm forward shearing, Option 2, Loading Sequence B.*

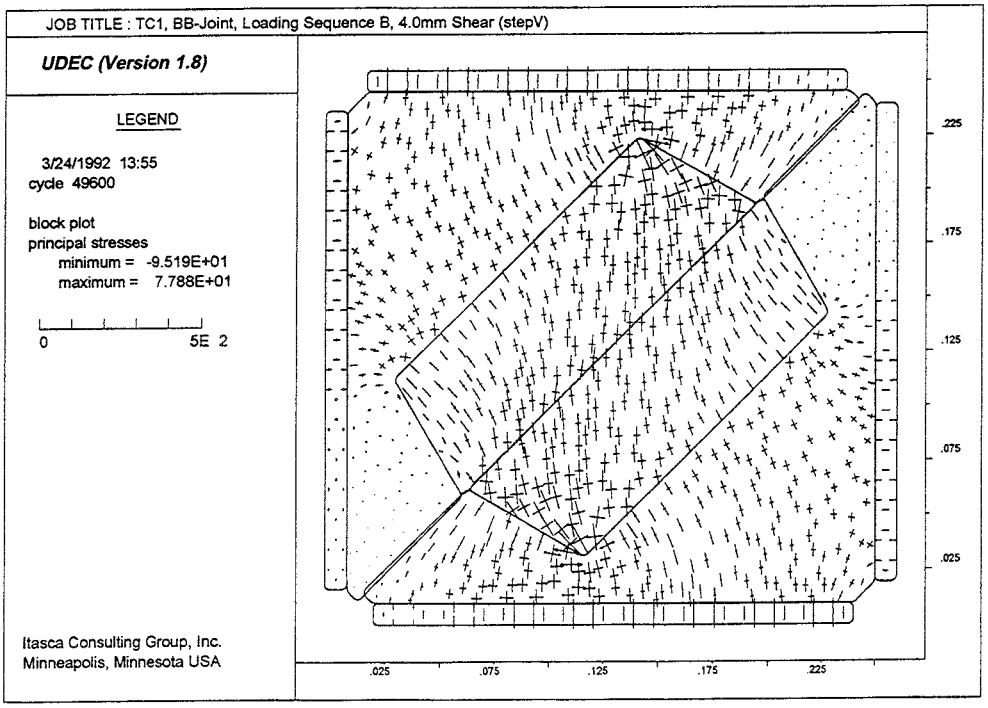

Figure 6-25. *Principal stress vectors at 4.0 mm forward shearing, Option 2, Loading Sequence B.*

6.2 Additional Results

In this section additional results are presented. Table 6.1 gives a description of the plots presented here.

Table 6.1 Description of additional plots

PLOT	FIGURE
Normal stress distribution along joint at 25 MPa boundary loading, Option 1, Loading Sequence A.	6.26 (a)
Normal stress distribution along joint at 25 MPa boundary loading, Option 2, Loading Sequence A.	6.26 (b)
Hydraulic aperture distribution along joint at 25 MPa boundary loading, Option 1, Loading Sequence A.	6.27 (a)
Hydraulic aperture distribution along joint at 25 MPa boundary loading, Option 2, Loading Sequence A.	6.27 (b)
Normal stress distribution along joint at 0.0 mm shear, Option 1, Loading Sequence B.	6.28 (a)
Normal stress distribution along joint at 0.0 mm shear, Option 2, Loading Sequence B.	6.28 (b)
Hydraulic aperture distribution along joint at 0.0 mm shear, Option 1, Loading Sequence B.	6.29 (a)
Hydraulic aperture distribution along joint at 0.0 mm shear, Option 2, Loading Sequence B.	6.29 (b)
Average normal stress on joint versus average shear displacement along joint for Option 1 and 2, Loading Sequence B.	6.30

(a)

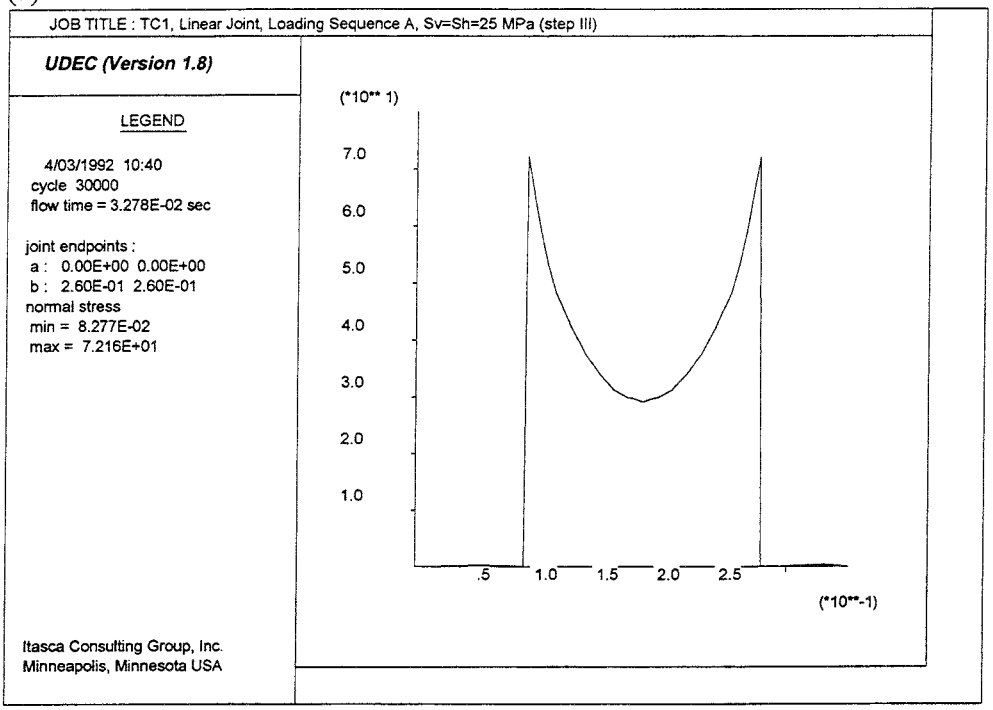

(b)

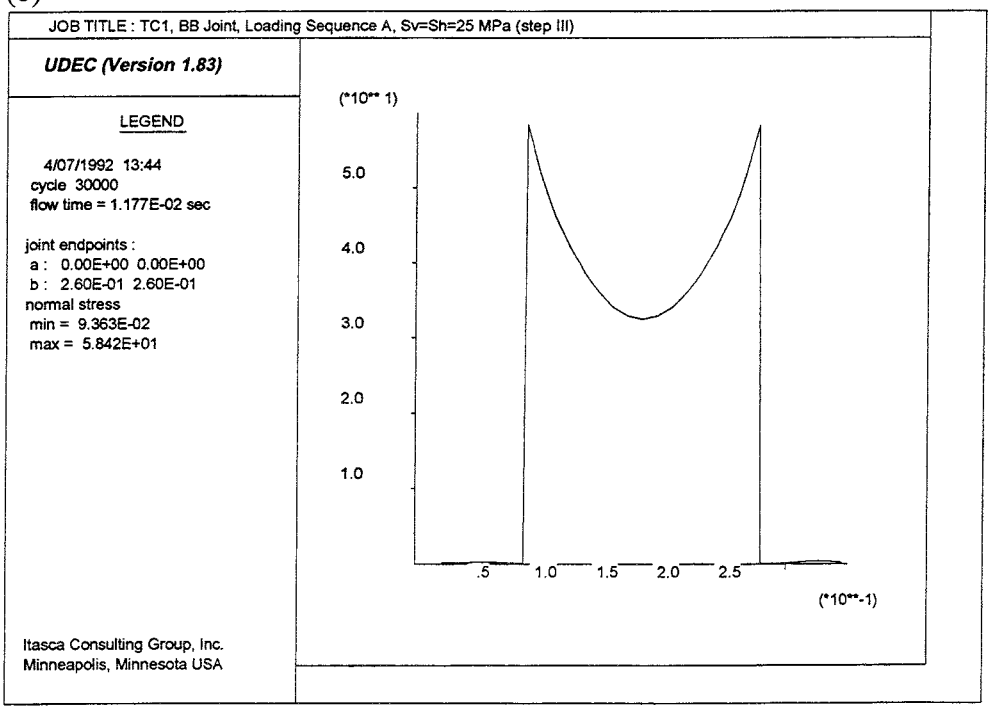

Figure 6-26. *Normal stress distribution along joint at 25 MPa boundary loading, Loading Sequence A: (a) Option 1; (b) Option 2.*

(a)

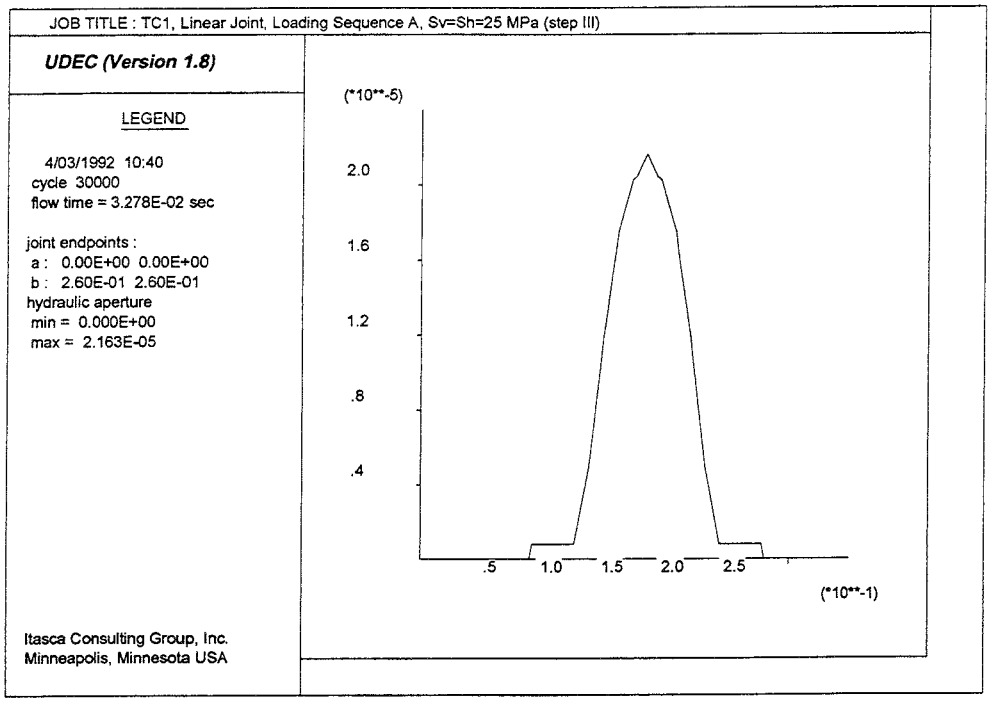

(b)

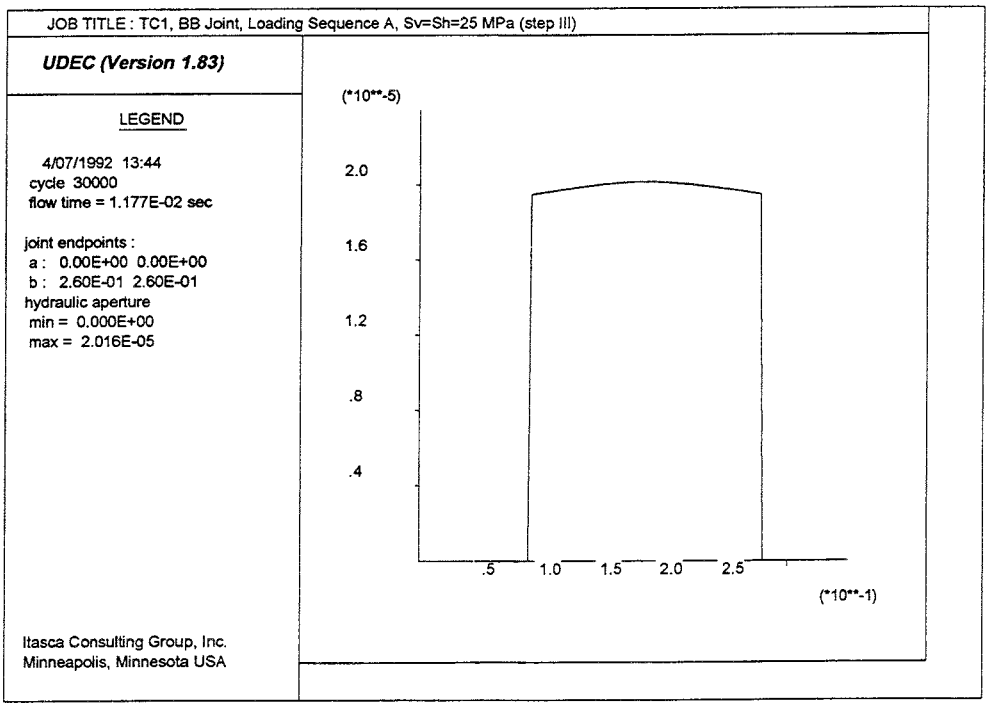

Figure 6-27. *Hydraulic aperture distribution along joint at 25 MPa boundary loading, Loading Sequence A: (a) Option 1; (b) Option 2.*

(a)

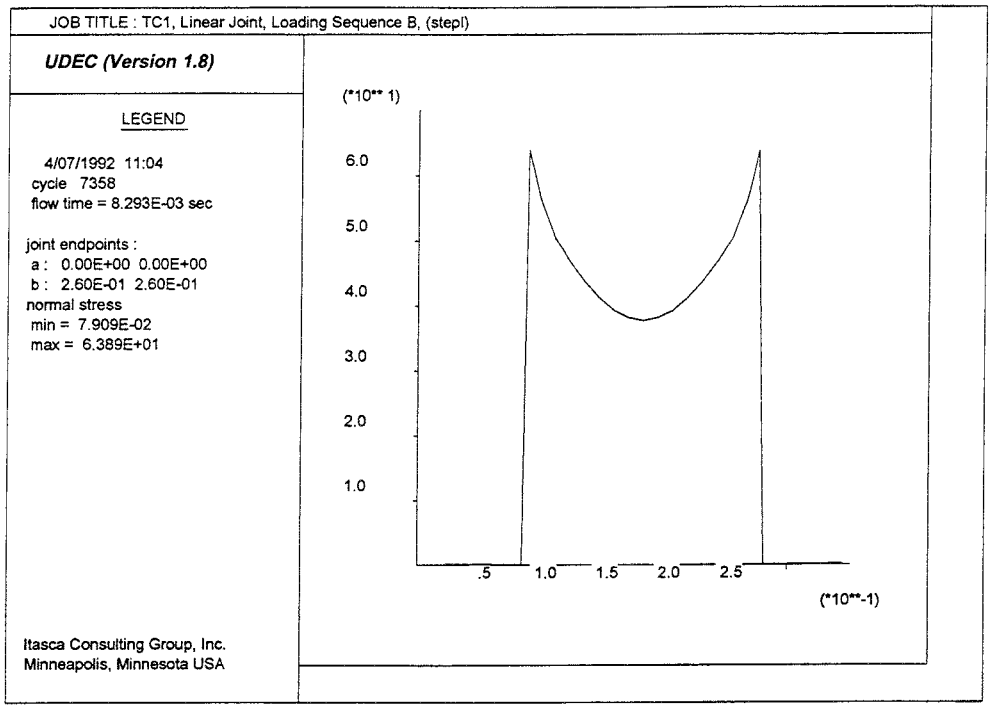

(b)

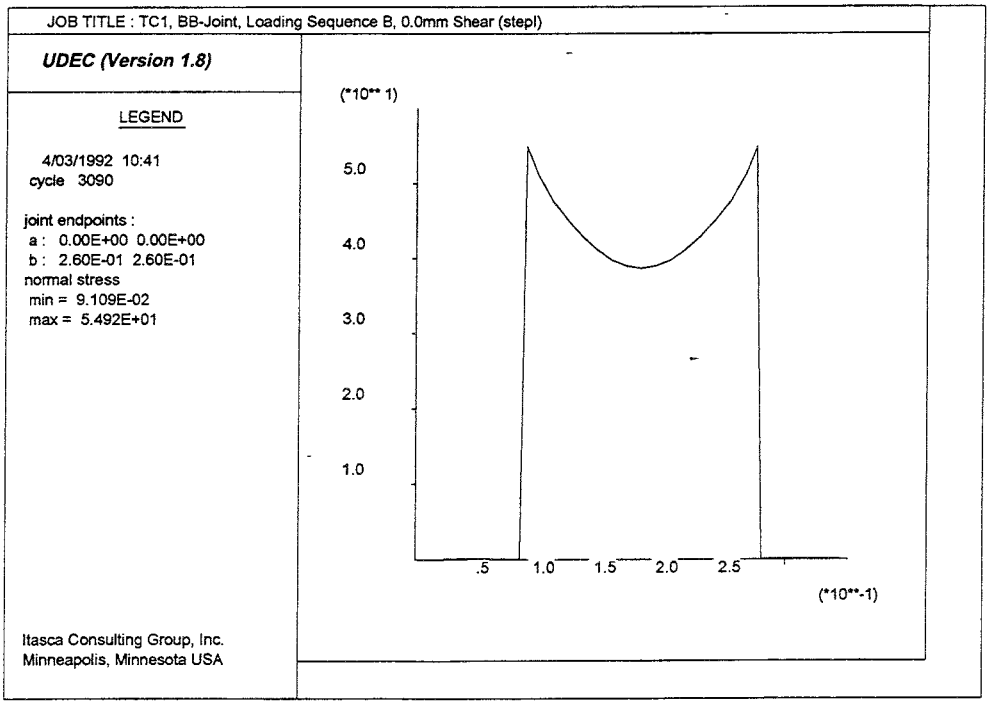

Figure 6-28. *Normal stress distribution along joint at 0.0 mm shear, Loading Sequence B: (a) Option 1; (b) Option 2.*

(a)

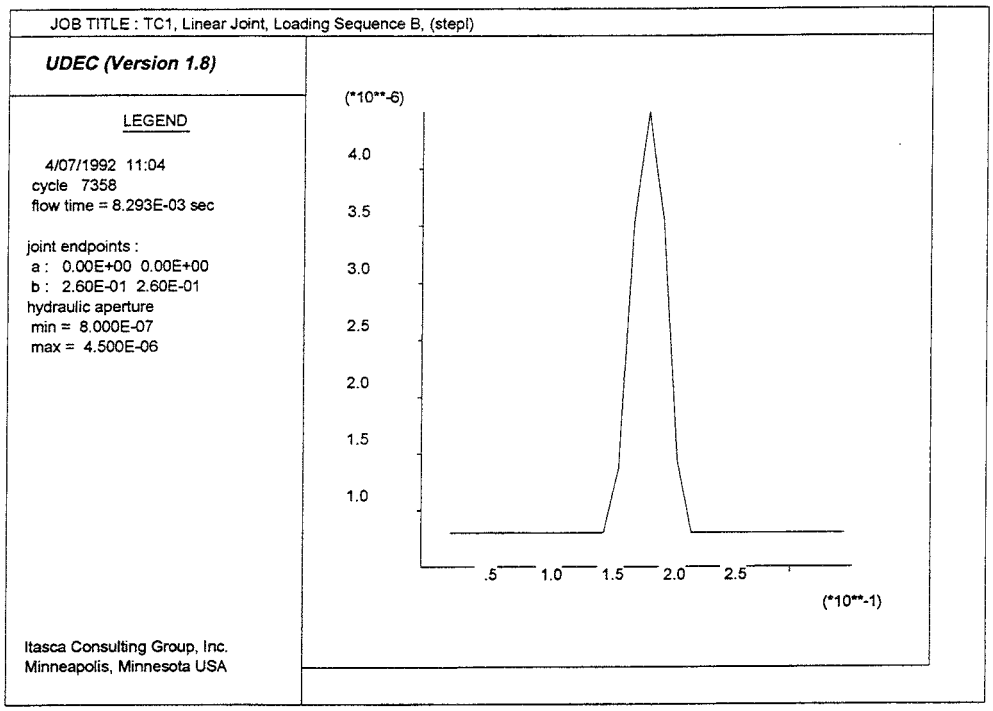

(b)

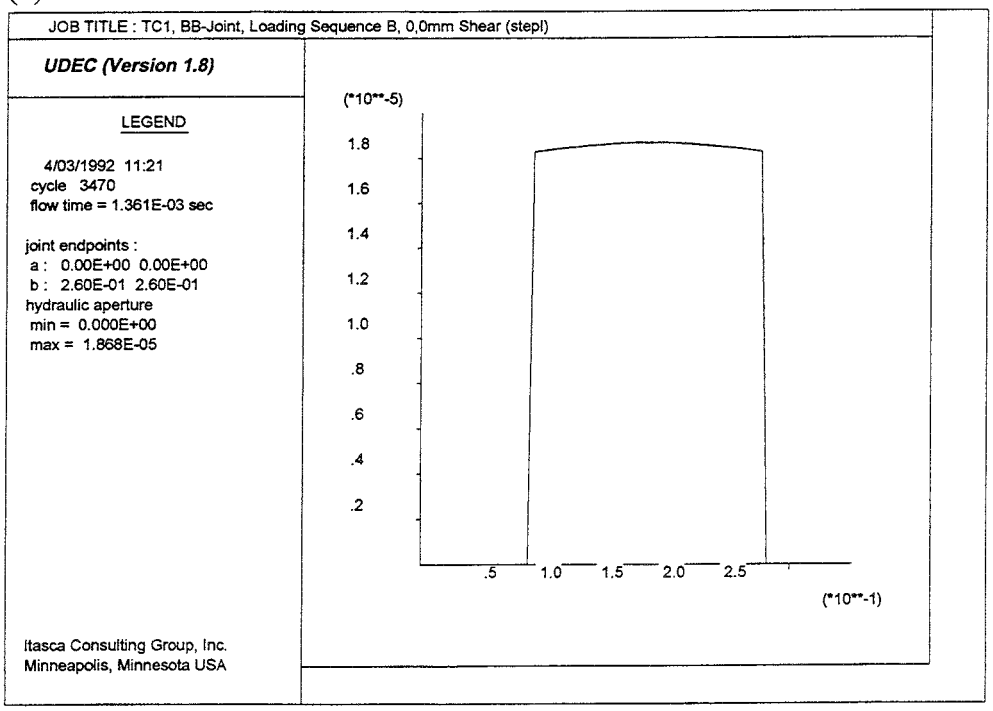

Figure 6-29. *Hydraulic aperture distribution along joint at 0.0 mm shear, Loading Sequence B: (a) Option 1; (b) Option 2*

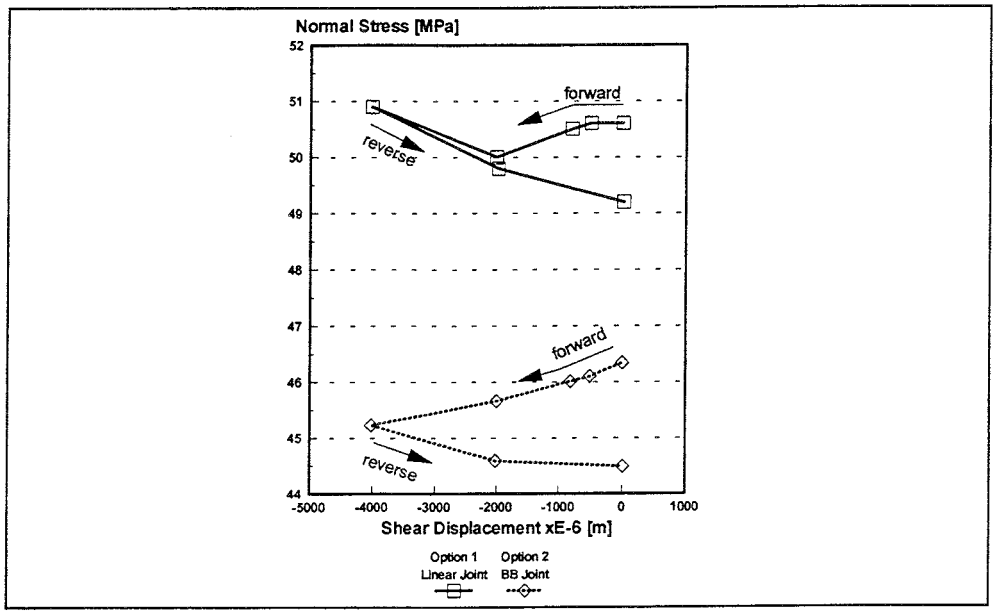

Figure 6-30. *Average normal stress versus average shear displacement along joint for Options 1 and 2.*

7 DISCUSSION OF THE RESULTS

7.1 General For Option 1 and 2

The results of the modeling raise the following interesting general points for Option 1 and 2:

1. A stress boundary condition cannot be used to determine post peak behavior. If a load (or stress) boundary condition is used in a laboratory test, the post peak data recorded will be wrong if the loading mechanism has a lower stiffness than the failure curve of the specimen. In this case the data will reflect the loading mechanism and not the specimen. In a numerical simulation with a stress boundary condition the loading mechanism has no stiffness at all so the applied load will not drop off due to sample displacement. Also, if a stress boundary is used in a shear experiment, the shear force generated along the joint surface will have to be balanced by a change in the distribution of joint normal stress.

2. The normal stress along the joint is not the same at all monitoring locations. This is due to the bending in the epoxy itself and, the lower stiffness in the epoxy-epoxy interface. The normal stress distribution for Option 1, Loading Sequence A, (at 25 MPa boundary loading) and B (at 0.0 mm shear) is shown in Fig 6-26 (a) and 6-28 (a) respectively. As can be seen from these figures the stress distribution along the joint is different, however the average normal stress is the same. The difference in normal stress distribution is due to the different boundary conditions used for the two models. Stress boundaries have been applied to the Loading Sequence A model, whereas displacement boundaries have been used for Loading Sequence B. Stress boundaries give more bending in the model compared to the model with displacement boundaries. This larger bending results in larger difference in stress between the joint ends and the middle of the joint. A higher normal stress results in a smaller aperture at the ends of the joint. The ends of the joint will control the flow rate for the entire joint. This will lead to errors if the flow rate is used to determine an average joint aperture.

3. Neither of the models induce an average normal stress of 25 MPa at 25 MPa boundary loading as indicated in the problem definition. This is mainly due to the fact that the model is loaded over its whole boundary, while in reality, the flat jacks only load the portion of the boundary which corresponds to the projection of the specimen.

4. Figure 6-30 shows the average normal stress versus average shear displacement along the joint. As can be seen from this figure, the average normal stress could be held fairly constant during the shearing sequence for both Option 1 and 2. The difference is less than 2 MPa or roughly 4%. The lower stress level in Option 2 is due to the way average stress is calculated. The average is calculated using only points E-I. This gives too much weight to the stress peaks at the ends of the joint. The distribution of stresses for Option 1 and Option 2 are different because of different joint normal stiffness. However, a proper average should result in the same average stress level.

   The slight change in normal stress along the joint during the shearing sequence is the reason for the changes in aperture and flow mentioned in item 2., section 7.2 below.

7.2 Specific For Option 1

The results of this modeling raise the following interesting points for Option 1:

1. The joint closes to its residual aperture at the ends for all loading steps except for the case of 5 MPa normal boundary loading.

2. When shearing a non-dilatant joint as in this problem, the joint apertures should remain constant during the shearing sequence. However, in the model presented here, a slight change (< 1 μm) in the average aperture occurs resulting in a slight change in flow rate. If the flow rates are plotted in the same scale as for Option 2, they will appear constant. Consequently, this minor change in aperture and flow rates can essentially be considered as noise.

7.3 Specific For Option 2

The results of this modeling raise the following interesting points for Option 2:

1. For Loading Sequence B displacement boundary condition was used. However, displacement boundary condition has drawbacks as well. A displacement boundary will result in less bending of the sample and thus a different normal stress distribution along the joint. Also, it is more difficult to maintain a constant normal stress if the joint is dilatant. A component of normal displacement must be estimated and removed during shear. The sample is not allowed to rotate when a displacement boundary is used so that any change in normal stress distribution caused by rotation may not be evident.

2. The use of a relatively low joint stiffness limit (200 GPa/m) produces a more constant stress distribution along the joint compared to Option 1 where a joint stiffness of 500 GPa/m was used, see Fig 6-26 a) and b).

3. In the Barton-Bandis joint model implementation in UDEC the joint dilation is a function of the shear displacement and the mobilized roughness. It does not take into account displacement from the original start point during shear reversal. This results in the dilation being recovered immediately upon shear reversal since the mobilized roughness goes to zero. The dilation is then accumulated during the reverse shear displacement and is nearly the same as at the end of the original 4.0 mm shear.

8 RECOMMENDATIONS

1. The boundary conditions for, Loading Sequence B, should be specified. The boundary condition suggestions included in the definition of the test were not compatible with the requested results. This will lead to different modeling groups using different assumptions to model the boundaries. The different boundary conditions will lead to different results in the simulated rock joint behavior.

2. There should be some mechanism in place to allow the various groups to compare assumptions and results prior to final reporting. This would help to ensure that the same problem is being solved by all participants.

3. Examples of the requested output plots and diagrams would be useful to allow a consistent reporting format.

4. If the Epoxy-Epoxy interface is actually supposed to be a gap, it should be modelled as a gap. Currently, it is defined as a very soft interface.

9 REFERENCES

Barton, N., 1982. "Modeling Rock Joint Behavior from In Situ Block Tests: Implications for Nuclear Waste Repository Design," Technical Report ONWI-308.

Barton, N., S. Bandis and K. Bakhtar, 1985. "Strength, Deformation and Conductivity Coupling of Rock Joints," Int. J. Rock Mech. Min. Sci. & Geomech. Abstr., 22(3), 121-140.

Board, M., 1989. "UDEC (Universal Distinct Element Code) Version ICG1.5," Vols. 1-3. U.S. NRC, NUREG/CR-5429, September.

Brady, B.H.G., M. L. Cramer and R. D. Hart, 1985. "Preliminary Analysis of a Loading Test on a Large Basalt Block," Int. J. Rock Mech., 22(5), 345-348.

Brady, B.H.G., S. M. Hsiung and A. H. Chowdhury, 1990a. "Qualification Studies on the Distinct Element Code UDEC Against Some Benchmark Analytical Problems," CNWRA Report to U.S. NRC, CNWRA 90-004, January.

Brady, B. H., S. H. Hsiung, A. H. Chowdhury and J. Philip, 1990b. "Verification Studies on the UDEC Computational Model of Jointed Rock," in Mechanics of Jointed and Faulted Rock, pp. 551-558. Rotterdam: A. A. Balkema.

Christianson, M., 1989. "Sensitivity of the Stability of a Waste Emplacement Drift to Variation in Assumed Rock Joint Parameters in Welded Tuff," U.S. Nuclear Regulatory Commission, NUREG/CR-5336, April.

Cundall, P. A., 1971. "A Computer Model for Simulating Progressive Large Scale Movements in Blocky Rock Systems," in Proceedings of the Symposium of the International Society for Rock Mechanics (Nancy, France, 1971), Vol. 1, Paper No. II-8.

Cundall, P. A., 1980. "UDEC - A Generalized Distinct Element Program for Modelling Jointed Rock," Peter Cundall Associates, Report PCAR-1-80, U.S. Army, European Research Office, Contract DAJA37-79-C-0548.

Cundall, P. A., 1988. "Formulation of a Three-Dimensional Distinct Element Model — Part I: A Scheme to Detect and Represent Contacts in a System Composed of Many Polyhedral Blocks," Int. J. Rock Mech., Min. Sci. & Geomech. Abstr., 25, 107-116.

Cundall, P. A., and J. Marti, 1979. "Some New Developments in Discrete Numerical Methods for Dynamic Modelling of Jointed Rock Masses," in Proceedings of the Rapid Excavation and Tunnelling Conference, 1979 (Atlanta, June 1979), Vol. 2, pp. 1466-1477. Baltimore: Port City Press.

Cundall, P. A., and O.D.L. Strack, 1983. "Modeling of Microscopic Mechanisms in Granular Material," in Mechanics of Granular Materials: New Models and Constitutive Relations. J. T. Jenkins and M. Satake, Eds. Amsterdam: Elsevier Scientific Publications, B.V.

Cundall, P. A., J. Marti, P. Beresford, N. Last and M. Asgian, 1978. "Computer Modeling of Jointed Rock Masses," U.S. Army, Engineer Waterways Experiment Station, Technical Report WES-TR-N-78-4, August.

Cundall, P. A., and J. V. Lemos, 1990. "Numerical Simulation of Fault Instabilities with the Continuously-Yielding Joint Model," in Rockbursts and Seismicity in Mines, pp. 147-152. C. Fairhurst, Ed. Rotterdam: A. A. Balkema.

Decovalex, 1991. International co-operative project for the DEvelopment of COupled models and their VAlidation against EXperiments in nuclear waste isolation. Test Case 1, Coupled Stress-Flow Model, Decovalex Doc 91/105.

Hart, R. D., P. A. Cundall and M. L. Cramer, 1985. "Analysis of a Loading Test on a Large Basalt Block," in Research and Engineering — Applications in Rock Masses, Vol. 2, pp. 759-768. E. Ashworth, Ed. Boston: A. A. Balkema.

Hart, R., P. Cundall and J. Lemos, 1988. "Formulation of a Three-Dimensional Distinct Element Model — Part II: Mechanical Calculations for Motion and Interaction of a System Composed of Many Polyhedral Blocks," Int. J. Rock Mech., Min. Sci. & Geomech. Abstr., 25, 117-126.

Hart, R. D., 1991. "An Introduction to Distinct Element Modelling for Rock Engineering," to be published in the proceedings of the 7th International Congress on Rock Mechanics (Aachen, Germany, September 1991), Vol. 3; to be published in Comprehensive Rock Engineering, 1992.

Itasca Consulting Group, Inc., 1991. UDEC Version 1.7. Minneapolis, Minnesota: ICG.

Johansson, E., M. Hakala and L. J. Lorig, 1991a. "Rock Mechanical, Thermomechanical and Hydraulic Behaviour of the Near Field for Spent Nuclear Fuel," Nuclear Waste Commission of Finnish Power Companies Report YJT-91-21, October.

Johansson, E., M. Hakala, E. Peltonen, J.-P. Aslo and L. Lorig, 1991b. "Comparisons of Computed Two- and Three-Dimensional Thermo-mechanical Response of Jointed Rock," in Proceedings of the 7th International Congress on Rock Mechanics (Aachen, September 1991), pp. 115-119. Rotterdam: A. A. Balkema.

Karlekar, B. V., and R. M. Desmond, 1982. Heat Transfer, 2nd Ed. St. Paul, Minnesota: West Publishing Co.

Lemos, J. V., and L. J. Lorig, 1990. "Hydromechanical Modelling of Jointed Rock Masses Using the Distinct Element Method," in Mechanics of Jointed and Faulted Rock, pp. 605-612. Rotterdam: A. A. Balkema.

Lemos, J. V., R. D. Hart and P. A. Cundall, 1985. "A Generalized Distinct Element Program for Modelling Jointed Rock Mass: A Keynote Lecture," in Proceedings of the International Symposium on Fundamentals of Rock Joints (Bjorkliden, 15-20 September 1985), pp. 335-343. Lulea, Sweden: Centek Publishers.

Lorig, L. J., and P. A. Cundall, 1987. "Modeling of Reinforced Concrete Using the Distinct Element Method," in Fracture of Concrete and Rock, pp. 459-471. S. P. Shah and S. E. Swartz, Eds. Bethel, Conn.: SEM.

Lorig, L. J., and B. Dasgupta, 1989. Analysis of Emplacement Borehole Rock and Liner Be~havior for a Repository at Yucca Mountain, U.S. NRC, NUREG / CR-5427, September.

Plesha, M. E., and E. C. Aifantis, 1983. "On the Modeling of Rocks with Microstructure," in Rock Mechanics — Theory-Experiment-Practice (Proceedings of the 24th U.S. Symposium on Rock Mechanics, Texas A&M University, 1983), pp. 27-35. New York: Association of Engineering Geologists

Voegele, M., E. Hardin, D. Lingle, M. Board and N. Barton, 1981. "Site Characterization of Joint Permeability Using the Heated Block Test," in Rock Mechanics from Research to Application (Proceedings of the 22nd U.S. Symposium on Rock Mechanics (MIT, 1981), pp. 120-127. Cambridge: MIT.

Walton, O. R., 1980 "Particle Dynamic Modeling of Geologic Materials," Lawrence Livermore National Laboratory, Report UCRL-52915.

Zimmerman, Roger M., Robert L. Schuch, Donald S. Mason, Michael L. Wilson, Michael E. Hall, Mark P. Board, Robert P. Bellman and Mark L. Blanford, 1986. Final Report: G-Tunnel Heated Block Experiment. SAND84-2620. May.

NOMENCLATURE FOR FIGURE 2.1

Contacts:

F_n	normal and shear forces
Δu_n, Δu_s	increment normal, shear displacements
k_n,k_s	normal, shear stiffness
μ	friction coefficient

Rigid Blocks:

F_i	block force vector
F_i^c	contact force vector
I	moment of inertia
M	block moment
$\ddot{u}_i$	translational acceleration
x_i	position vector
$\ddot{\theta}$	angular acceleration
e_{ij}	permutation tensor

Deformable Blocks:

C( )	functional form of constitutive law
F_i^c	contact force vector
F_i^e	gridpoint force vector
$\dot{u}$	gridpoint velocity vector
$\Delta\varepsilon_{ij}$	incremental strain in zone
σ_{ij}	stress tensor in zone
Δt	timestep
m	zone mass
$n\Delta$	unit outward normal vector
ds	incremental segment

DATA FILE FOR OPTION 1, LOADING SEQUENCE A

```
round 0.001
set ovtol 0.01

bl  mat 2 0,0 0,.26 .26,.26 .26,0
*
*create metal platens
*
split .01 .00 .01 .26
split .25 .00 .25 .26
split .00 .01 .26 .01
split .00 .25 .26 .25
*
*trim ends
*
split .01 .02 .02 .01
split .01 .24 .02 .25
split .25 .24 .24 .25
split .24 .01 .25 .02
split .00 .02 .01 .02
split .02 .00 .02 .01
split .00 .24 .01 .24
split .02 .25 .02 .26
split .24 .25 .24 .26
split .25 .24 .26 .24
split .25 .02 .26 .02
split .24 .00 .24 .01
*
*discard corner pieces
*
del area=1.1e-3
*
*split epoxy block
*
split 0,0 .26,.26
*
*bottom half of sample
*
crack .062825,.062825 .116620,.031767
crack .116620,.031767 .228233,.143380
crack .197175,.197175 .228233,.143380
*
*top half of sample
*
crack .062825,.062825 .031792,.116645
crack .031792,.116645 .143380,.228233
crack .197175,.197175 .143380,.228233
*
```

```
*Generate finite difference zones
*
gen .09 .12 .13 .17 edge 0.02
gen .13 .17 .09 .12 quad 0.015
gen 0 0.5 0 0.5 edge 0.02

*Material properties
*
*Steel
prop mat=1 k=144.927e3 g=78.740e3 dens=7000e-6
*
*Epoxy
*
prop mat=2 k=8.333e3 g=3.846e3 dens=2250e-6
*
*Rock
*
prop mat=3 k=36.667e3 g=22.000e3 dens=2600e-6
*
*Interface properties
*
*Extra crack
prop jmat=3 jcoh=1e10 jtens=1e10 jfric=1 jkn=1e10 jks=1e10
*Steel-Epoxy
*
prop jmat=4 jcoh=0 jfric=.176 jkn=1.0e5 jks=1.0e3
*
*Epoxy-Epoxy
*
prop jmat=5 jcoh=0 jfric=.0175 jkn=0.1e3 jks=0.1e3
*
*Rock-Rock (Linear)
*
*Mechanical properties
prop jmat=6 jcoh=0 jfric=.532 jkn=500.0e3 jks=16.0e3
*Fluid flow properties
prop jmat 6 azero=80e-6 ares=80e-8 jperm=8.33e7 empb=1 expa=3
*
*Rock-Rock (Barton-Bandis)
*
prop jmat=7 JRCo=1.95212 JCSo=156.207 Ln=.200 Lo=.100 Phir=26.5
prop jmat=7 aper 0.080e-3 jkn=2.0e7 jks=15.8e3 azero=80e-6
*
*Rock-Epoxy
*
prop jmat=8 jcoh=1e6 jfric=1 jkn=500.0e3 jks=16.0e3
*
*Assign Steel Properties
*
change .00 .01 .00 .26 mat=1
change .00 .26 .00 .01 mat=1
```

```
change .00 .26 .25 .26 mat=1
change .25 .26 .00 .26 mat=1

*Assign Rock Properties
*
change .09 .11 .14 .16 mat=3
change .09 .11 .06 .08 mat=10
change .14 .16 .09 .11 mat=10
change .18 .20 .14 .16 mat=10
*
*Joint Cons
*
change jcons 2
*
*Assign joint Steel-Epoxy
*
change interface 1,2 jmat 4
*
*Assign joint Epoxy-Epoxy
*
change interface 2,2 jmat 5
*
*Assign extra cracks
*
change interface 10 10 jmat 3
*
*Assign joint Rock-Rock
*
change interface 10 3 jcons 2 jmat 6 *linear
*
*change interface 10,3 jmat 7 jcons 7 *Barton-Bandis
*
*Assign joint Rock-Epoxy
*
change interface 2,3 jmat 8
change interface 2 10 jmat 8
change .09 .11 .06 .08 mat=3
change .14 .16 .09 .11 mat=3
change .18 .20 .14 .16 mat=3
*
*Histories

*Horizontal stress histories at points A, B, C, and D
his sxx .0734 .13 *A
his sxx .13 .1866 *B
his sxx .1866 .13 *C
his sxx .13 .0734 *D
*Vertical stress histories at points A, B, C, and D
his syy .0734 .13 *A
his syy .13 .1866 *B
his syy .1866 .13 *C
```

```
his syy .13 .0734 *D
*Shear stress histories at points A, B, C, and D
his sxy .0734 .13 *A
his sxy .13 .1866 *B
his sxy .1866 .13 *C
his sxy .13 .0734 *D

*Minor principal stress histories at points A, B, C, and D
*his smax .0734 .13 *A
*his smax .13 .1866 *B
*his smax .1866 .13 *C
*his smax .13 .0734 *D
*Major principal stress histories at points A, B, C, and D
*his smin .0734 .13 *A
*his smin .13 .1866 *B
*his smin .1866 .13 *C
*his smin .13 .0734 *D
*Horizontal displacement component at points A, B, C, and D
his xdis .0734 .13 *A
his xdis .13 .1866 *B
his xdis .1866 .13 *C
his xdis .13 .0734 *D
*Vertical displacement component at points A, B, C, and D
his ydis .0734 .13 *A
his ydis .13 .1866 *B
his ydis .1866 .13 *C
his ydis .13 .0734 *D
*Normal stress at points E, F, G, H, and I
hist nstre 4104 *E
hist nstre 1604 *F
hist nstre 345  *G
hist nstre 2368 *H
hist nstre 3014 *I
*Shear stress at point E, F, G, H, and I
hist sstr 4104 *E
hist sstr 1604 *F
hist sstr 345  *G
hist sstr 2368 *H
hist sstr 3014 *I
*Normal displacement at points E, F, G, H, and I
hist ndis 4104 *E
hist ndis 1604 *F
hist ndis 345  *G
hist ndis 2368 *H
hist ndis 3014 *I
*Shear displacement at points E, F, G, H, and I
hist sdis 4104 *E
hist sdis 1604 *F
hist sdis 345  *G
hist sdis 2368 *H
hist sdis 3014 *I
```

```
*Mean aperture for joint at points E, F, G, H, and I(contact offset 20)
hist addr 4104 20 *E
hist addr 1604 20 *F
hist addr 345  20 *G
hist addr 2368 20 *H
hist addr 3014 20 *I

*Domain pressure at points E, F, G, H, and I
hist addr 4137 4 *E
hist addr 1206 4 *F
hist addr 6763 4 *G
hist addr 2477 4 *H
hist addr 1486 4 *I
*Flow rate at points E, F, G, H, and I
hist addr 4104 21 *E (outlet)
hist addr 1604 21 *F
hist addr 345  21 *G
hist addr 2368 21 *H
hist addr 3014 21 *I (Injection)
hist damp
hist unbal
*
*Bottom and Right boundary fixed in normal direction
*
bound -0.01 .2601 -0.01 0.001 yvel 0 *bottom boundary
bound .2599 .2601 -.01 .261 xvel 0 *right boundary
head
TC1, Linear Joint, Loading Sequence A, Sv=Sh=0 MPa (step 0)
save d:\tc1a0.sav
*
bound corner 3001 3264 stress -5 0 0 *left boundary
bound corner 3441 3579 stress 0 0 -5 *top boundary
*
mscale on
damp auto
*
*Fluid properties for water
*
fluid dens=1000e-6 bulkw=2e3
*
*Fluid condition=steady state
*
set sflow on
*
*Fix domain pressures at point E to 0 and 5m head at point I
*
pfix domain 4137 press 0 *point E
pfix domain 1486 press 49.05e-3 *point I
*
*Fix domain pressure to 0 in domains adjecent to domain=1486 to avoid
fluid pressure
```

```
*
pfix domain 3533 press 0
pfix domain 16948 press 0
pfix domain 3080 press 0

*Set maximum hydraulic aperture=ARES x CAPRATIO
*
set capratio=100
*
*Set default material number for new contacts
*
set jmatdf 6 *linear rock joint properties
*
*Set default constitutive relation for new contacts
set jcondf 2 *Mohr-Coulomb joint, i.e linear
*
head
TC1, Linear Joint, Loading Sequence A, Sv=Sh=5+ MPa (step I)
cy 10000
save d:\tc1aI.sav
*
*Increase bound stresses to 15 MPa by adding 10 MPa
*
bound corner 3001 3264 stress -10 0 0 *left boundary
bound corner 3441 3579 stress 0 0 -10 *top boundary
head
TC1, Linear Joint, Loading Sequence A, Sv=Sh=15+ MPa (step II)
cy 10000
save d:\tc1aII.sav
*
*Increase bound stresses to 25 MPa by adding 10 MPa
*
bound corner 3001 3264 stress -10 0 0 *left boundary
bound corner 3441 3579 stress 0 0 -10 *top boundary
head
TC1, Linear Joint, Loading Sequence A, Sv=Sh=25 MPa (step III)
cy 10000
save d:\tc1aIII.sav
*
*Decrease bound stresses to 15 MPa by subtracting 10 MPa
*
bound corner 3001 3264 stress 10 0 0 *left boundary
bound corner 3441 3579 stress 0 0 10 *top boundary
head
TC1, Linear Joint, Loading Sequence A, Sv=Sh=15- MPa (step IV)
cy 10000
save d:\tc1aIV.sav
*
*Decrease bound stresses to 5 MPa by subtracting 10 MPa
*
bound corner 3001 3264 stress 10 0 0 *left boundary
```

```
bound corner 3441 3579 stress 0 0 10 *top boundary
head
TC1, Linear Joint, Loading Sequence A, Sv=Sh=5- MPa (step V)
cy 10000
save d:\tc1aV.sav

*Decrease bound stresses to 0 MPa by subtracting 5 MPa
*
pfix domain 1486 press 0 *point I
bound corner 3001 3264 stress 5 0 0 *left boundary
bound corner 3441 3579 stress 0 0 5 *top boundary
head
TC1, Linear Joint, Loading Sequence A, Sv=Sh=0 MPa (step VI)
cy 10000
save d:\tc1aVI.sav
*
ret
```

DATA FILE FOR OPTION 1, LOADING SEQUENCE B

```
* set rounding length to avoid contact type change during * * shear
*
round .0024
*
* define block
*
bl mat=2 0,0 0,.26 .26,.26 .26,0
*
* create metal plattens
*
split .01 .00 .01 .26
split .25 .00 .25 .26
split .00 .01 .26 .01
split .00 .25 .26 .25
*
* trim ends
*
split .01 .02 .02 .01
split .01 .24 .02 .25
split .25 .24 .24 .25
split .24 .01 .25 .02
split .00 .02 .01 .02
split .02 .00 .02 .01
split .00 .24 .01 .24
split .02 .25 .02 .26
split .24 .25 .24 .26
split .25 .24 .26 .24
split .25 .02 .26 .02
split .24 .00 .24 .01
*
* discard corner pieces
*
del area = 1.1e-3
*
* split epoxy block
*
split 0,0 .26,.26
*
* bottom half of sample
*
crack .062825,.062825 .116620,.031767
crack .116620,.031767 .228233,.143380
crack .197175,.197175 .228233,.143380
*
* top half of sample
*
crack .062825,.062825 .031792,.116645
crack .031792,.116645 .143380,.228233
```

```
crack .197175,.197175 .143380,.228233
*
* zone model
*
gen 0 .5 0 .5 edge .02
*
* Material properites
*
* Steel
*
prop mat=1 k=144.927e3 g=78.740e3 dens=7000e-6
*
* Epoxy
*
prop mat=2 k=8.333e3 g=3.846e3 dens=2250e-6
*
* Rock
*
prop mat=3 k=36.667e3 g=22.000e3 dens=2600e-6
*
* Interface properties
*
* Steel-Epoxy
*
prop jmat 4 jcoh=0 jfric=.176 jkn 1.0e5 jks 1.0e3
*
* Epoxy-Epoxy
*
prop jmat 5 jcoh=0 jfric=.0175 jkn 0.1e3 jks 0.1e3
prop jmat 5 azero 80e-6 ares 80e-8 jperm 8.33e7 empb 1 expa 3
*
* Rock-Rock (linear)
*
prop jmat 6 jcoh=0 jfric=.532 jkn 500.0e3 jks 16.0e3 azero 80.0e-6
prop jmat 6 ares 80e-8 jperm 8.33e7 empb 1 expa 3
*
* Rock-Rock (Barton-Bandis)
*
prop jmat 7 JRCo=1.95212 JCSo=156.207 Ln=.200 Lo=.100 Phir=26.5
sig=240 &
        jkn 2.0e5 jks 15.8e3 azero 80.0e-6
*
* Rock-Epoxy
*
prop jmat 8 jcoh=1e9 jfric=1.0 jkn 500.0e3 jks 16.0e3
*
* assign steel properties
*
change .00 .01 .00 .26 mat 1
change .00 .26 .00 .01 mat 1
change .00 .26 .25 .26 mat 1
```

```
change .25 .26 .00 .26 mat 1
*
* assign rock properties
*
change .075,.175 .075 .175 mat 3
change .075,.150 .050 .100 mat 3
change .150,.225 .150 .200 mat 3
*
* joint constuitive model
*
change jcons 2
*
* assign joint steel-epoxy
*
change inter 1,2 jmat 4
*
* assign joint epoxy-epoxy
*
change inter 2,2 jmat 5
*
* assign joint rock-rock
*
* linear
 change inter 3,3 jmat 6 jcons 2
*
* assign joint rock-epoxy
*
change inter 2,3 jmat 8
*
* make new contacts use epoxy-epoxy material type
*
set jcondf 2
set jmatdf 5
*
* avoid contact overlaps on epoxy-epoxy contacts
*
set ovtol .1
*
* set roller boundaries along bottom and right side
*
bound -0.01 .2601 -.01 .001 yvel=0
bound .2599 .2601 -.01 .261 xvel=0
*
* inhibit deletion of contacts
*
set delc off
*
* set histories
*
reset hist
hist nc 100
```

```
hist unbal
hist damp
hist nstr 4104
hist nstr 1604
hist nstr 345
hist nstr 2368
hist nstr 3014
hist sstr 4104
hist sstr 1604
hist sstr 345
hist sstr 2368
hist sstr 3014
hist ndis 4104
hist ndis 1604
hist ndis 345
hist ndis 2368
hist ndis 3014
hist sdis 4104
hist sdis 1604
hist sdis 345
hist sdis 2368
hist sdis 3014
hist sxx .0734,.1300
hist sxx .1300,.1866
hist sxx .1866,.1300
hist sxx .1300,.0734
hist sxy .0734,.1300
hist sxy .1300,.1866
hist sxy .1866,.1300
hist sxy .1300,.0734
hist syy .0734,.1300
hist syy .1300,.1866
hist syy .1866,.1300
hist syy .1300,.0734
hist xdis .0734,.1300
hist xdis .1300,.1866
hist xdis .1866,.1300
hist xdis .1300,.0734
hist ydis .0734,.1300
hist ydis .1300,.1866
hist ydis .1866,.1300
hist ydis .1300,.0734
hist type 20
*
save tc1b0.sav

*restore tc1b0.sav (state before loading the boundaries)
rest tc1b0.sav
*use boundary stress loading to determine boundary displacements
*for use in velocity boundary condition
*
```

```
bound corner 3001 3264 stress -25 0 0 *left boundary
bound corner 3441 3579 stress 0 0 -25 *top boundary
*
mscale on
damp auto
*
*Fluid properties for water
*
fluid dens=1000e-6 bulkw=2e3
*
*Fluid condition=steady state
*
set sflow on
*
*Fix domain pressures at point E to 0 and 5m head at point I
*
pfix domain 4137 press 0 *point E
pfix domain 1486 press 49.05e-3 *point I
*
*Fix domain pressure to 0 in domains adjecent to domain=1486 to avoid
fluid pressure
*
pfix domain 3533 press 0
pfix domain 10994 press 0
pfix domain 11493 press 0
*Set maximum hydraulic aperture=ARES x CAPRATIO
*
set capratio=100
*
head
TC1, Linear Joint, Loading Sequence B, Sv=Sh=25 MPa (step Ia)
cy 5000
save tc1bIa.sav

*
*data file for DECOVALEX TEST CASE 1
*Linear joint, loading sequence B.
*
*
*restore tc1a0.sav (state before loading the boundaries)
rest tc1b0.sav
*use velocity boundaries to obtain an average normal stress
*of 49.7MPa, 358 cy is required
*

mscale on
damp auto
*
*Fluid properties for water
*
fluid dens=1000e-6 bulkw=2e3
```

```
*
*Fluid condition=steady state
*
set sflow on
*
*Fix domain pressures at point E to 0 and 5m head at point I
*
pfix domain 4137 press 0 *point E
pfix domain 1486 press 49.05e-3 *point I
*
*Fix domain pressure to 0 in domains adjecent to domain=1486 to avoid
fluid pressure
*
pfix domain 3533 press 0
pfix domain 10994 press 0
pfix domain 11493 press 0
*Set maximum hydraulic aperture=ARES x CAPRATIO
*
set capratio=100
*
bound corner 3001 3264 xvel 3.0 *left boundary
bound corner 3441 3579 yvel -3.0 *top boundary
cy 358
bound corner 3001 3264 xvel 0.0 *left boundary
bound corner 3441 3579 yvel 0.0 *top boundary
cy 5000
head
TC1, Linear Joint, Loading Sequence B, (stepI)
save tc1bIb.sav
* 0.5 mm shear forward
rest tc1bib.sav
boun corn 3441 3579 yvel -0.1617 *top bound
boun corn 3441 3579 xvel -0.1617 *top bound
boun corn 3001 3264 xvel -0.1617 *left bound
boun corn 3001 3264 yvel -0.1617 *left bound
his type 20
his ncyc 100
cy 3466
save tc1biia.sav
boun corn 3441 3579 yvel 0 *top bound
boun corn 3441 3579 xvel 0 *top bound
boun corn 3001 3264 xvel 0 *left bound
boun corn 3001 3264 yvel 0 *left bound
head
TC1, Linear Joint, Loading Sequence B, 0.5mm shear, (stepII)
cy 3000
save tc1bIIb.sav
*0.8 mm shear forward
 rest tc1biib.sav
boun corn 3441 3579 yvel -0.1617 *top bound
boun corn 3441 3579 xvel -0.1617 *top bound
```

```
boun corn 3001 3264 xvel -0.1617 *left bound
boun corn 3001 3264 yvel -0.1617 *left bound
his type 20
his ncyc 100
head
TC1, Linear Joint, Loading Sequence B, 0.8mm shear, (stepIII)
cy 2068
save tc1biiia.sav
his ncyc 100
boun corn 3441 3579 yvel 0 *top bound
boun corn 3441 3579 xvel 0 *top bound
boun corn 3001 3264 xvel 0 *left bound
boun corn 3001 3264 yvel 0 *left bound
head
TC1, Linear Joint, Loading Sequence B, 0.8mm shear, (stepIII)
cy 3000
save tc1bIIIb.sav
*2.0 mm shear forward
rest tc1biiib.sav
boun corn 3441 3579 yvel -0.1617 *top bound
boun corn 3441 3579 xvel -0.1617 *top bound
boun corn 3001 3264 xvel -0.1617 *left bound
boun corn 3001 3264 yvel -0.1617 *left bound
his type 20
his ncyc 100
head
TC1, Linear Joint, Loading Sequence B, 2.0mm shear, (stepIV)
cy 7193
save tc1biva.sav
his ncyc 100
boun corn 3441 3579 yvel 0 *top bound
boun corn 3441 3579 xvel 0 *top bound
boun corn 3001 3264 xvel 0 *left bound
boun corn 3001 3264 yvel 0 *left bound
head
TC1, Linear Joint, Loading Sequence B, 2.0mm shear, (stepIV)
cy 5000
save tc1bIVb.sav
*4.0 mm shear forward
rest tc1bivb.sav
boun corn 3441 3579 yvel -0.1617 *top bound
boun corn 3441 3579 xvel -0.1617 *top bound
boun corn 3001 3264 xvel -0.1617 *left bound
boun corn 3001 3264 yvel -0.1617 *left bound
his type 20
his ncyc 100
head
TC1, Linear Joint, Loading Sequence B, 4.0mm shear, (stepV)
cy 7656
save tc1bva.sav
his ncyc 100
```

```
boun corn 3441 3579 yvel 0 *top bound
boun corn 3441 3579 xvel 0 *top bound
boun corn 3001 3264 xvel 0 *left bound
boun corn 3001 3264 yvel 0 *left bound
head
TC1, Linear Joint, Loading Sequence B, 4.0mm shear, (stepV)
cy 5000
save tc1bVb.sav
*2.0 mm shear reverse
rest tc1bvb.sav
boun corn 3441 3579 yvel 0.1617 *top bound
boun corn 3441 3579 xvel 0.1617 *top bound
boun corn 3001 3264 xvel 0.1617 *left bound
boun corn 3001 3264 yvel 0.1617 *left bound
his type 20
his ncyc 100
head
TC1, Linear Joint, Loading Sequence B, reverse 2.0mm shear, (stepVI)
cy 14275
save tc1bvia.sav
his ncyc 100
boun corn 3441 3579 yvel 0 *top bound
boun corn 3441 3579 xvel 0 *top bound
boun corn 3001 3264 xvel 0 *left bound
boun corn 3001 3264 yvel 0 *left bound
head
TC1, Linear Joint, Loading Sequence B, reverse 2.0mm shear, (stepVI)
cy 5000
save tc1bvib.sav
*0.0 mm reverse
rest tc1bvib.sav
boun corn 3441 3579 yvel 0.1617 *top bound
boun corn 3441 3579 xvel 0.1617 *top bound
boun corn 3001 3264 xvel 0.1617 *left bound
boun corn 3001 3264 yvel 0.1617 *left bound
his type 20
his ncyc 100
head
TC1, Linear Joint, Loading Sequence B, reverse 0.0mm shear, (stepVII)
cy 11100
save tc1bviia.sav
his ncyc 100
boun corn 3441 3579 yvel 0 *top bound
boun corn 3441 3579 xvel 0 *top bound
boun corn 3001 3264 xvel 0 *left bound
boun corn 3001 3264 yvel 0 *left bound
head
TC1, Linear Joint, Loading Sequence B, reverse 0.0mm shear, (stepVII)
cy 5000
save tc1bVIIb.sav
ret
```

DATA FILE FOR OPTION 2, LOADING SEQUENCE A

```
round 0.001
set delc off
set ovtol 0.01
bl  mat 2 0,0 0,.26 .26,.26 .26,0
*
*create metal platens
*
split .01 .00 .01 .26
split .25 .00 .25 .26
split .00 .01 .26 .01
split .00 .25 .26 .25
*
*trim ends
*
split .01 .02 .02 .01
split .01 .24 .02 .25
split .25 .24 .24 .25
split .24 .01 .25 .02
split .00 .02 .01 .02
split .02 .00 .02 .01
split .00 .24 .01 .24
split .02 .25 .02 .26
split .24 .25 .24 .26
split .25 .24 .26 .24
split .25 .02 .26 .02
split .24 .00 .24 .01
*
*discard corner pieces
*
del area=1.1e-3
*
*split epoxy block
*
split 0,0 .26,.26
*
*bottom half of sample
*
crack .062825,.062825 .116620,.031767
crack .116620,.031767 .228233,.143380
crack .197175,.197175 .228233,.143380
*
*top half of sample
*
crack .062825,.062825 .031792,.116645
crack .031792,.116645 .143380,.228233
crack .197175,.197175 .143380,.228233
*
*Generate finite difference zones
*
```

```
gen .09 .12 .13 .17 edge 0.02
gen .13 .17 .09 .12 quad 0.015
gen 0 0.5 0 0.5 edge 0.02

*Material properties
*
*Steel
prop mat=1 k=144.927e3 g=78.740e3 dens=7000e-6
*
*Epoxy
*
prop mat=2 k=8.333e3 g=3.846e3 dens=2250e-6
*
*Rock
*
prop mat=3 k=36.667e3 g=22.000e3 dens=2600e-6
*
*Interface properties
*
*Steel-Epoxy
*
prop jmat=4 jcoh=0 jfric=.176 jkn=1.0e5 jks=1.0e3
*
*Epoxy-Epoxy
*
prop jmat=5 jcoh=0 jfric=.0175 jkn=0.1e3 jks=0.1e3
*
*Rock-Rock (Linear)
*
*Mechanical properties
prop jmat=6 jcoh=0 jfric=.532 jkn=500.0e3 jks=16.0e3
*Fluid flow properties
prop jmat 6 azero=80e-6 ares=80e-8 jperm=8.33e7 empb=1 expa=3
*

*Rock-Rock (BArton-Bandis)
*
prop jmat=7 JRCo=1.95212 JCSo=156.207 Ln=.200 Lo=.100 Phir=26.5
prop jmat=7 jkn=2.0e5 jks=15.8e3 sig 240
prop jmat 7 empb=1 expa=3 ares=80e-8 jperm=8.33e7
*
*Rock-Epoxy
*
prop jmat=8 jcoh=1e6 jfric=1 jkn=500.0e3 jks=16.0e3
*
*Assign Steel Properties
*
change .00 .01 .00 .26 mat=1
change .00 .26 .00 .01 mat=1
change .00 .26 .25 .26 mat=1
change .25 .26 .00 .26 mat=1
```

```
*
*Assign Rock Properties
*
change .09 .11 .14 .16 mat=3
change .09 .11 .06 .08 mat=10
change .14 .16 .09 .11 mat=10
change .18 .20 .14 .16 mat=10
*
*Joint Cons
*
change jcons 2
*
*Assign joint Steel-Epoxy
*
change interface 1,2 jmat 4
*
*Assign joint Epoxy-Epoxy
*
change interface 2,2 jmat 5
*
*Assign joint Rock-Rock
*
change interface 10,3 jmat 7 jcons 7 *Barton-Bandis
*
*Assign joint Rock-Epoxy
*
change interface 2,3 jmat 8
change interface 2 10 jmat 8
*change back blocks in lower half from mat=10 to mat=3
change .09 .11 .06 .08 mat=3
change .14 .16 .09 .11 mat=3
change .18 .20 .14 .16 mat=3
*
*Histories

*Horizontal stress histories at points A, B, C, and D
his sxx .0734 .13 *A
his sxx .13 .1866 *B
his sxx .1866 .13 *C
his sxx .13 .0734 *D
*Vertical stress histories at points A, B, C, and D
his syy .0734 .13 *A
his syy .13 .1866 *B
his syy .1866 .13 *C
his syy .13 .0734 *D
*Shear stress histories at points A, B, C, and D
his sxy .0734 .13 *A
his sxy .13 .1866 *B
his sxy .1866 .13 *C
his sxy .13 .0734 *D
*Minor principal stress histories at points A, B, C, and D
```

```
*his smax .0734 .13 *A
*his smax .13 .1866 *B
*his smax .1866 .13 *C
*his smax .13 .0734 *D
*Major principal stress histories at points A, B, C, and D
*his smin .0734 .13 *A
*his smin .13 .1866 *B
*his smin .1866 .13 *C
*his smin .13 .0734 *D
*Horizontal displacement component at points A, B, C, and D
his xdis .0734 .13 *A
his xdis .13 .1866 *B
his xdis .1866 .13 *C
his xdis .13 .0734 *D
*Vertical displacement component at points A, B, C, and D
his ydis .0734 .13 *A
his ydis .13 .1866 *B
his ydis .1866 .13 *C
his ydis .13 .0734 *D
*Normal stress at points E, F, G, H, and I
hist nstre 4104 *E
hist nstre 1604 *F
hist nstre 345  *G
hist nstre 2368 *H
hist nstre 3014 *I
*Shear stress at point E, F, G, H, and I
hist sstr 4104 *E
hist sstr 1604 *F
hist sstr 345  *G
hist sstr 2368 *H
hist sstr 3014 *I
*Normal displacement at points E, F, G, H, and I
hist ndis 4104 *E
hist ndis 1604 *F
hist ndis 345  *G
hist ndis 2368 *H
hist ndis 3014 *I
*Shear displacement at points E, F, G, H, and I
hist sdis 4104 *E
hist sdis 1604 *F
hist sdis 345  *G
hist sdis 2368 *H
hist sdis 3014 *I
*Mean aperture for joint at points E, F, G, H, and I(contact offset 20)
hist addr 4104 20 *E
hist addr 1604 20 *F
hist addr 345  20 *G
hist addr 2368 20 *H
hist addr 3014 20 *I
*Domain pressure at points E, F, G, H, and I
hist addr 4137 4 *E
```

```
hist addr 1206 4 *F
hist addr 6763 4 *G
hist addr 2477 4 *H
hist addr 1486 4 *I
*Flow rate at points E, F, G, H, and I
hist addr 4104 21 *E (outlet)
hist addr 1604 21 *F
hist addr 345  21 *G
hist addr 2368 21 *H
hist addr 3014 21 *I (Injection)
hist damp
hist unbal
*
*Bottom and Right boundary fixed in normal direction
*
bound -0.01 .2601 -0.01 0.001 yvel 0 *bottom boundary
bound .2599 .2601 -.01 .261 xvel 0 *right boundary
head
TC1, BB Joint, Loading Sequence A, Sv=Sh=0 MPa (step 0)
save tc2a0.sav
*
bound corner 3001 3264 stress -5 0 0 *left boundary
bound corner 3441 3579 stress 0 0 -5 *top boundary
*
damp auto
*
*Fluid properties for water
*
fluid dens=1000e-6 bulkw=2e3
*
*Fluid condition=steady state
*
set sflow on
*
*Fix domain pressures at point E to 0 and 5m head at point I
*
pfix domain 4137 press 0 *point E
pfix domain 1486 press 49.05e-3 *point I
*
*Fix domain pressure to 0 in domains adjecent to domain=1486 to avoid
fluid pressure
*
pfix domain 3533 press 0
pfix domain 16948 press 0
pfix domain 3080 press 0
*Set maximum hydraulic aperture=ARES x CAPRATIO
*
set capratio=100
*
*Set default material number for new contacts
*
```

```
set jmatdf 7 *BB rock joint properties
*
*Set default constitutive relation for new contacts
set jcondf 7 *BB joint, i.e unlinear
*
*turn on joint reversal logic
jhist on 0.1
head
TC1, BB Joint, Loading Sequence A, Sv=Sh=5+ MPa (step I)
cy 10000
save tc2aI.sav
*
*Increase bound stresses to 15 MPa by adding 10 MPa
*
bound corner 3001 3264 stress -10 0 0 *left boundary
bound corner 3441 3579 stress 0 0 -10 *top boundary
head
TC1, BB Joint, Loading Sequence A, Sv=Sh=15+ MPa (step II)
cy 10000
save tc2aII.sav
*
*Increase bound stresses to 25 MPa by adding 10 MPa
*
bound corner 3001 3264 stress -10 0 0 *left boundary
bound corner 3441 3579 stress 0 0 -10 *top boundary
head
TC1, BB Joint, Loading Sequence A, Sv=Sh=25 MPa (step III)
cy 10000
save tc2aIII.sav
*
*Decrease bound stresses to 15 MPa by subtracting 10 MPa
*
bound corner 3001 3264 stress 10 0 0 *left boundary
bound corner 3441 3579 stress 0 0 10 *top boundary
head
TC1, BB Joint, Loading Sequence A, Sv=Sh=15- MPa (step IV)
cy 10000
save tc2aIV.sav
*
*Decrease bound stresses to 5 MPa by subtracting 10 MPa
*
bound corner 3001 3264 stress 10 0 0 *left boundary
bound corner 3441 3579 stress 0 0 10 *top boundary
head
TC1, BB Joint, Loading Sequence A, Sv=Sh=5- MPa (step V)
cy 10000
save tc2aV.sav
*
*Decrease bound stresses to 0 MPa by subtracting 5 MPa
*
bound corner 3001 3264 stress 5 0 0 *left boundary
```

```
bound corner 3441 3579 stress 0 0 5 *top boundary
pfix domain 1486 press 0 *point I
head
TC1, BB Joint, Loading Sequence A, Sv=Sh=0 MPa (step VI)
cy 10000
save tc2aVI.sav
*
ret
```

DATA FILE FOR OPTION 2, LOADING SEQUENCE B

```
* set rounding length to avoid contact type change during *shear
*
round .0024
*
* define block
*
bl mat=2 0,0 0,.26 .26,.26 .26,0
*
* create metal plattens
*
split .01 .00 .01 .26
split .25 .00 .25 .26
split .00 .01 .26 .01
split .00 .25 .26 .25
*
* trim ends
*
split .01 .02 .02 .01
split .01 .24 .02 .25
split .25 .24 .24 .25
split .24 .01 .25 .02
split .00 .02 .01 .02
split .02 .00 .02 .01
split .00 .24 .01 .24
split .02 .25 .02 .26
split .24 .25 .24 .26
split .25 .24 .26 .24
split .25 .02 .26 .02
split .24 .00 .24 .01
*
* discard corner pieces
*
del area = 1.1e-3
*
* split epoxy block
*
split 0,0 .26,.26
*
* bottom half of sample
*
crack .062825,.062825 .116620,.031767
crack .116620,.031767 .228233,.143380
crack .197175,.197175 .228233,.143380
*
* top half of sample
*
crack .062825,.062825 .031792,.116645
crack .031792,.116645 .143380,.228233
crack .197175,.197175 .143380,.228233
```

```
*
* zone model
*
gen 0 .5 0 .5 edge .02
*
* Material properites
*
* Steel
*
prop mat=1 k=144.927e3 g=78.740e3 dens=7000e-6
*
* Epoxy
*
prop mat=2 k=8.333e3 g=3.846e3 dens=2250e-6
*
* Rock
*
prop mat=3 k=36.667e3 g=22.000e3 dens=2600e-6
*
* Interface properties
*
* Steel-Epoxy
*
prop jmat 4 jcoh=0 jfric=.176 jkn 1.0e5 jks 1.0e3
*
* Epoxy-Epoxy
*
prop jmat 5 jcoh=0 jfric=.0175 jkn 0.1e3 jks 0.1e3
*
* Rock-Rock (linear)
*
prop jmat 6 jcoh=0 jfric=.532 jkn 500.0e3 jks 16.0e3 azero 80.0e-6
*
* Rock-Rock (Barton-Bandis)
*
prop jmat 7 JRCo=1.95212 JCSo=156.207 Ln=.200 Lo=.100 Phir=26.5
sig=240 &
        jkn 2.0e5 jks 15.8e3 azero 80.0e-6
*
* Rock-Epoxy
*
prop jmat 8 jcoh=1e9 jfric=1.0 jkn 500.0e3 jks 16.0e3
*
* assign steel properties
*
change .00 .01 .00 .26 mat 1
change .00 .26 .00 .01 mat 1
change .00 .26 .25 .26 mat 1
change .25 .26 .00 .26 mat 1
*
* assign rock properties
```

```
*
change .075,.175 .075 .175 mat 3
change .075,.150 .050 .100 mat 3
change .150,.225 .150 .200 mat 3
*
* joint constuitive model
*
change jcons 2
*
* assign joint steel-epoxy
*
change inter 1,2 jmat 4
*
* assign joint epoxy-epoxy
*
change inter 2,2 jmat 5
*
* assign joint rock-rock
*
* linear
* change inter 3,3 jmat 6 jcons 2
* Barton Bandis
change inter 3,3 jmat 7 jcons 7
*
* assign joint rock-epoxy
*
change inter 2,3 jmat 8
*
* make new contacts use epoxy-epoxy material type
*
set jcondf 2
set jmatdf 5
*
* avoid contact overlaps on epoxy-epoxy contacts
*
set ovtol .1
*
* set roller boundaries along bottom and right side
*
bound -0.01 .2601 -.01 .001 yvel=0
bound .2599 .2601 -.01 .261 xvel=0
*
* inhibit deletion of contacts
*
set delc off
*
* set histories
*
reset hist
hist nc 100
hist unbal
```

```
hist damp
hist nstr 4104
hist nstr 1604
hist nstr 345
hist nstr 2368
hist nstr 3014
hist sstr 4104
hist sstr 1604
hist sstr 345
hist sstr 2368
hist sstr 3014
hist ndis 4104
hist ndis 1604
hist ndis 345
hist ndis 2368
hist ndis 3014
hist sdis 4104
hist sdis 1604
hist sdis 345
hist sdis 2368
hist sdis 3014
hist sxx .0734,.1300
hist sxx .1300,.1866
hist sxx .1866,.1300
hist sxx .1300,.0734
hist sxy .0734,.1300
hist sxy .1300,.1866
hist sxy .1866,.1300
hist sxy .1300,.0734
hist syy .0734,.1300
hist syy .1300,.1866
hist syy .1866,.1300
hist syy .1300,.0734
hist xdis .0734,.1300
hist xdis .1300,.1866
hist xdis .1866,.1300
hist xdis .1300,.0734
hist ydis .0734,.1300
hist ydis .1300,.1866
hist ydis .1866,.1300
hist ydis .1300,.0734
hist type 4
*
* set velocity boundary to load joint
*
bound corner 3441 3579 yvel = -3.0
bound corner 3001 3264 xvel =  3.0
damp auto
*
cycle 1090
*
```

```
bound corner 3001 3264 yvel = 0 xvel = 0
bound corner 3441 3579 yvel = 0 xvel = 0
*
cy 2000
*
sav tc2bi.sav
*
* now do shear of joint
*
*0.5 mm shear forward
*
* shear (non dilatant)
*
bound corner 3001 3264 yvel = -0.22
bound corner 3001 3264 xvel = -0.22
bound corner 3441 3579 yvel = -0.22
bound corner 3441 3579 xvel = -0.22
*
cyc 4000
*
* shear (dilatant)
*
bound corner 3001 3264 yvel = -0.1960
bound corner 3001 3264 xvel = -0.2040
bound corner 3441 3579 yvel = -0.1960
bound corner 3441 3579 xvel = -0.2040
*
cyc 10710
save tc2bii.sav
*
*0.8 mm shear forward
*
cyc 3100
save tc2biii.sav
*
* 2.0 mm shear forward
*
cyc 10500
save tc2biv.sav
*
* 4.0 mm shear forward
*
cyc 18200
sav tc2bv.sav
*
* do reverse shear
*
*2.0 mm shear reverse
jhist on 0.1
*
* shear (reverse dilatant)
```

```
*
bound corner 3001 3264 yvel =  0.1980
bound corner 3001 3264 xvel =  0.2020
bound corner 3441 3579 yvel =  0.1980
bound corner 3441 3579 xvel =  0.2020
cyc 4000
*
* shear (non dilatant)
*
bound corner 3001 3264 yvel = 0.22
bound corner 3001 3264 xvel = 0.22
bound corner 3441 3579 yvel = 0.22
bound corner 3441 3579 xvel = 0.22
*
cyc 32200
sav tc2bvi.sav
*
* shear 0.0 mm (reverse)
*
cyc 16800
sav tc2bvii.sav
ret
```

RESULTS AT MONITORING POINTS A-D, OPTION 1, LOADING SEQUENCE A

Sh=Sv=0 initial state

POINT	Sxx [MPa]	Syy [MPa]	Sxy [MPa]	S1 [MPa]	S2 [MPa]	Ux xE-4 [m]	Uy xE-4 [m]
A	0.00	0.00	0.00	0.00	0.00	0.00	0.00
B	0.00	0.00	0.00	0.00	0.00	0.00	0.00
C	0.00	0.00	0.00	0.00	0.00	0.00	0.00
D	0.00	0.00	0.00	0.00	0.00	0.00	0.00

Sh=Sv=5MPa loading

POINT	Sxx [MPa]	Syy [MPa]	Sxy [MPa]	S1 [MPa]	S2 [MPa]	Ux xE-4 [m]	Uy xE-4 [m]
A	-7.76	-5.91	-0.28	-7.80	-5.87	1.17	-1.14
B	-5.88	-7.75	-0.32	-7.80	-5.83	1.15	-1.17
C	-6.10	-6.26	0.91	-7.09	-5.27	1.00	-1.03
D	-6.23	-6.04	0.90	-7.04	-5.23	1.03	-1.00

Sh=Sv=15MPa loading

POINT	Sxx [MPa]	Syy [MPa]	Sxy [MPa]	S1 [MPa]	S2 [MPa]	Ux xE-4 [m]	Uy xE-4 [m]
A	-23.31	-17.76	-0.85	-23.44	-17.63	3.50	-3.42
B	-17.68	-23.27	-0.97	-23.43	-17.52	3.44	-3.50
C	-18.31	-18.80	2.71	-21.28	-15.83	3.00	-3.10
D	-18.72	-18.11	2.69	-21.12	-15.71	3.09	-3.00

Sh=Sv=25MPa loading

POINT	Sxx [MPa]	Syy [MPa]	Sxy [MPa]	S1 [MPa]	S2 [MPa]	Ux xE-4 [m]	Uy xE-4 [m]
A	-38.92	-29.67	-1.45	-39.14	-29.45	5.83	-5.70
B	-29.55	-38.84	-1.66	-39.13	-29.26	5.74	-5.83
C	-30.52	-31.38	-4.51	-35.48	-26.42	5.00	-5.17
D	-31.23	-30.18	-4.46	-35.20	-26.21	5.14	-5.00

Sh=Sv=15MPa unloading

POINT	Sxx [MPa]	Syy [MPa]	Sxy [MPa]	S1 [MPa]	S2 [MPa]	Ux xE-4 [m]	Uy xE-4 [m]
A	-23.30	-17.75	-0.85	-23.42	-17.63	3.50	-3.42
B	-17.68	-23.26	-0.97	-23.42	-17.51	3.44	-3.49
C	-18.30	-18.80	2.70	-21.26	-15.84	3.00	-3.10
D	-18.72	-18.10	2.68	-21.11	-15.71	3.08	-3.00

Sh=Sv=5MPa unloading

POINT	Sxx [MPa]	Syy [MPa]	Sxy [MPa]	S1 [MPa]	S2 [MPa]	Ux xE-4 [m]	Uy xE-4 [m]
A	-7.73	-5.90	-0.28	-7.78	-5.86	1.16	-1.14
B	-5.87	-7.72	-0.32	-7.78	-5.81	1.14	-1.16
C	-6.09	-6.26	0.89	-7.06	-5.28	1.00	-1.03
D	-6.23	-6.02	0.88	-7.01	-5.24	1.03	-1.00

Sh=Sv=0MPa unloading

POINT	Sxx [MPa]	Syy [MPa]	Sxy [MPa]	S1 [MPa]	S2 [MPa]	Ux xE-4 [m]	Uy xE-4 [m]
A	0.00	0.00	0.00	0.00	0.00	-0.02	0.02
B	0.00	0.00	0.00	0.00	0.00	-0.02	0.02
C	0.00	0.00	0.00	0.00	0.00	-0.02	0.02
D	0.00	0.00	0.00	0.00	0.00	-0.02	0.02

RESULTS AT MONITORING POINTS E-I, OPTION 1, LOADING SEQUENCE A

Sh=Sv=0 initial state

POINT	Sn [MPa]	Ss [MPa]	Un xE-6 [m]	Us xE-6 [m]	b xE-6 [m]	e xE-6 [m]	P xE-2 [MPa]	Q xE-6 [m^3/s]
E	0.00	0.00	0.00	0.00	80.00	80.00	0.00	0.00
F	0.00	0.00	0.00	0.00	80.00	80.00	0.00	0.00
G	0.00	0.00	0.00	0.00	80.00	80.00	0.00	0.00
H	0.00	0.00	0.00	0.00	80.00	80.00	0.00	0.00
I	0.00	0.00	0.00	0.00	80.00	80.00	0.00	0.00

Sh=Sv=5MPa loading

POINT	Sn [MPa]	Ss [MPa]	Un xE-6 [m]	Us xE-6 [m]	b xE-6 [m]	e xE-6 [m]	P xE-2 [MPa]	Q xE-6 [m^3/s]
E	14.25	-0.27	-28.41	16.79	51.59	51.59	0.00	5.37
F	7.50	-0.14	-15.00	8.48	65.00	65.00	1.49	5.37
G	5.83	0.00	-11.65	0.01	68.35	68.35	2.54	5.37
H	7.48	0.14	-14.95	-8.54	65.05	65.05	3.61	5.37
I	14.19	0.27	-28.29	-16.80	51.71	51.71	4.91	5.37

Sh=Sv=15MPa loading

POINT	Sn [MPa]	Ss [MPa]	Un xE-6 [m]	Us xE-6 [m]	b xE-6 [m]	e xE-6 [m]	P xE-2 [MPa]	Q xE-10 [m^3/s]
E	43.01	-0.82	-85.29	50.75	0.80	0.80	0.00	1.96
F	22.51	-0.41	-45.03	25.61	34.97	34.97	2.47	1.97
G	17.50	0.00	-35.03	0.11	44.97	44.97	2.47	1.85
H	22.50	0.41	-45.02	-25.62	34.98	34.98	2.47	1.95
I	42.98	0.81	-85.26	-50.58	0.80	0.80	4.91	1.93

Sh=Sv=25MPa loading

POINT	Sn [MPa]	Ss [MPa]	Un xE-6 [m]	Us xE-6 [m]	b xE-6 [m]	e xE-6 [m]	P xE-2 [MPa]	Q xE-11 [m^3/s]
E	72.16	-1.38	-142.50	85.35	0.80	0.80	0.00	2.60
F	37.55	-0.69	-75.08	42.99	4.92	4.92	2.47	2.60
G	29.16	0.00	-58.37	0.25	21.63	21.63	2.47	2.56
H	37.54	0.69	-75.06	-42.85	4.94	4.94	2.47	2.57
I	72.09	1.37	-142.40	-84.90	0.80	0.80	4.91	2.57

Sh=Sv=15MPa unloading

POINT	Sn [MPa]	Ss [MPa]	Un xE-6 [m]	Us xE-6 [m]	b xE-6 [m]	e xE-6 [m]	P xE-2 [MPa]	Q xE-10 [m^3/s]
E	43.12	-0.82	-85.17	50.68	0.80	0.80	0.00	1.96
F	22.49	-0.41	-45.01	25.54	34.99	34.99	2.47	1.96
G	17.50	0.00	-35.02	0.07	44.98	44.98	2.47	1.98
H	22.48	0.41	-45.00	-25.61	35.00	35.00	2.47	1.90
I	43.04	0.82	-85.10	-50.57	0.80	0.80	4.91	1.93

Sh=Sv=5MPa unloading

POINT	Sn [MPa]	Ss [MPa]	Un xE-6 [m]	Us xE-6 [m]	b xE-6 [m]	e xE-6 [m]	P xE-2 [MPa]	Q xE-6 [m^3/s]
E	14.47	-0.28	-28.17	16.67	51.83	51.83	0.00	5.40
F	7.46	-0.13	-14.97	8.36	65.03	65.03	1.49	5.40
G	5.80	0.00	-11.64	-0.03	68.36	68.36	2.54	5.40
H	7.42	0.14	-14.91	-8.50	65.09	65.09	3.61	5.40
I	14.34	0.27	-28.04	-16.74	51.96	51.96	4.91	5.40

Sh=Sv=0MPa unloading

POINT	Sn [MPa]	Ss [MPa]	Un xE-6 [m]	Us xE-6 [m]	b xE-6 [m]	e xE-6 [m]	P xE-2 [MPa]	Q xE-6 [m^3/s]
E	0.00	0.00	1.03	-0.02	80.00	80.00	0.00	0.00
F	0.00	0.00	1.00	-0.03	80.00	80.00	0.00	0.00
G	0.00	0.00	0.94	-0.01	80.00	80.00	0.00	0.00
H	0.00	0.00	0.90	-0.02	80.00	80.00	0.00	0.00
I	0.00	0.00	0.85	-0.01	80.00	80.00	0.00	0.00

RESULTS AT MONITORING POINTS A-D, OPTION 1, LOADING SEQUENCE B

Shear=0mm

POINT	Sxx [MPa]	Syy [MPa]	Sxy [MPa]	S1 [MPa]	S2 [MPa]	Ux xE-4 [m]	Uy xE-4 [m]
A	-36.55	-30.66	7.00	-41.21	-26.01	6.59	-6.45
B	-30.25	-36.29	6.44	-40.38	-26.16	6.54	-6.58
C	-36.75	-30.68	6.87	-41.23	-26.21	5.56	-5.71
D	-30.33	-36.53	6.34	-40.49	-26.38	5.61	-5.57

Shear=0.5mm forward

POINT	Sxx [MPa]	Syy [MPa]	Sxy [MPa]	S1 [MPa]	S2 [MPa]	Ux xE-4 [m]	Uy xE-4 [m]
A	-27.66	-31.26	9.46	-39.09	-19.83	1.54	-11.35
B	-29.58	-44.99	3.96	-45.95	-28.62	1.63	-11.62
C	-27.67	-31.02	9.14	-38.63	-20.05	4.25	-7.16
D	-29.83	-45.39	4.08	-46.39	-28.83	4.15	-6.88

Shear=0.8mm forward

POINT	Sxx [MPa]	Syy [MPa]	Sxy [MPa]	S1 [MPa]	S2 [MPa]	Ux xE-4 [m]	Uy xE-4 [m]
A	-22.68	-31.68	11.02	-39.08	-15.28	-1.46	-14.26
B	-29.16	-50.21	2.45	-50.49	-28.88	-1.28	-14.63
C	-22.55	-31.28	10.57	-38.35	-15.48	3.47	-8.05
D	-29.51	-50.73	2.70	-51.06	-29.18	3.27	-7.66

Shear=2.0mm forward

POINT	Sxx [MPa]	Syy [MPa]	Sxy [MPa]	S1 [MPa]	S2 [MPa]	Ux xE-4 [m]	Uy xE-4 [m]
A	-16.15	-35.14	12.73	-41.53	-12.82	-12.45	-24.90
B	-28.80	-64.01	-2.32	-64.17	-28.65	-11.95	-25.67
C	-15.33	-34.15	12.34	-40.27	-12.37	1.24	-10.57
D	-28.87	-64.85	-1.81	-64.94	-28.78	0.71	-9.78

Shear=4.0mm forward

POINT	Sxx [MPa]	Syy [MPa]	Sxy [MPa]	S1 [MPa]	S2 [MPa]	Ux xE-4 [m]	Uy xE-4 [m]
A	-16.04	-33.99	12.92	-40.75	-12.51	-26.48	-39.14
B	-28.81	-63.27	-2.22	-63.41	-28.67	-26.11	-39.77
C	-15.22	-33.12	12.55	-39.59	-12.08	1.32	-10.28
D	-28.92	-64.06	-1.73	-64.15	-28.83	0.91	-9.63

Shear=2.0mm reverse

POINT	Sxx [MPa]	Syy [MPa]	Sxy [MPa]	S1 [MPa]	S2 [MPa]	Ux xE-4 [m]	Uy xE-4 [m]
A	-47.68	-31.02	4.34	-48.74	-29.95	-5.90	-19.05
B	-31.12	-26.55	8.45	-37.59	-20.08	-6.08	-19.07
C	-47.34	-30.70	4.73	-48.59	-29.45	6.91	-4.15
D	-30.72	-26.20	8.52	-37.27	-19.65	7.09	-4.13

Shear=0.0mm reverse

POINT	Sxx [MPa]	Syy [MPa]	Sxy [MPa]	S1 [MPa]	S2 [MPa]	Ux xE-4 [m]	Uy xE-4 [m]
A	-65.99	-30.63	-1.70	-66.08	-30.55	11.57	-1.93
B	-35.47	-15.67	11.85	-41.02	-12.78	10.94	-1.61
C	-66.46	-30.03	-1.31	-66.50	-29.98	9.74	-0.86
D	-34.67	-15.14	11.80	-40.22	-12.45	10.38	-1.21

RESULTS AT MONITORING POINTS E-I, OPTION 1, LOADING SEQUENCE B

Shear 0 mm

POINT	Sn [MPa]	Ss [MPa]	Un xE-6 [m]	Us xE-6 [m]	b xE-6 [m]	e xE-6 [m]	P xE-2 [MPa]	Q xE-11 [m^3/s]
E	63.89	0.00	-127.80	-0.26	0.80	0.80	0.00	1.60
F	43.79	0.01	-87.62	-0.52	0.80	0.80	1.47	1.60
G	37.72	-0.01	-75.50	0.30	4.50	4.50	2.46	1.60
H	43.72	0.00	-87.48	0.17	0.80	0.80	2.99	1.60
I	63.75	-0.01	-127.50	0.44	0.80	0.80	4.91	1.60

Shear 0.5 mm forward

POINT	Sn [MPa]	Ss [MPa]	Un xE-6 [m]	Us xE-6 [m]	b xE-6 [m]	e xE-6 [m]	P xE-2 [MPa]	Q xE-11 [m^3/s]
E	64.39	8.06	-128.80	-503.90	0.80	0.80	0.00	1.61
F	43.96	8.01	-87.99	-500.70	0.80	0.80	1.48	1.61
G	37.63	8.02	-75.28	-501.40	4.72	4.72	2.48	1.61
H	43.50	8.00	-86.95	-500.00	0.80	0.80	2.98	1.61
I	63.49	8.05	-127.00	-503.30	0.80	0.80	4.91	1.61

Shear 0.8 mm forward

POINT	Sn [MPa]	Ss [MPa]	Un xE-6 [m]	Us xE-6 [m]	b xE-6 [m]	e xE-6 [m]	P xE-2 [MPa]	Q xE-11 [m^3/s]
E	64.35	12.86	-128.70	-803.50	0.80	0.80	0.00	1.56
F	44.12	12.77	-88.28	-798.00	0.80	0.80	1.43	1.56
G	37.73	12.79	-45.47	-799.20	4.53	4.53	2.55	1.56
H	43.40	12.76	-86.74	-797.00	0.80	0.80	3.04	1.56
I	63.04	12.84	-126.10	-802.50	0.80	0.80	4.91	1.56

Shear 2.0 mm forward

POINT	Sn [MPa]	Ss [MPa]	Un xE-6 [m]	Us xE-6 [m]	b xE-6 [m]	e xE-6 [m]	P xE-2 [MPa]	Q xE-11 [m^3/s]
E	60.31	32.07	-120.60	-2017.00	0.80	0.80	0.00	1.14
F	45.53	24.12	-91.04	-2011.00	0.80	0.80	1.04	1.14
G	39.57	20.90	-79.17	-2019.00	0.83	0.83	2.31	1.14
H	44.30	23.37	-88.41	-2011.00	0.80	0.80	3.55	1.14
I	60.23	31.71	-120.50	-2012.00	0.80	0.80	4.91	1.14

Shear 4.0 mm forward

POINT	Sn [MPa]	Ss [MPa]	Un xE-6 [m]	Us xE-6 [m]	b xE-6 [m]	e xE-6 [m]	P xE-2 [MPa]	Q xE-11 [m^3/s]
E	62.99	33.51	-126.00	-4018.00	0.80	0.80	0.00	1.15
F	45.08	23.85	-90.16	-4015.00	0.80	0.80	1.16	1.15
G	39.18	20.65	-78.24	-4023.00	1.76	1.76	2.44	1.15
H	43.98	23.14	-87.77	-4015.00	0.80	8.00	3.43	1.15
I	63.03	33.19	-126.10	-4013.00	0.80	0.80	4.91	1.15

Shear 2.0 mm reverse

POINT	Sn [MPa]	Ss [MPa]	Un xE-6 [m]	Us xE-6 [m]	b xE-6 [m]	e xE-6 [m]	P xE-2 [MPa]	Q xE-11 [m^3/s]
E	60.85	0.82	-121.70	-1975.00	0.80	0.80	0.00	1.40
F	43.61	-8.55	-87.26	-1991.00	0.80	0.80	1.27	1.40
G	38.21	-11.74	-76.33	-1998.00	3.76	3.76	2.45	1.40
H	43.72	-9.20	-87.44	-1994.00	0.80	0.80	3.24	1.40
I	62.64	0.61	-125.30	-1978.00	0.80	0.80	4.91	1.40

Shear 0.0 mm reverse

POINT	Sn [MPa]	Ss [MPa]	Un xE-6 [m]	Us xE-6 [m]	b xE-6 [m]	e xE-6 [m]	P xE-2 [MPa]	Q xE-11 [m^3/s]
E	57.26	-30.21	-114.50	13.84	0.80	0.80	0.00	1.13
F	44.79	-23.62	-89.57	11.82	0.80	0.80	1.04	1.13
G	40.91	-21.60	-81.82	21.62	0.80	0.80	2.30	1.13
H	45.27	-24.00	-90.54	14.19	0.80	0.80	3.55	1.13
I	57.65	-30.67	-115.30	21.12	0.80	0.80	4.91	1.13

RESULTS AT MONITORING POINTS A-D, OPTION 2, LOADING SEQUENCE A

Sh=Sv=0 nitial state

POINT	Sxx [MPa]	Syy [MPa]	Sxy [MPa]	S1 [MPa]	S2 [MPa]	Ux xE-4 [m]	Uy xE-4 [m]
A	0.00	0.00	0.00	0.00	0.00	0.00	0.00
B	0.00	0.00	0.00	0.00	0.00	0.00	0.00
C	0.00	0.00	0.00	0.00	0.00	0.00	0.00
D	0.00	0.00	0.00	0.00	0.00	0.00	0.00

Sh=Sv=5MPa loading

POINT	Sxx [MPa]	Syy [MPa]	Sxy [MPa]	S1 [MPa]	S2 [MPa]	Ux xE-4 [m]	Uy xE-4 [m]
A	-8.32	-5.38	-0.49	-8.33	-5.38	1.39	-1.38
B	-5.35	-8.04	-0.53	-8.31	-5.35	1.38	-1.39
C	-6.46	-5.70	0.53	-7.39	-4.77	1.01	-1.04
D	-5.67	-6.39	0.52	-7.32	-4.74	1.03	-1.01

Sh=Sv=15MPa loading

POINT	Sxx [MPa]	Syy [MPa]	Sxy [MPa]	S1 [MPa]	S2 [MPa]	Ux xE-4 [m]	Uy xE-4 [m]
A	-24.59	-16.02	-0.10	-24.59	-16.02	4.07	-4.01
B	-15.95	-24.55	-0.22	-24.55	-15.94	4.04	-4.07
C	-19.68	-17.04	3.83	-22.41	-14.31	3.04	-3.13
D	-16.96	-19.46	3.80	-22.21	-14.21	3.12	-3.04

Sh=Sv=25MPa loading

POINT	Sxx [MPa]	Syy [MPa]	Sxy [MPa]	S1 [MPa]	S2 [MPa]	Ux xE-4 [m]	Uy xE-4 [m]
A	-39.82	-26.24	0.27	-39.82	-26.31	6.74	-6.65
B	-26.12	-39.74	0.07	-39.74	-26.12	6.68	-6.73
C	-33.09	-28.96	5.97	-37.34	-24.70	5.07	-5.24
D	-28.83	-32.73	5.93	-37.02	-24.53	5.21	-5.07

Sh=Sv=15MPa unloading

POINT	Sxx [MPa]	Syy [MPa]	Sxy [MPa]	S1 [MPa]	S2 [MPa]	Ux xE-4 [m]	Uy xE-4 [m]
A	-24.61	-15.99	-0.09	-24.61	-15.99	4.06	-4.00
B	-15.91	-24.56	-0.22	-24.57	-15.90	4.02	-4.05
C	-19.70	-17.00	3.82	-22.40	-14.30	3.04	-3.13
D	-16.93	-19.48	3.80	-22.21	-14.19	3.11	-3.04

Sh=Sv=5MPa unloading

POINT	Sxx [MPa]	Syy [MPa]	Sxy [MPa]	S1 [MPa]	S2 [MPa]	Ux xE-4 [m]	Uy xE-4 [m]
A	-8.35	-5.33	-0.08	-8.35	-5.33	1.37	-1.35
B	-5.30	-8.33	-0.13	-8.34	-5.30	1.36	-1.37
C	-6.48	-5.65	1.24	-7.37	-4.76	1.01	-1.04
D	-5.63	-6.40	1.24	-7.31	-4.72	1.03	-1.01

Sh=Sv=0MPa unloading

POINT	Sxx [MPa]	Syy [MPa]	Sxy [MPa]	S1 [MPa]	S2 [MPa]	Ux xE-4 [m]	Uy xE-4 [m]
A	0.00	0.00	0.00	0.00	0.00	-0.51	0.54
B	0.00	0.00	0.00	0.00	0.00	-0.53	0.55
C	0.00	0.00	0.00	0.00	0.00	-0.39	0.39
D	0.00	0.00	0.00	0.00	0.00	-0.39	0.39

RESULTS AT MONITORING POINTS E-I, OPTION 2, LOADING SEQUENCE A

Sh=Sv=0 initial state

POINT	Sn [MPa]	Ss [MPa]	Un xE-6 [m]	Us xE-6 [m]	b xE-6 [m]	e xE-6 [m]	P xE-2 [MPa]	Q xE-6 [m^3/s]
E	0.00	0.00	-30.00	0.00	51.00	51.00	0.00	0.00
F	0.00	0.00	-30.00	0.00	51.00	51.00	0.00	0.00
G	0.00	0.00	-30.00	0.00	51.00	51.00	0.00	0.00
H	0.00	0.00	-30.00	0.00	51.00	51.00	0.00	0.00
I	0.00	0.00	-30.00	0.00	51.00	51.00	0.00	0.00

Sh=Sv=5MPa loading

POINT	Sn [MPa]	Ss [MPa]	Un xE-6 [m]	Us xE-6 [m]	b xE-6 [m]	e xE-6 [m]	P xE-2 [MPa]	Q xE-6 [m^3/s]
E	12.06	-0.37	-59.44	16.92	21.52	21.52	0.00	0.27
F	7.79	-0.12	-57.58	8.62	23.44	23.44	1.39	0.27
G	6.50	0.00	-56.60	0.02	24.41	24.41	2.55	0.27
H	7.76	0.12	-57.56	-8.65	23.46	23.46	3.52	0.27
I	12.00	0.37	-59.42	-16.90	21.54	21.54	4.91	0.27

Sh=Sv=15MPa loading

POINT	Sn [MPa]	Ss [MPa]	Un xE-6 [m]	Us xE-6 [m]	b xE-6 [m]	e xE-6 [m]	P xE-2 [MPa]	Q xE-6 [m^3/s]
E	36.20	-2.87	-62.25	43.19	19.42	19.42	0.00	0.18
F	23.41	-0.91	-61.62	21.22	20.19	20.19	1.32	0.18
G	19.58	-0.00	-61.14	0.14	20.60	20.60	2.56	0.18
H	23.39	0.91	-61.63	-21.26	20.19	20.19	3.58	0.18
I	36.14	2.86	-62.24	-43.06	19.42	19.42	4.91	0.18

Sh=Sv=25MPa loading

POINT	Sn [MPa]	Ss [MPa]	Un xE-6 [m]	Us xE-6 [m]	b xE-6 [m]	e xE-6 [m]	P xE-2 [MPa]	Q xE-6 [m^3/s]
E	58.42	-6.30	-62.86	58.56	19.48	19.48	0.00	0.17
F	38.56	-2.04	-62.57	28.47	19.92	19.92	1.28	0.17
G	32.45	-0.01	-62.27	0.19	20.16	20.16	2.53	0.17
H	38.54	2.02	-62.59	-28.55	19.92	19.92	3.56	0.17
I	58.37	6.27	-62.86	-58.39	19.48	19.48	4.91	0.17

Sh=Sv=15MPa unloading

POINT	Sn [MPa]	Ss [MPa]	Un xE-6 [m]	Us xE-6 [m]	b xE-6 [m]	e xE-6 [m]	P xE-2 [MPa]	Q xE-6 [m^3/s]
E	36.19	-2.87	-62.20	43.15	20.78	20.78	0.00	0.22
F	23.37	-0.91	-61.52	21.18	21.58	21.58	1.36	0.22
G	19.63	-0.01	-61.03	0.15	22.63	22.63	2.55	0.22
H	23.34	0.91	-61.53	-21.23	21.58	21.58	3.55	0.22
I	36.10	2.86	-62.19	-43.06	20.79	20.79	4.91	0.22

Sh=Sv=5MPa unloading

POINT	Sn [MPa]	Ss [MPa]	Un xE-6 [m]	Us xE-6 [m]	b xE-6 [m]	e xE-6 [m]	P xE-2 [MPa]	Q xE-6 [m^3/s]
E	12.05	-0.38	-58.87	16.96	24.65	24.65	0.00	0.42
F	7.74	-0.12	-56.75	8.63	26.84	26.84	1.41	0.42
G	6.55	-0.00	-55.55	0.14	28.54	28.54	2.58	0.42
H	7.71	0.12	-56.74	-8.56	26.86	26.86	3.49	0.42
I	11.96	0.37	-58.83	-16.85	24.68	24.68	4.91	0.42

Sh=Sv=0MPa unloading

POINT	Sn [MPa]	Ss [MPa]	Un xE-6 [m]	Us xE-6 [m]	b xE-6 [m]	e xE-6 [m]	P xE-2 [MPa]	Q xE-6 [m^3/s]
E	0.00	0.00	-22.01	3.41	61.57	61.57	0.00	0.00
F	0.00	0.00	-22.32	3.40	61.27	61.27	0.00	0.00
G	0.00	0.00	-21.07	3.55	63.43	63.43	0.00	0.00
H	0.00	0.00	-22.33	3.55	61.27	61.27	0.00	0.00
I	0.00	0.00	-22.00	3.51	61.57	61.57	0.00	0.00

RESULTS AT MONITORING POINTS A-D, OPTION 2, LOADING SEQUENCE B

Shear=0.0mm initial state

POINT	Sxx [MPa]	Syy [MPa]	Sxy [MPa]	S1 [MPa]	S2 [MPa]	Ux xE-4 [m]	Uy xE-4 [m]
A	-37.63	-28.54	6.63	-41.12	-25.05	7.34	-7.20
B	-28.19	-37.36	6.11	-40.41	-25.14	7.30	-7.32
C	-37.04	-27.84	7.36	-41.12	-23.76	5.40	-5.51
D	-27.52	-36.80	6.87	-40.45	-23.87	5.42	-5.41

Shear=0.5mm forward

POINT	Sxx [MPa]	Syy [MPa]	Sxy [MPa]	S1 [MPa]	S2 [MPa]	Ux xE-4 [m]	Uy xE-4 [m]
A	-16.58	-31.86	12.54	-38.90	-9.54	-0.78	-14.55
B	-25.88	-62.43	-1.87	-62.53	-25.78	-0.28	-15.27
C	-15.53	-31.17	12.06	-37.72	-8.98	1.33	-9.99
D	-26.47	-61.80	-0.77	-61.82	-26.45	0.78	-9.22

Shear=0.8mm forward

POINT	Sxx [MPa]	Syy [MPa]	Sxy [MPa]	S1 [MPa]	S2 [MPa]	Ux xE-4 [m]	Uy xE-4 [m]
A	-16.11	-31.78	12.27	-38.50	-9.39	-2.95	-16.63
B	-26.09	-63.40	-2.25	-63.53	-25.96	-2.41	-17.40
C	-15.59	-31.29	12.12	-37.88	-9.00	1.32	-10.00
D	-26.32	-61.91	-1.04	-61.94	-26.29	0.75	-9.22

Shear=2.0mm forward

POINT	Sxx [MPa]	Syy [MPa]	Sxy [MPa]	S1 [MPa]	S2 [MPa]	Ux xE-4 [m]	Uy xE-4 [m]
A	-16.31	-30.74	12.62	-38.06	-8.99	-11.46	-25.04
B	-25.55	-61.96	-1.92	-62.06	-25.45	-11.03	-25.68
C	-15.26	-30.08	12.08	-36.84	-8.50	1.31	-9.79
D	-26.14	-61.26	-0.83	-61.28	-26.12	0.83	-9.10

Shear=4.0mm forward

POINT	Sxx [MPa]	Syy [MPa]	Sxy [MPa]	S1 [MPa]	S2 [MPa]	Ux xE-4 [m]	Uy xE-4 [m]
A	-16.03	-29.00	12.66	-36.74	-8.29	-25.66	-39.08
B	-24.98	-60.02	-1.65	-60.10	-24.90	-25.38	-39.55
C	-14.97	-28.34	12.14	-35.51	-7.80	1.37	-9.31
D	-25.56	-59.33	-0.66	-59.34	-25.55	1.03	-8.78

Shear=2.0mm reverse

POINT	Sxx [MPa]	Syy [MPa]	Sxy [MPa]	S1 [MPa]	S2 [MPa]	Ux xE-4 [m]	Uy xE-4 [m]
A	-62.58	-25.92	-1.36	-62.63	-25.87	-2.90	-17.46
B	-31.29	-15.39	11.08	-36.98	-9.70	-3.67	-16.94
C	-61.38	-26.36	-0.47	-61.39	-26.35	8.92	-0.73
D	-31.03	-26.36	10.95	-39.89	-17.50	9.70	-1.26

Shear=0.0mm reverse

POINT	Sxx [MPa]	Syy [MPa]	Sxy [MPa]	S1 [MPa]	S2 [MPa]	Ux xE-4 [m]	Uy xE-4 [m]
A	-62.78	-26.38	-1.22	-62.82	-26.34	11.21	-3.21
B	-30.84	-15.60	11.46	-36.98	-9.46	10.52	-2.77
C	-61.75	-26.83	-0.24	-61.75	-26.83	8.93	-2.77
D	-30.66	-15.02	11.36	-36.63	-9.05	9.63	-0.94

RESULTS AT MONITORING POINTS E-I, OPTION 2, LOADING SEQUENCE B

Shear=0.0mm initial state

POINT	Sn [MPa]	Ss [MPa]	Un xE-6 [m]	Us xE-6 [m]	b xE-6 [m]	e xE-6 [m]	P xE-2 [MPa]	Q xE-7 [m^3/s]
E	54.92	-0.16	-62.66	1.42	18.26	18.26	0.00	1.40
F	42.90	-0.03	-62.39	0.34	18.54	18.54	1.21	1.40
G	38.60	-0.03	-62.25	0.40	18.68	18.68	2.45	1.40
H	42.87	0.03	-62.39	-0.38	18.48	18.48	3.69	1.40
I	54.88	0.10	-62.66	-0.89	18.27	18.27	4.91	1.40

Shear=0.5mm forward

POINT	Sn [MPa]	Ss [MPa]	Un xE-6 [m]	Us xE-6 [m]	b xE-6 [m]	e xE-6 [m]	P xE-2 [MPa]	Q xE-7 [m^3/s]
E	54.64	27.98	-62.66	-500.70	18.40	18.40	0.00	1.45
F	43.63	22.47	-62.41	-499.30	18.68	18.68	1.22	1.45
G	39.28	20.30	-62.28	-509.80	18.85	18.85	2.46	1.45
H	42.22	21.78	-62.37	-509.60	18.74	18.74	3.70	1.45
I	50.76	26.06	-62.58	-520.90	18.51	18.51	4.91	1.45

Shear=0.8mm forward

POINT	Sn [MPa]	Ss [MPa]	Un xE-6 [m]	Us xE-6 [m]	b xE-6 [m]	e xE-6 [m]	P xE-2 [MPa]	Q xE-7 [m^3/s]
E	53.73	27.72	-62.64	-803.50	18.94	18.94	0.00	1.61
F	43.12	22.40	-62.39	-802.30	19.35	19.35	1.22	1.61
G	39.20	20.44	-62.28	-812.30	19.57	19.57	2.46	1.61
H	42.56	22.13	-62.38	-811.10	19.40	19.40	3.69	1.61
I	51.45	26.59	-62.60	-822.00	19.05	19.05	4.91	1.61

Shear=2.0mm forward

POINT	Sn [MPa]	Ss [MPa]	Un xE-6 [m]	Us xE-6 [m]	b xE-6 [m]	e xE-6 [m]	P xE-2 [MPa]	Q xE-7 [m^3/s]
E	54.14	27.97	-62.65	-1995.00	21.82	21.82	0.00	2.75
F	43.15	22.47	-62.40	-1994.00	23.05	23.05	1.27	2.75
G	38.89	20.32	-62.26	-2005.00	23.70	23.70	2.49	2.75
H	41.82	21.80	-62.35	-2005.00	23.27	23.27	3.69	2.75
I	50.33	26.07	-62.57	-2015.00	22.26	22.26	4.91	2.75

Shear=4.0mm forward

POINT	Sn [MPa]	Ss [MPa]	Un xE-6 [m]	Us xE-6 [m]	b xE-6 [m]	e xE-6 [m]	P xE-2 [MPa]	Q xE-7 [m^3/s]
E	54.28	27.93	-62.66	-4006.00	27.63	27.63	0.00	6.22
F	42.29	21.93	-62.37	-4007.00	30.44	30.44	1.25	6.22
G	37.94	19.73	-62.22	-4018.00	30.65	30.65	2.49	6.22
H	41.17	21.36	-62.32	-4017.00	30.49	30.49	3.72	6.22
I	50.49	26.03	-62.57	-4026.00	28.61	28.61	4.91	6.22

Shear=2.0mm reverse

POINT	Sn [MPa]	Ss [MPa]	Un xE-6 [m]	Us xE-6 [m]	b xE-6 [m]	e xE-6 [m]	P xE-2 [MPa]	Q xE-7 [m^3/s]
E	50.20	-25.77	-62.57	-2006.00	21.49	21.49	0.00	2.47
F	41.27	-21.30	-62.35	-2016.00	22.37	22.37	1.23	2.47
G	38.32	-19.81	-62.24	-2014.00	22.79	22.79	2.45	2.47
H	41.65	-21.49	-62.35	-2025.00	22.14	22.14	2.66	2.47
I	51.53	-26.43	-62.61	-2024.00	21.37	21.37	4.91	2.47

Shear=0.0mm reverse

POINT	Sn [MPa]	Ss [MPa]	Un xE-6 [m]	Us xE-6 [m]	b xE-6 [m]	e xE-6 [m]	P xE-2 [MPa]	Q xE-7 [m^3/s]
E	49.41	-25.29	-62.55	-0.90	27.98	27.98	0.00	5.82
F	41.43	-21.29	-62.36	-8.11	30.13	30.13	1.26	5.82
G	38.67	-19.90	-62.26	-5.20	30.62	30.62	2.44	5.82
H	41.53	-21.34	-62.32	-16.62	30.10	30.10	3.62	5.82
I	51.41	-26.29	-62.32	-18.90	27.51	27.51	4.91	5.82

List of SKB reports

Annual Reports

1977-78
TR 121
KBS Technical Reports 1 – 120
Summaries
Stockholm, May 1979

1979
TR 79-28
The KBS Annual Report 1979
KBS Technical Reports 79-01 – 79-27
Summaries
Stockholm, March 1980

1980
TR 80-26
The KBS Annual Report 1980
KBS Technical Reports 80-01 – 80-25
Summaries
Stockholm, March 1981

1981
TR 81-17
The KBS Annual Report 1981
KBS Technical Reports 81-01 – 81-16
Summaries
Stockholm, April 1982

1982
TR 82-28
The KBS Annual Report 1982
KBS Technical Reports 82-01 – 82-27
Summaries
Stockholm, July 1983

1983
TR 83-77
The KBS Annual Report 1983
KBS Technical Reports 83-01 – 83-76
Summaries
Stockholm, June 1984

1984
TR 85-01
Annual Research and Development Report 1984
Including Summaries of Technical Reports Issued during 1984. (Technical Reports 84-01 – 84-19)
Stockholm, June 1985

1985
TR 85-20
Annual Research and Development Report 1985
Including Summaries of Technical Reports Issued during 1985. (Technical Reports 85-01 – 85-19)
Stockholm, May 1986

1986
TR 86-31
SKB Annual Report 1986
Including Summaries of Technical Reports Issued during 1986
Stockholm, May 1987

1987
TR 87-33
SKB Annual Report 1987
Including Summaries of Technical Reports Issued during 1987
Stockholm, May 1988

1988
TR 88-32
SKB Annual Report 1988
Including Summaries of Technical Reports Issued during 1988
Stockholm, May 1989

1989
TR 89-40
SKB Annual Report 1989
Including Summaries of Technical Reports Issued during 1989
Stockholm, May 1990

1990
TR 90-46
SKB Annual Report 1990
Including Summaries of Technical Reports Issued during 1990
Stockholm, May 1991

1991
TR 91-64
SKB Annual Report 1991
Including Summaries of Technical Reports Issued during 1991
Stockholm, April 1992

1992
TR 92-46
SKB Annual Report 1992
Including Summaries of Technical Reports Issued during 1992
Stockholm, May 1993

1993
TR 93-34
SKB Annual Report 1993
Including Summaries of Technical Reports Issued during 1993
Stockholm, May 1994

1994

TR 94-33

SKB Annual Report 1994

Including Summaries of Technical Reports Issued during 1994.
Stockholm, May 1995

List of SKB Technical Reports 1995

TR 95-01

Biotite and chlorite weathering at 25°C. The dependence of pH and (bi) carbonate on weathering kinetics, dissolution stoichiometry, and solubility; and the relation to redox conditions in granitic aquifers

Maria Malmström[1], Steven Banwart[1], Lara Duro[2], Paul Wersin[3], Jordi Bruno[3]
[1] Royal Institute of Technology, Department of Inorganic Chemistry, Stockholm, Sweden
[2] Universidad Politécnica de Cataluña, Departmento de Inginería Química, Barcelona, Spain
[3] MBT Tecnología Ambiental, Cerdanyola, Spain
January 1995

TR 95-02

Copper canister with cast inner component. Amendment to project on Alternative Systems Study (PASS), SKB TR 93-04

Lars Werme, Joachim Eriksson
Swedish Nuclear Fuel and Waste Management Co, Stockholm, Sweden
March 1995

TR 95-03

Prestudy of final disposal of long-lived low and intermediate level waste

Marie Wiborgh (ed.)
Kemakta Konsult AB, Stockholm, Sweden
January 1995

TR 95-04

Spent nuclear fuel corrosion: The application of ICP-MS to direct actinide analysis

R S Forsyth[1], U-B Eklund[2]
[1] Caledon-Consult AB, Nyköping, Sweden
[2] Studsvik Nuclear AB, Nyköping, Sweden
March 1995

TR 95-05

Groundwater sampling and chemical characterisation of the Laxemar deep borehole KLX02

Marcus Laaksoharju[1], John Smellie[2]
Ann-Chatrin Nilsson[3], Christina Skårman[1]
[1] GeoPoint AB, Sollentuna, Sweden
[2] Conterra AB, Uppsala, Sweden
[3] KTH, Stockholm, Sweden
February 1995

TR 95-06

Palaeohydrological implications in the Baltic area and its relation to the groundwater at Äspö, south-eastern Sweden – A literature study

Bill Wallin
Geokema AB, Lidingö, Sweden
March, 1995

TR 95-07

Äspö Hard Rock Laboratory Annual Report 1994

SKB
April 1995

TR 95-08

Feasibility study for siting of a deep repository within the Storuman municipality

Swedish Nuclear Fuel and Waste Management Co., Stockholm
January 1995

TR 95-09

A thermodynamic data base for Tc to calculate equilibrium solubilities at temperatures up to 300°C

Ignasi Puigdomènech[1], Jordi Bruno[2]
[1] Studsvik AB, Nyköping, Sweden
[2] Intera Information Technologies SL, Cerdanyola, Spain
April 1995

TR 95-10

Investigations of subterranean microorganisms. Their importance for performance assessment of radioactive waste disposal

Karsten Pedersen[1], Fred Karlsson[2]
[1] Göteborg University, General and Marine Microbiology, The Lundberg Institute, Göteborg, Sweden
[2] Swedish Nuclear Fuel and Waste Management Co., Stockholm, Sweden
June 1995

TR 95-11
Solute transport in fractured media – The important mechanisms for performance assessment
Luis Moreno, Björn Gylling, Ivars Neretnieks
Department of Chemical Engineering and Technology, Royal Institute of Technology, Stockholm, Sweden
June 1995

TR 95-12
Literature survey of matrix diffusion theory and of experiments and data including natural analogues
Yvonne Ohlsson, Ivars Neretnieks
Department of Chemical Engineering and Technology, Royal Institute of Technology, Stockholm, Sweden
August 1995

TR 95-13
Interactions of trace elements with fracture filling minerals from the Äspö Hard Rock Laboratory
Ove Landström[1], Eva-Lena Tullborg[2]
[1] Studsvik Eco & Safety AB
[2] Terralogica AB
June 1995

TR 95-14
Consequences of using crushed crystalline rock as ballast in KBS-3 tunnels instead of rounded quartz particles
Roland Pusch
Clay Technology AB
February 1995

TR 95-15
Estimation of effective block conductivities based on discrete network analyses using data from the Äspö site
Paul R La Pointe[1], Peter Wallmann[1], Sven Follin[2]
[1] Golder Associates Inc., Seattle, WA, USA
[2] Golder Associates AB, Lund, Sweden
September 1995

TR 95-16
Temperature conditions in the SKB study sites
Kaj Ahlbom[1], Olle Olsson[1], Stefan Sehlstedt[2]
[1] Conterra AB
[2] MRM Konsult AB
June 1995

TR 95-17
Measurements of colloid concentrations in the fracture zone, Äspö Hard Rock Laboratory, Sweden
Anna Ledin, Anders Düker, Stefan Karlsson, Bert Allard
Department of Water and Environmental Studies,Linköping University, Linköping, Sweden
June 1995

TR 95-18
Thermal evidence of caledonide foreland, molasse sedimentation in Fennoscandia
Eva-Lena Tullborg[1], Sven Åke Larsson[1], Lennart Björklund[1], Lennart Samuelsson[2], Jimmy Stigh[1]
[1] Department of Geology, Earth Sciences Centre, Göteborg University, Göteborg, Sweden
[2] Geological Survey of Sweden, Earth Sciences Centre, Göteborg, Sweden
November 1995

TR 95-19
Compaction of bentonite blocks. Development of technique for industrial production of blocks which are manageable by man
Lars-Erik Johannesson, Lennart Börgesson, Torbjörn Sandén
Clay Technology AB, Lund, Sweden
April 1995

TR 95-20
Modelling of the physical behaviour of water saturated clay barriers. Laboratory tests, material models and finite element application
Lennart Börgesson[1], Lars-Erik Johannesson[1], Torbjörn Sandén[1], Jan Hernelind[2]
[1] Clay Technology AB, Lund, Sweden
[2] FEM-Tech AB, Västerås, Sweden
September 1995

TR 95-21
Conceptual model for concrete long time degradation in a deep nuclear waste repository
Björn Lagerblad, Jan Trägårdh
Swedish Cement and Concrete Research Institute
February 1994

TR 95-22
The use of interaction matrices for identification, structuring and ranking of FEPs in a repository system. Application on the far-field of a deep geological repository for spent fuel
Kristina Skagius[1], Anders Ström[2], Marie Wiborgh[1]
[1] Kemakta, Stockholm, Sweden
[2] Swedish Nuclear Fuel and Waste Management Co, Stockholm, Sweden
November 1995

TR 95-23
Spent nuclear fuel. A review of properties of possible relevance to corrosion processes
Roy Forsyth
Caledon Consult AB
April 1995

TR 95-24
Studies of colloids and their importance for repository performance assessment
Marcus Laaksoharju[1], Claude Degueldre[2], Christina Skårman[1]
[1] GeoPoint AB, Sollentuna, Sweden
[2] University of Geneva, Switzerland
December 1995

TR 95-25
Sulphate reduction in the Äspö HRL tunnel
Marcus Laaksoharju (ed.)
GeoPoint AB, Sollentuna, Sweden
December 1995

TR 95-26
The Äspö redox investigations in block scale. Project summary and implications for repository performance assessment
Steven Banwart (ed.)
Dept. of Civil and Environmental Engineering, University of Bradford, UK
November 1995

TR 95-27
Survival of bacteria in nuclear waste buffer materials. The influence of nutrients, temperature and water activity
Karsten Pedersen[1], Mehrdad Motamedi[1], Ola Karnland[2]
[1] Department of General and Marine Microbiology, the Lundberg Institute, Göteborg University, Göteborg, Sweden
[2] Clay Technology AB, Lund, Sweden
December 1995

TR 95-28
DECOVALEX I – Test Case 2: Calculation of the Fanay-Augères THM Test – Thermomechanical modelling of a fractured rock volume
Lennart Börgesson[1], Jan Hernelind[2]
[1] Clay Technology AB, Lund, Sweden
[2] Fem-Tech AB, Västerås, Sweden
December 1995

TR 95-29
DECOVALEX I – Test Case 3: Calculation of the Big Ben Experiment – Coupled modelling of the thermal, mechanical and hydraulic behaviour of water-unsaturated buffer material in a simulated deposition hole
Lennart Börgesson[1], Jan Hernelind[2]
[1] Clay Technology AB, Lund, Sweden
[2] Fem-Tech AB, Västerås, Sweden
December 1995

TR 95-30
DECOVALEX I – Bench-Mark Test 3: Thermo-hydro-mechanical modelling
Jan Israelsson
Itasca Geomekanik AB
December 1995